NEONOR
Neotectonics in Norway

NGU Report 98.016

Neotectonics in Norway

Annual Technical Report 1997

NGU
Norges geologiske undersøkelse
Geological Survey of Norway
P.O.Box 3006 - Lade
N-7002 Trondheim, Norway

REPORT

Report no.: 98.016	ISSN 0800-3416	Grading: ÅPEN

Title:

Neotectonics in Norway, Annual Technical Report 1997

Editors:	Client:
John Dehls and Odleiv Olesen	NGU, Amoco, Phillips, Norsk Hydro, Statkraft, NPD, SK, NFR, NORSAR
Contributors: L. Bockmann, A. Braathen, H. Bungum, R. Bøe, J. Dehls, S. Fanavoll, W. Fjeldskaar, E. Hicks, E. Larsen, C. Lindholm, O. Longva, E. Mauring, O. Olesen, L. Olsen, F. Riis, L. Rise, J. S. Rønning, T. Skogseth, J. F. Tønnesen	Contributing institutes: NGU, NORSAR, Norwegian Mapping Authority (SK), IKU Petroleum Research, Rogaland Research, NPD, NTNU
Deposit name and grid-reference:	Number of pages: 149 Price (NOK): kr. 850,- Map enclosures: 1

Fieldwork carried out:	Date of report:	Project no.:	Person responsible:
1997	15/02-1998	2757.00	

Summary:

Neotectonic crustal deformations have been reported at a large number of locations in Norway (both on local and regional scales). The NEONOR Project represents a national effort by several national research and mapping institutions to investigate these phenomena through a multidisciplinary approach. Both the industry and the Norwegian Research Council contribute with major financial support. The main objectives of the NEONOR Project are to systematically collect data, and to provide answers to the questions: 1) How can recent crustal deformation be characterised in time and space? 2) What processes cause the neotectonic crustal deformations? 3) What are the implications for migration and occurrence of fluids (especially hydrocarbons and groundwater) in bedrock? 4) What are the implications for geohazard related to constructing sensitive installations like pipelines, gas-terminals and hydropower-plants.

The initial phase of the project includes a systematic collection and characterisation of known deformations. New geological, geodetic and seismological data are, however, also acquired. In northern Norway there are now good evidences of postglacial crustal deformation in Rana, Beiarn, Kåfjord and Masi. Many of the other neotectonic claims in Norway can, however, be attributed to other effects than tectonic. The detailed studies have showed that areas of postglacial faults are characterised by increased seismicity, reactivation of regional zones of weakness and anomalous land uplift. There are good evidences for a conjugate set of normal faults perpendicular to the extensive system of NE-SW trending reverse faults in northern Fennoscandia. A new seismic micro-network in the Rana area has revealed an area of increased seismicity in the Sjona fjord. Nearly 100 earthquakes are detected in less than a half year. Focal plane mechanisms indicate a general N-S trending compression that may activate the reverse E-W trending Båsmoen fault. Studies of commercial 3D seismic data from the northern North Sea have unveiled evidences of Quaternary deformation. Glacio-isostatic modelling reveals local areas that have a significant difference between the observed uplift and the calculated uplift. This is assumed to be areas that experience tectonic movements today. The final phase of the NEONOR project will involve an integrated interpretation of the compiled neotectonic datasets.

Keywords: Geofysikk	Geologi	Neotektonikk
Isostasi	Forkastning	Seismologi
Geologisk risiko	Landhevning	Fagrapport

CONTENTS

LIST OF FIGURES

1 INTRODUCTION

The initiative for a national neotectonic research project was taken in 1995 by NORSAR and the Geological Survey of Norway (NGU). The Norwegian Petroleum Directorate (NPD) and NGU did at the same time make plans for compiling a neotectonic map of Norway at the scale 1:3 million. These two initiatives were merged into the 'Neotectonics in Norway - NEONOR Project' in 1996. The Norwegian Mapping Authority (SK) has joined the project and is contributing with expertise on geodesy. The Norwegian Research Council (NFR) has financed three years of a four-year Doctoral fellowship (Dr. Scient) for Erik Hicks at NORSAR/UiO and a two year Post Doctoral fellowship for John Dehls at NGU. NORSAR will fund the final year of the four-year Doctoral fellowship. The NEONOR Project is financed by Amoco Norway, Norsk Hydro, Phillips Petroleum, Statkraft, NFR, NGU, NPD, SK and NORSAR. Mark Shahly, Chris Dart, Philip J. Goldsmith and Ivar Hågensen are representatives of the four industrial partners in the steering committee. Philip J. Goldsmith is chairman. NGU, NORSAR, OD and SK are represented by Odleiv Olesen, Hilmar Bungum, Fridtjof Riis and Lars Bockmann, respectively. Stein Fanavoll, IKU Petroleum Research, Willy Fjeldskaar, Rogaland Research and Terje Skogseth, Norwegian University of Science and Technology (Dept. of Surveying and Mapping) are carrying out substantial parts of the research project on a contract basis. Conrad Lindholm and Hilmar Bungum, NORSAR were instrumental in the planning phase of the project proposal.

The project started in June 1997 and the present report documents the status for the activities that have been carried out by NGU, NORSAR, NPD, SK, IKU and RF since then (task numbers refer to the project proposal):

- Classification and quality assessment of existing neotectonic reports (Task 1).
- Collation and interpretation of marine seismic data (both 2D and 3D) from IKU, NPD and the petroleum industry, aimed at mapping recent offshore faulting (Task 2).
- Production of a 1:3 million scale map of neotectonic phenomena in Norway (Task 3).
- Acquisition of new geological and geophysical data at six specified sites and regions expected to have potential in terms of neotectonic information (Tasks 4 & 9).
- Acquisition and interpretation of local and regional high-resolution geodetic data, also by means of GPS networks (Tasks 5, 6 & 7).
- Acquisition of local seismological data by means of new seismic stations (micro-networks) (Task 10).
- Joint interpretation of acquired neotectonic data and geodynamic modelling aimed to understand the recent and present day crustal dynamics (Task 11).
- One Dr. Scient fellowship and one Post Doctoral fellowship are essential parts of the project, and these will run over four and two years, respectively.

The project will continue for two more years and will be finished in December 1999.

Neotectonics are, according to the International Association for Quaternary Research (INQUA), defined as "Any earth movements or deformations of the geodetic reference level, their mechanisms, their geological origin (however old they may be), their implications for various practical purposes and their future extrapolations (INQUA 1982)." These studies have long been addressed within plate margin areas where large movements occur, while intraplate areas have not been considered similarly interesting because of the lower deformation rates. The traditional view that Norway does not exhibit major earthquakes or large crustal surface deformations has obscured the fact that several observations have documented the contrary, however not on scales comparable with plate margin deformations. Geologic mapping over the last thirty years in northern Fennoscandia has revealed a system of postglacial surface deformations (e.g. Kujansuu 1964, Lundquist & Lagerbäck 1976, Olesen 1988). More recent studies of earthquake occurrence (e.g. Bungum *et al.* 1991) have revealed several regions of unexplained high seismic activity, but a correlation between earthquake distribution and surface deformation is still pending. We believe that this type of information is poorly integrated and emphasised in the scientific community and consequently also generally in society.

A detailed investigation involving quality analysis of existing reports, improved understanding of the characteristics of crustal deformations through more and better observations, and a unified interpretation of the observations, is a prerequisite for a better understanding of the dynamic processes that are active in Norwegian regions at present. Such understanding is desirable from a scientific point of view, but also has practical implications, including various aspects of geological risks. Active faulting in the offshore region can amongst other effects lead to major submarine landslides, and may also have implications for migration and sealing properties of faults (with consequences for petroleum potential). The study of the postglacial faults on land could lead to a better understanding of the offshore faults, as the on-land faults are more readily available to study. Greatly improved measurement techniques in the fields of geodesy, seismology and applied geophysics should guarantee for the success for a neotectonic research programme in Norway.

2 CLASSIFICATION AND QUALITY ASSESSMENT OF REPORTED NEOTECTONIC PHENOMENA (TASK 1)

2.1 NEOTECTONIC PHENOMENA IN NORTHERN NORWAY

By Odleiv Olesen and John Dehls, NGU

2.1.1 Introduction

Neotectonic crustal deformations have been reported at a large number of locations in Norway (both on local and regional scales). The NEONOR project represents an effort to investigate and classify these phenomena through a multidisciplinary approach. The definition of postglacial faulting is tectonic faulting that has occurred since the end of the last glaciation. Criteria for identification of postglacial faulting have been presented earlier by Fenton (1991, 1994) and Muir Wood (1993):

1) Offset of an original continuous surface or sediment of postglacial or late glacial age.

2) Reasonably consistent direction and amount of slip along the length of the fault.

3) The ratio of displacement to overall length of the feature should be less than 1/1000. For most faults this ratio is between 1/10,000 and 1/100.000.

4) Exclusion of gravity sliding as the driving mechanism of faults in areas of moderate to high relief.

5) No signs of glacial modification (such as striation or ice-plucking) of fault scarps especially those controlled by banding, bedding or schistosity.

6) Exclusion of mechanisms such as glaciotectonics (ice push features), collapse due to ice melting, differential compaction or deposition over a pre-existing erosional scarp being the cause of an apparent offset in overburden.

Slight glacial modification of scarps suggests late glacial or interglacial age for a fault scarp.

We can when applying these criteria, objectively rank neotectonic claims similar to the review of seismotectonics in Sweden by Muir Wood (1993). He classified the claims into five grades;

(A) Almost certainly neotectonics,

(B) Probably neotectonics,

(C) Possibly neotectonics,

(D) Probably not neotectonics

(E) Very unlikely to be neotectonics.

Muir Wood (1993) reported 10 claims in Norway. We have added 31 more accounts to the list in Appendix 2.1. A tentative assessment of the additional claims is also included. Eight of the claims are situated in the offshore area and the others are located on mainland Norway.

The locations of 17 reported claims of neotectonic activity in Norway have been visited for closer geological and geomorphological examination during the initial phase of the NEONOR Project: Lygre (Fusa), Vøringsfossen, Mosstølen (Suldal), Ragnhildnuten (Sandnes), Yrkje, Vindafjorden, Ulvegrovene (Forsand), Ranafjord, Austerdalsisen, Beiarn, Skjomen, Vassdal-fjell, Kåfjord, Nordreisa, Masi, Gæssajavri and Skipskjølen (Varanger Peninsula). We have in addition visited one locality in northern Finland.

This section details the results from the studies of the sites in northern Norway (Fig. 2.1.1). The results of the studies of the sites in southern Norway are presented in the next section. For each site, the M-711 series map-sheet number is included as well as the UTM coordinates with WGS84 datum.

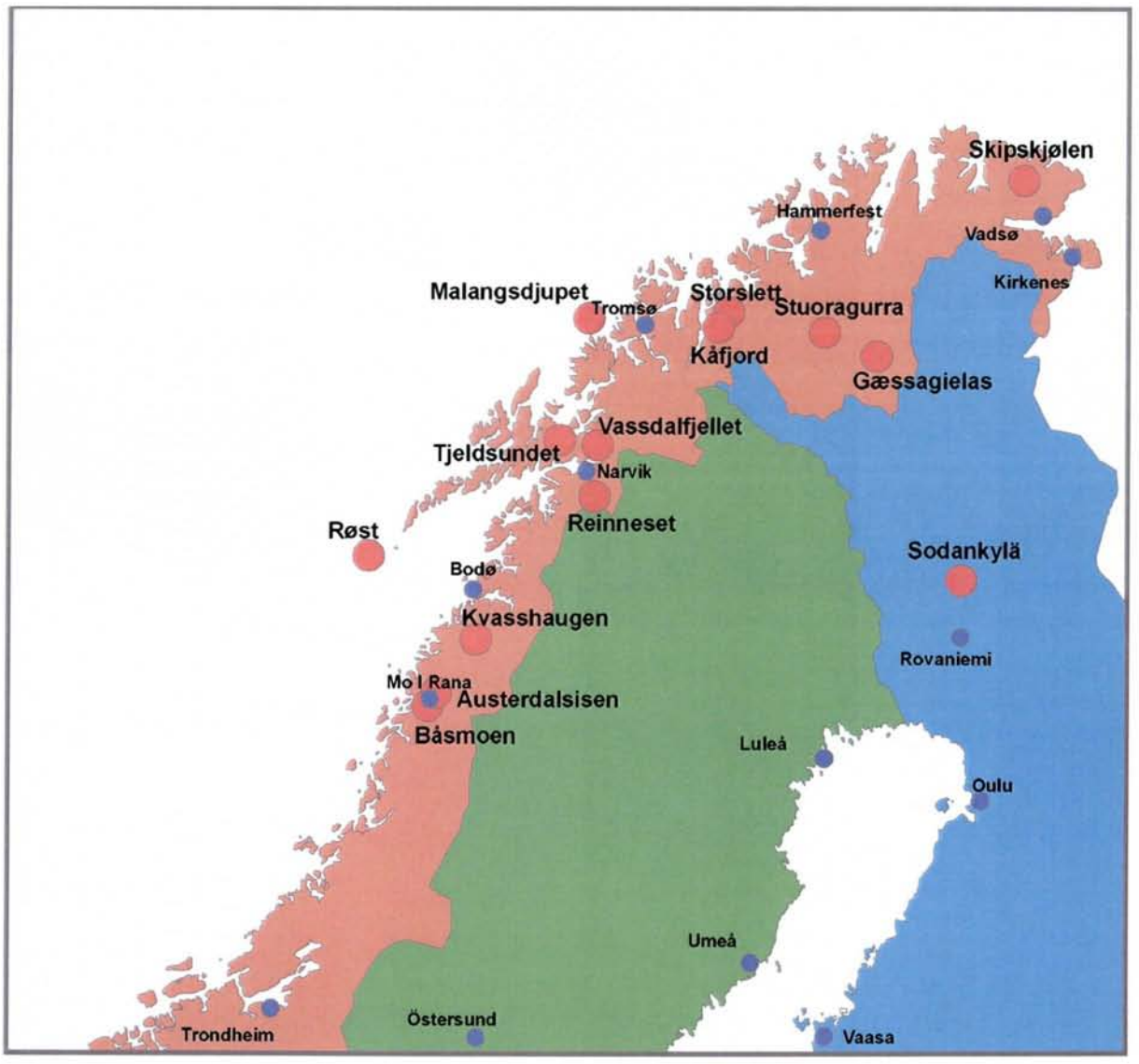

Fig. 2.1.1. Locations of sites of reported neotectonic activity visited in northern Norway.

2.1.2 Skipskjølen, Varanger Peninsula, Finnmark

(Map Sheet 2435 IV Skipskjølen, UTM 602.500,7811.400 - 605.300,7809.000, Zone 35)

WNW-ESE trending 4 km long escarpment (Fig. 2.1.2) within the Trollfjord-Komagelv Fault Zone has been observed from aerial photographs (Olesen *et al.* 1992b) and has been classified as a potential postglacial fault. The northern block seemed to be downfaulted.

A field-check of the location revealed that the scarp is not as steep as it appeared on the aerial photograph and seems to be sculptured and rounded by the moving inland ice (Fig. 2.1.3). The height of the scarp is varying considerable along the scarp. We do therefore conclude that the scarp does not represent a postglacial fault and it is most likely formed by glacial erosion. We can, however, not exclude that the fault was active in an interstadial or during deglaciation.

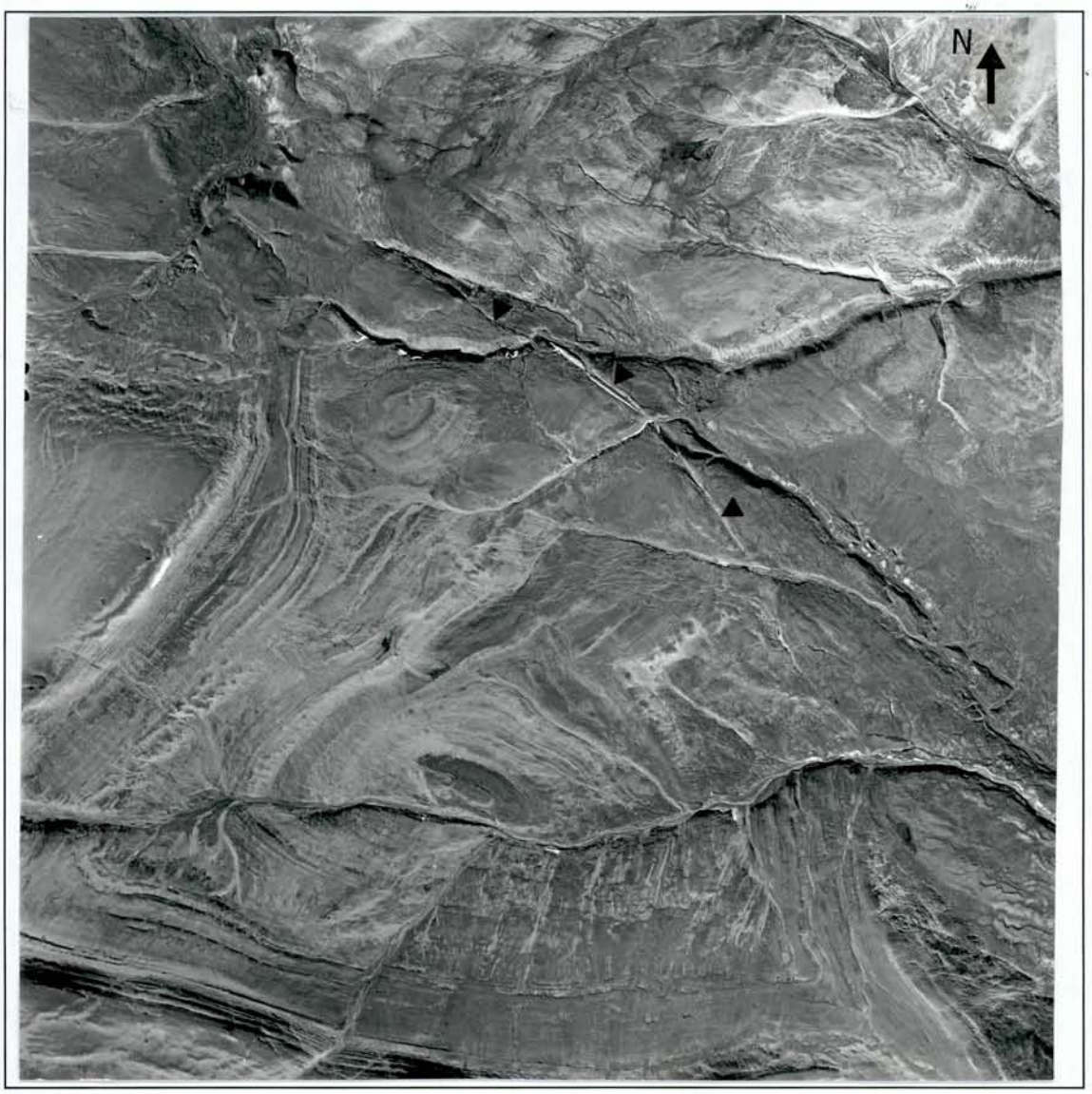

Fig. 2.1.2. Aerial photograph of a 4 km long NW trending escarpment (shown by the arrows) along the regional Trollfjord-Komagelv Fault Zone. Olesen et al. (1992b) classified it as a potential postglacial fault from aerial photographs. The northern block seemed to be downfaulted.

Fig. 2.1.3. Photograph of the escarpment looking west. The escarpment is trending through the central part of the photograph (along the uppermost snowdrift). The scarp obviously does not appear as sharp as on the aerial photographs.

2.1.3 Gæssagielas, Karasjok, Finnmark

(Map Sheet 2033 III Bæivasgieddi, UTM 421.000,7674.400, Zone 35)

Olsen (1989) has, during interpretation of aerial photographs for Quaternary mapping, interpreted an E-W trending 1.5 km long assumed Late Quaternary fault. The northern block seemed to be depressed. A landslide was observed at the scarp, which is situated at a small hill above the tree line. A closer field examination revealed a 1 m high diffuse scarp (Fig. 2.1.4). The till cover in the area is thin and there are several outcrops along the hill. The scarp is parallel to the underlying bedrock foliation and therefore interpreted to represent a till-draped escarpment in the bedrock.

(A)

(B)

Fig. 2.1.4. Oblique aerial photograph of 1.5 km long scarp on Gæssagielas, Karasjok. (A) looking south, (B) looking east. The scarp has, during interpretation of aerial photographs for Quaternary mapping, been inferred to represent a potential postglacial fault (Olsen 1989) but it has not been field-checked earlier. The northern block seemed to be depressed. See text for further discussion.

2.1.4 Stuoragurra Fault, Masi, Finnmark

(Map Sheets 1933 IV Masi, 1934 III Suoluvuobmi, 1934 II Iesjavri, 1934 I, Cåkkarassa and 2034 IV Skoganvarre)

The Stuoragurra Fault (SF) was identified in 1983 during the course of a collaborative project between the Geological Surveys of Norway and Sweden, and details on the SF have been reported by Olesen (1988), Muir Wood (1989a), Olesen *et al.* (1992a, b, c) and Roberts *et al.* (1997). The SF, located within the Mierujav'ri Sværholt Fault Zone (MSFZ), is an 80 km long fault zone, (Fig. 2.1.5) which contains numerous segments of eastward dipping (30-50°) faults with up to 10 m of reverse displacement and a 7 m high escarpment. The SF crosscuts glaciofluvial deposits northeast of Iešjav'ri (Olesen 1988) and an esker northeast of Masi and is consequently younger than 9.000 years. Similar fault scarps occur in adjacent parts of Finland (Kujansuu 1964) and Sweden (Lundquist & Lagerbäck 1976, Lagerbäck 1979, 1990). The postglacial fault coincides locally with an 5-10 m wide zone of lithified breccia and is composed of several thin (a few cm wide) zones of fault gouge within a couple of metres wide zone. The fault is listric with a dip of c. 50° close to the surface and c. 30° at a depth of 40 m. The fault typically have an offset/length ratio of approximately 1/10.000 which is one of the criteria generally applied for the classification of neotectonic faults. (Secondary accommodation faults may have a larger offset/length ratio.) The fault cuts through an esker and other glaciofluvial features. Several groundwater springs occur along the Stuoragurra Fault. Large amounts of water poured out of the escarpment (Fig. 2.1.6) after the January 1996 earthquake (magnitude 4.0).

Precision levelling of benchmarks across the Stuoragurra fault has shown that the footwall has subsided relative to the hanging-wall block by 2.3 mm between 1987 and 1991. The annual average change in elevation of benchmarks based on precision levelling in 1954 and later in 1975 along the old road from Alta to Kautokeino has shown a significant deviation from the general postglacial upheaval of Fennoscandia. Instead of an increasing uplift from 2 mm/year in Alta to 5 mm/year in Kautokeino as is generally indicated on land upheaval maps of Fennoscandia, a subsidence of the inland area was observed. During Quaternary geological mapping in the Iešjav'ri area one submerged shoreline has been observed at the southern margin of this lake. The shoreline is located roughly a few dm below the present water-level, and we think that this indicates that a vertical crustal movement with a N-S gradient opposite to that of the general postglacial rebound has occurred during the last few hundred years. Relevelling in 1992 of the profile of 1954 and 1975 did, however, not reproduce this pattern (Olesen *et al.* 1992c), but did on the other hand reveal a 3.4 mm movement across a 3 km extrapolation of a fault scarp. Systematic mapping of the shorelines around Iešjav'ri will clarify the regional uplift pattern of the area.

Studies of the postglacial Stuoragurra Fault in the Precambrian of Finnmark showed that postglacial faulting is likely to occur in areas of increased seismicity, regional zones of weakness and anomalous land uplift (Olesen *et al.* 1992a, 1992b, Bungum & Lindholm 1997).

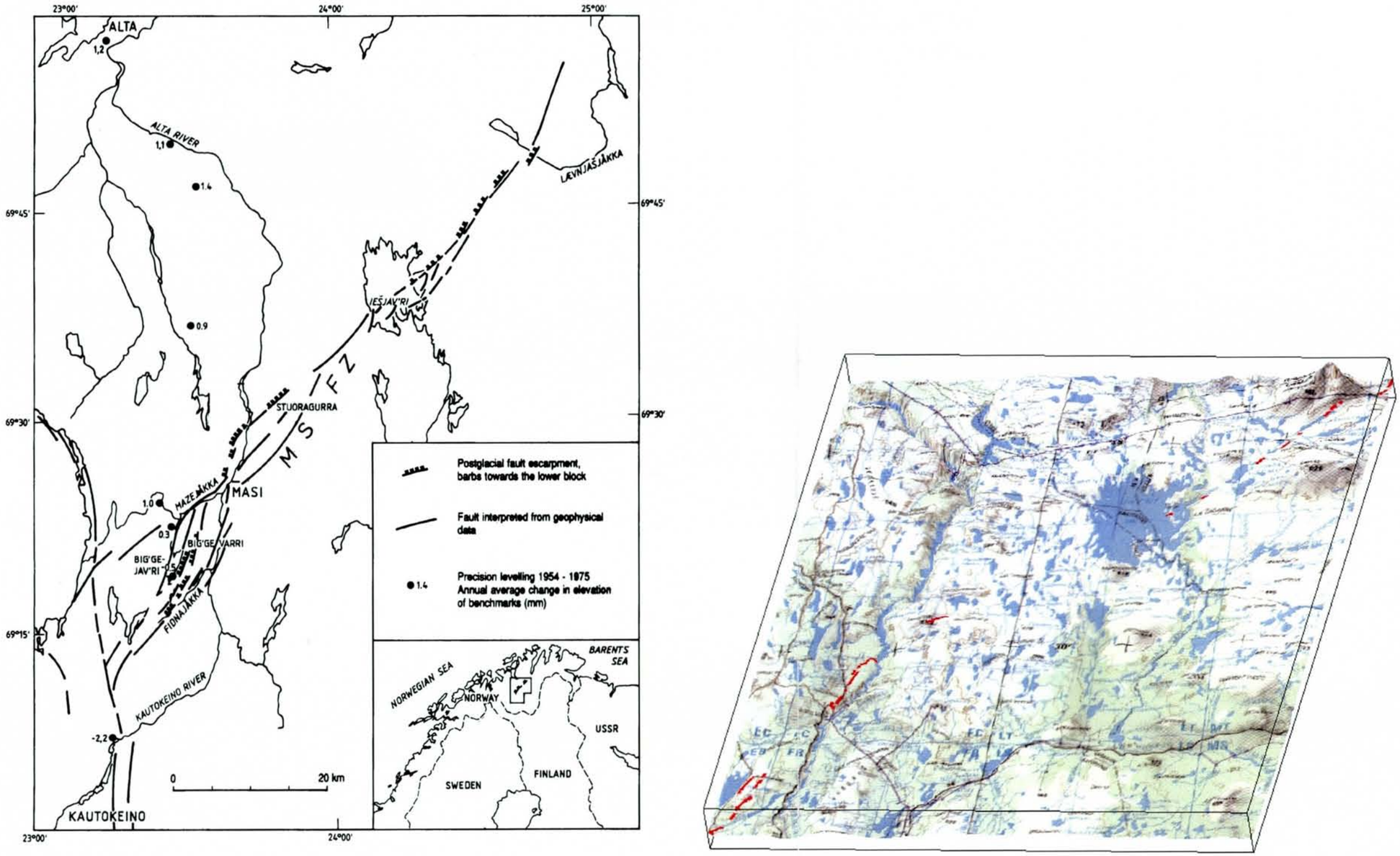

Fig. 2.1.5. The Stuoragurra postglacial fault is situated within the Proterozoic Mierujav'ri Sværholt Fault Zone (MSFZ) in Finnmark.

(A)

(B)

Fig. 2.1.6. (A) Oblique aerial photograph from August 1989 of the Stuoragurra Fault to the east of the Kautokeino River. The height of the escarpment on the picture is 4-5 m. Several groundwater springs occur along the fault. Large amounts of water poured out of the escarpment after the January 1996 earthquake (magnitude 4.0). (B) Photograph from August 1996 showing turf destroyed by the water and washed-out soil (only gravel is left). The photograph is from the central part of the oblique aerial photograph (A) where there are no signs

of gravel in the escarpment. A field visit to this location two days after the January 1996 earthquake did, however, not reveal any outpour of groundwater. This spring must therefore have been active some time later, but before August.

2.1.5 Storslett, Nordreisa, Troms

(Map Sheet 1734 IV Nordreisa, UTM 505.000,7740.000, Zone 34)

Wontka (1974) interpreted an up to 150 m high scarp to the southeast of Storslett (Fig. 2.1.7) in terms of a postglacial reactivation of the Caledonian Jyppyrä fault which has an apparent accumulated displacement of approximately 700 m. The height of the scarp varies considerably and it does also appear to be rounded by glacial erosion (Fig. 2.1.8). There does not seem to be any reactivation along the foliation (which has a dec./inc. of 68°/30°) or any fault plane in the escarpment. The scarp was most likely formed by plucking of the moving inland ice along the Caledonian fault.

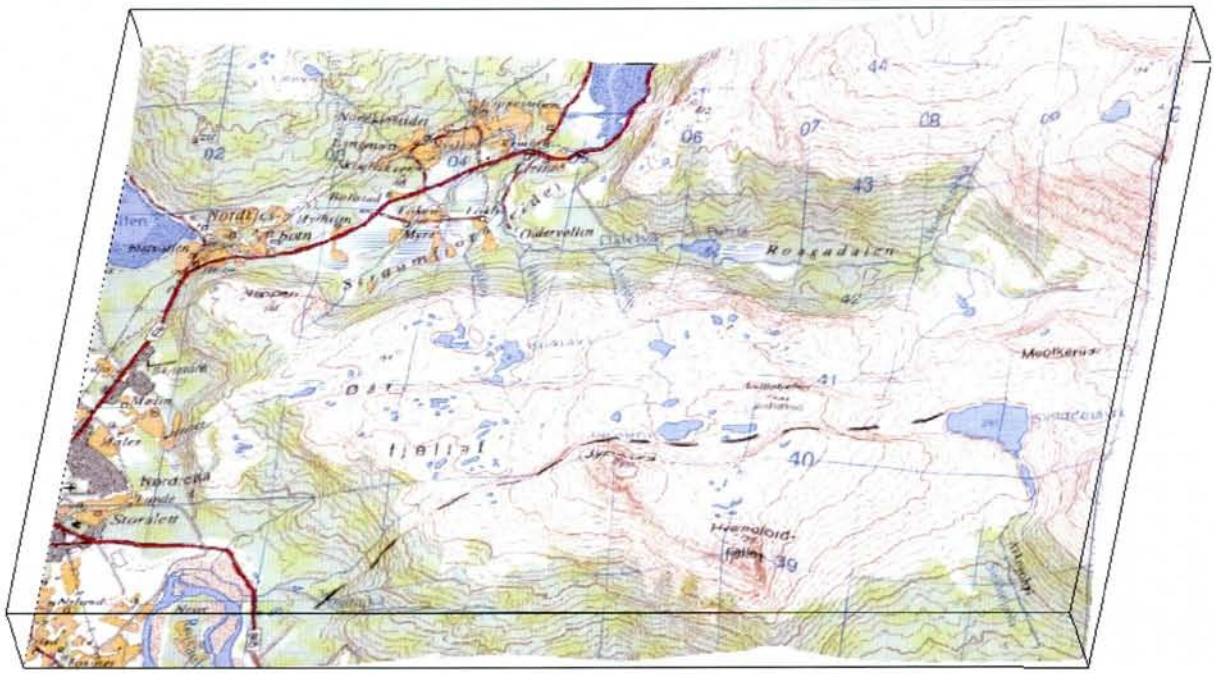

Fig. 2.1.7. Location of an approximately 150 m high escarpment, previously interpreted as a postglacial reactivation of the Caledonian Jyppyrä fault.

(A)

(B)

Fig. 2.1.8. (A) Approximately 50 m high escarpment along the Caledonian Jyppyrä fault which is situated three km to the east of the centre of Storslett in Nordreisa. (the photograph is looking to the west). (B) Detail of the escarpment looking east across the Reisa River. The top of the escarpment is rounded and there is a significant variation in offset along the scarp.

2.1.6 Nordmannvikdalen fault, Kåfjord, Troms

(Map Sheet 1634 II Kåfjord, UTM 487.000,7724.800-483.000,7727.800, Zone 34)

The Nordmannsvika postglacial fault (Fig. 2.1.9) which was discovered by Tolgensbakk & Sollid (1988) is a normal fault dipping 35-50° to the northeast (Fig. 2.1.10). The height of the escarpment is up to 1 metre. The fault does locally branch out in 2-3 sub-parallel faults causing an anastomosing appearance (Fig. 2.1.11). The fault is situated along the gradients of parallel gravity and magnetic anomalies, which are interpreted to represent structures in the underlying Proterozoic basement that is situated at a depth of c. 3 km in this area (Olesen *et al.* 1990b). The fault does also coincide with a NNW-SSE trending gradient in the depth to the Precambrian basement surface, which increases from a depth of 1-2 km in the Reisa area to more than 3 km in the Lyngen area to the west.

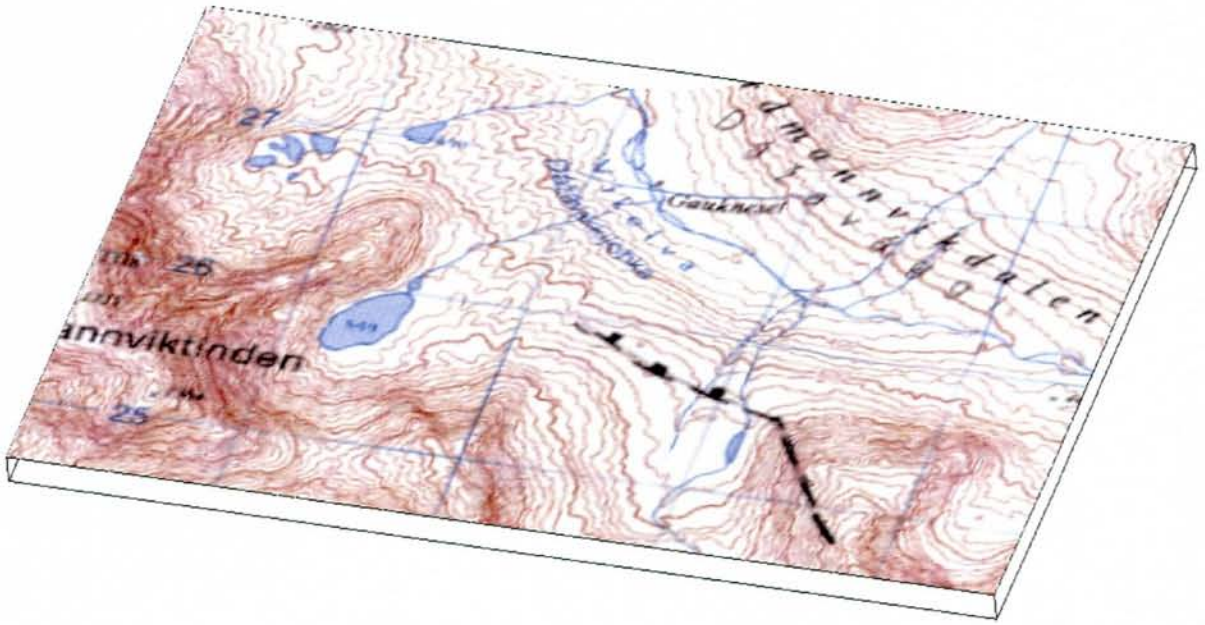

Fig. 2.1.9. The Nordmannsvika postglacial fault. 2X vertical exaggeration.

Ground penetrating radar (GPR) profiles at Kåfjord was carried out within the NEONOR Project to try to determine whether the Nordmannvikdalen fault is a gravitational induced fault or a true tectonic postglacial fault (Mauring *et al.* 1997, this report). Varnes *et al.* (1989) suggest that gravity induced sliding is most likely to occur when the elevation difference is greater than 300 m. At Kåfjord, the slope of the terrain is 10-12°, and the elevation difference between the fault scarp and the valley bottom is 150-200 m. Thus, gravitational sliding seems less likely, but still has to be considered.

(A)

(B)

Fig. 2.1.10. The Nordmannsvika postglacial fault discovered by Tolgensbakk & Solli (1988) is a normal fault dipping c. 45° to the northeast. The fault has an offset/length ratio of approximately 1/3000, which fulfils one of the important criteria generally applied for the classification of neotectonic faults. The faults cut through Quaternary deposits that are c. 10.000 years old. (A) Photograph of the Nordmannvikdalen fault from the westernmost slope of Kistefjellet looking towards the northwest. (B) Photograph taken in the opposite direction of the previous. Note the continuation of the fault through the mountain-slope in the background (western part of Kistefjellet). The dip of this exposed fault is c. 35° while GPR measurements reveal that the continuation at depth has a dip of 45-50°.

(A)

(B)

Fig. 2.1.11. Photographs of the escarpment of the Nordmannvikdalen postglacial fault. (A) The escarpment looking towards the southeast revealing a scarp height of 0.5-0.9 . (B) Photograph from a location further to the north-west along the escarpment (looking towards the north-west). The fault zone consists of two or three faults making up a set of lens-shaped blocks that have subsided up to 1 meter.

The GPR records (Mauring *et al.,* this report) show that the feature is a surface expression of a structure dipping 45-50° towards the north-east. An abrupt offset in the terrain surface corresponds with the position of the up-dip extrapolation of the most prominent radar reflector. This could indicate that the dipping reflector represents a structure that has been active during Holocene (i.e. postglacial activation). A relatively constant dip of the structure towards the north-east on two profiles indicates tectonic faulting. A third profile shows, however, a gentler dipping of the structure towards depth, which is in favour of gravitational induced faulting. To try to resolve this ambiguity, further investigations should include prolonging GPR profiles to the valley bottom in the north-eastern direction, to investigate the possibility of a gravitational induced fault. Also, a more extensive structural geological mapping programme should be carried out in the area. A preliminary interpretation of the structure is that it represents a normal, postglacial fault of tectonic origin.

2.1.7 Vassdalfjellet, Bjerkvik, Nordland

(Map Sheet 1432 III Gratangen, UTM 610.200,7609.000, Zone 33)

Bargel *et al.* (1995) describes a series of parallel east-west-oriented open fractures observed on the crest of Vassdalfjellet (Fig. 2.1.12). Some of these are over 1 m wide and many are so deep that their depth is difficult to assess. There have been vertical movements along some of the fractures (Fig. 2.1.13). Inspection in the field revealed a 100 m wide belt of 7-8 parallel faults situated close to a steep 600 m high wall along the southernmost slope of Vassdalfjellet. The longest fault is 600 m. Bargel *et al.* (1995) suggest that the features are due to stress features in the ridge or to more regional crustal movements after deglaciation, or a combination of these. The proximity to the almost vertical mountain wall with abundance of rock falls make us believe that the faults are gravity-driven.

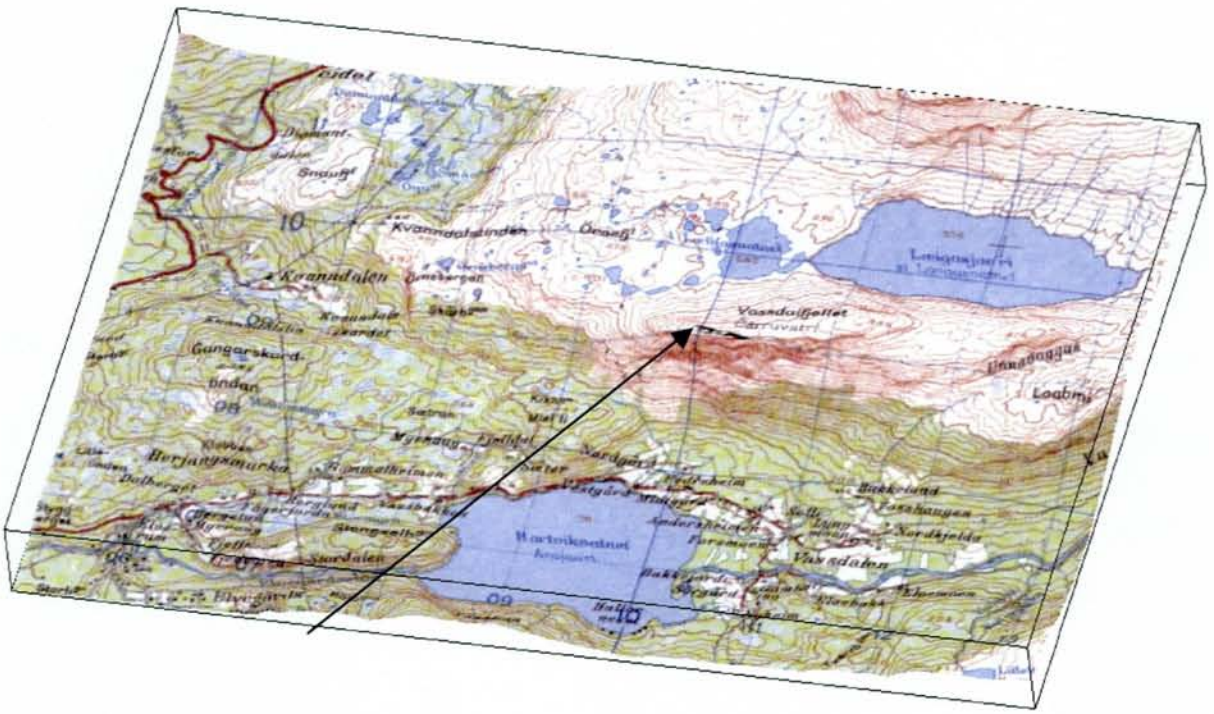

Fig. 2.1.12. Location of the open fractures on the crest of Vassdalfjellet.

Fig. 2.1.13. Open fractures on the top of Vassdalfjellet. Vertical movements can be observed along some of the clefts and fractures.

2.1.8 Reinneset, Skjomen, Nordland

(Map Sheet 1331 I Skjomen, UTM 597.700,7573.500, Zone 33)

On the headland between Skjomen and Sørskjomen, Bargel *et al.* (1995) interpreted a 1.5 to 10 m high escarpment in terms of a reverse postglacial fault dipping to the north. The fault continued to the west on the other side of Skjomenfjorden (Fig. 2.1.14). Foliated granite can be observed in a zone, a few dm wide at the foot of the escarpment. The dec./inc. of the foliation and fault wall is 260°/65°. Bargel *et al.* (1995) argue that the high, sharp-edged fault wall facing the direction of the moving inland ice points to a young age. An inspection of the locality shows that the top of the escarpment is rounded (Fig. 2.1.15) and that the height of the escarpment varies considerable over short distances along the fault. These observations point towards a formation due to erosion along an older zone of weakness. Since the escarpment is lying at the

headland between the Sørskjomen and Skjomen fjords it may have escaped the heaviest erosion from the two glaciers meeting at this point. We can, however, not exclude that the reverse fault could have been formed before the deglaciation or in an interstadial period and has been modified during the last glaciation.

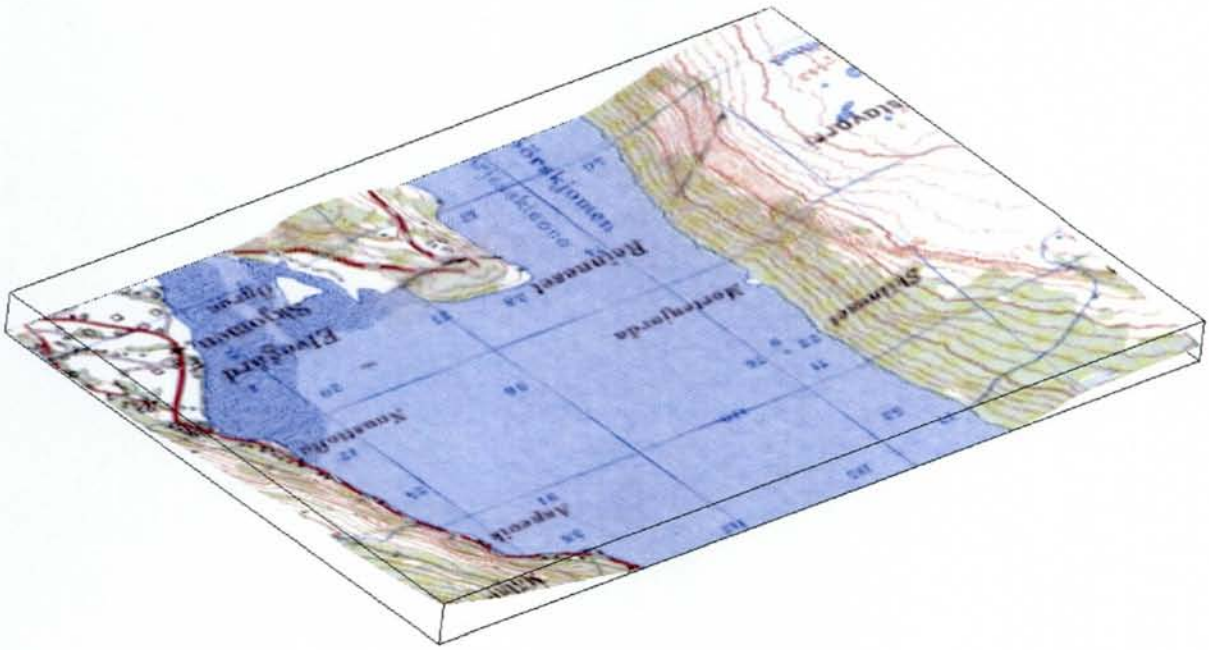

Fig. 2.1.14. Location of the proposed postglacial reverse fault crossing Skjomenfjorden. View is looking SW.

(A)

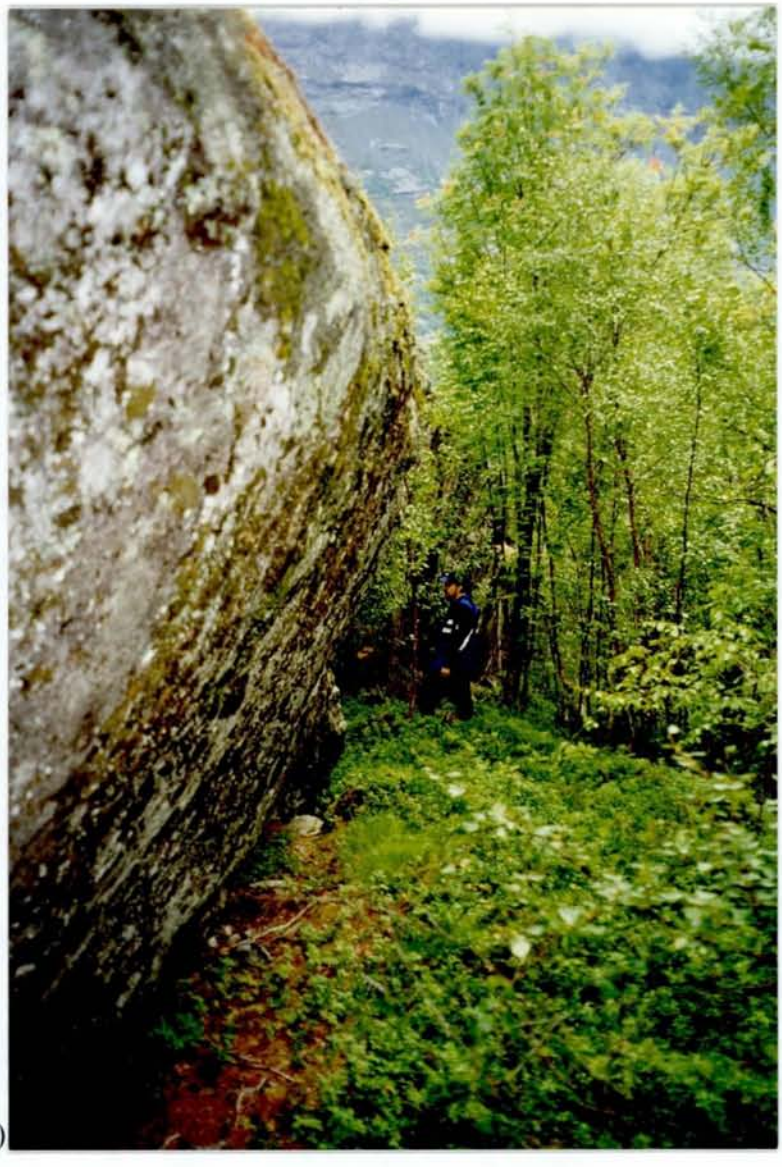

Fig. 2.1.15. Photographs of escarpment on the headland of Reinneset in Skjomen. (A) Rounded appearance of the escarpment (looking towards the east). (B, next page) Varying height of the escarpment. (C, next page) The escarpment on the western side of Sørskjomen viewed towards the west from Reinneset. There does not seem to be any offset of the bedrock surface at the top of the mountain in the uppermost part of the picture.

(B)

(C)

Fig. 2.1.15. *(See previous page)*

2.1.9 Kvasshaugen, Beiarn, Nordland

(Map Sheet 2028 Iv Arstaddalen, UTM 483.500,7411.800 - 485.400,7416.400, Zone 33)

Grønlie (1939) and Johnsen (1981) observed NNE-SSW trending clefts occurring along an approximately 5 km long NNE-SSW trending zone at the crest of Kvasshaugen (Fig. 2.1.16). These clefts are up to 20 m wide and 10 m deep and the eastern sides are generally down-faulted (Fig. 2.1.17). Clefts at a smaller scale can also be observed perpendicular to the foliation. The large-scale faults are suggested to be of postglacial age since there is no sign of glacial sculpturing along the escarpments. They have consequently been related to a WNW-ESE oriented extension. The faults were classified by Muir Wood (1993) as some of the most reliable claims of neotectonic surface fault rupture in Scandinavia but he pointed out that they may probably be of superficial character.

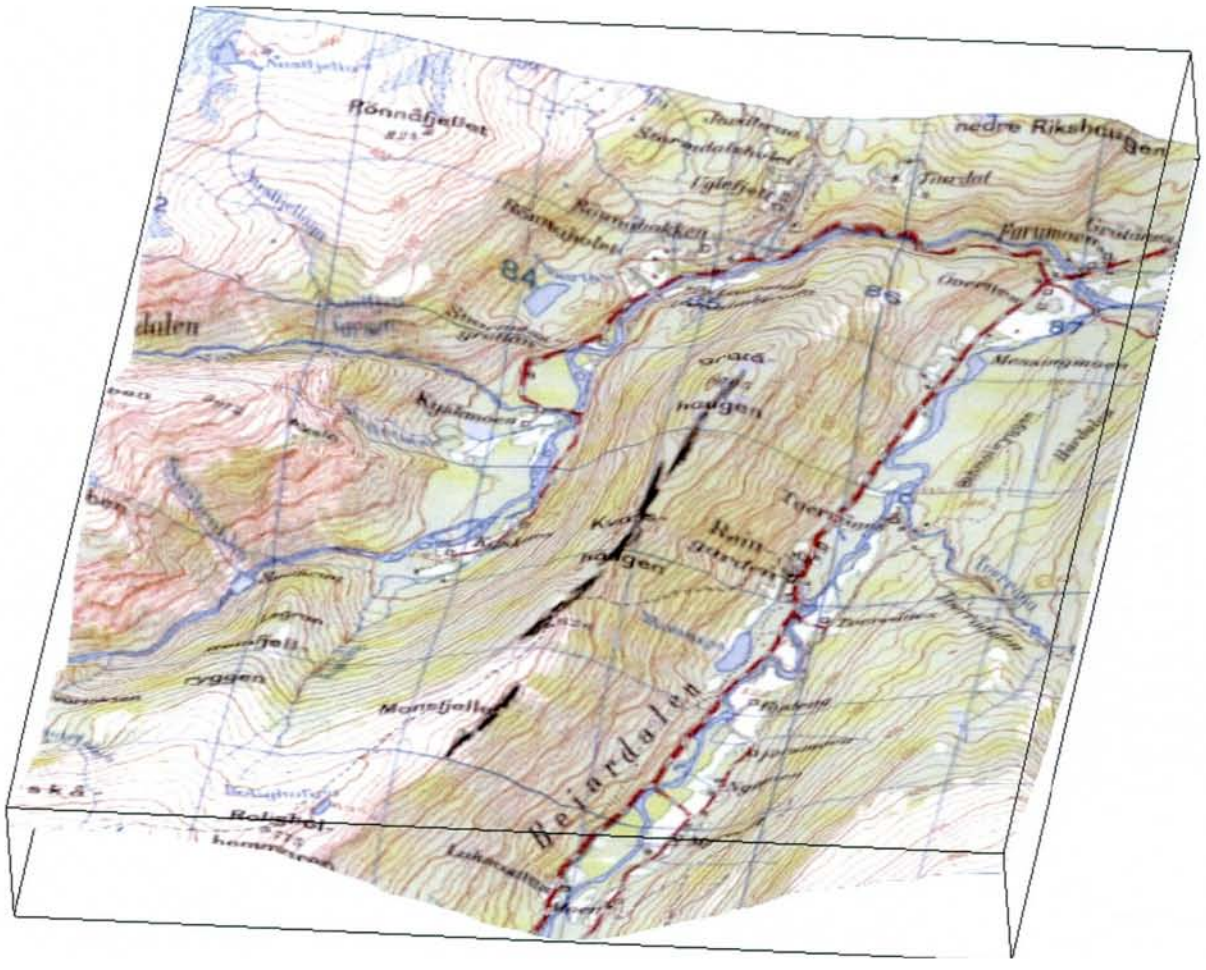

Fig. 2.1.16. Location of open clefts along the crest of Kvasshaugen.

When comparing these features to the sackung structures in the Alps, Rocky Mountains and New Zealand (Beck 1968, Zischinsky 1969, Varnes *et al.* 1989), it becomes evident that they belong to this group of structures which includes double-crested ridges, upslope-facing scarps,

linear troughs and downslope facing scarps. These characteristic geomorphic forms are produced by gravitational spreading (Fig. 2.1.18) of steep-sided ridges (Varnes *et al.* 1989). Several different interpretations of the origin of the structures have been proposed. Whether initiation of movements is by strong shaking, faulting, long-term creep, or a combination of factors has long been a matter of debate (Jibson 1996). Varnes *et al.* (1989) and McCalpin & Irvine (1995) argue that the movement originates from long-term, gravity-driven creep but the former does not exclude tectonism as a possible contribution. Other investigations in New Zealand, Slovakia and Russia conclude that earthquake shaking was the most likely trigger of movement (Jahn 1964, Beck 1968, Jibson 1996), partly because the sackung features occur in seismically active areas. The Kvasshaugen Mountain is also situated in a seismically active area so earthquake shaking could be a triggering mechanism.

(A) 

Fig. 2.1.17. *(See page 25)*

(B)

(C)

Fig. 2.1.17. *(See page 25)*

(D)

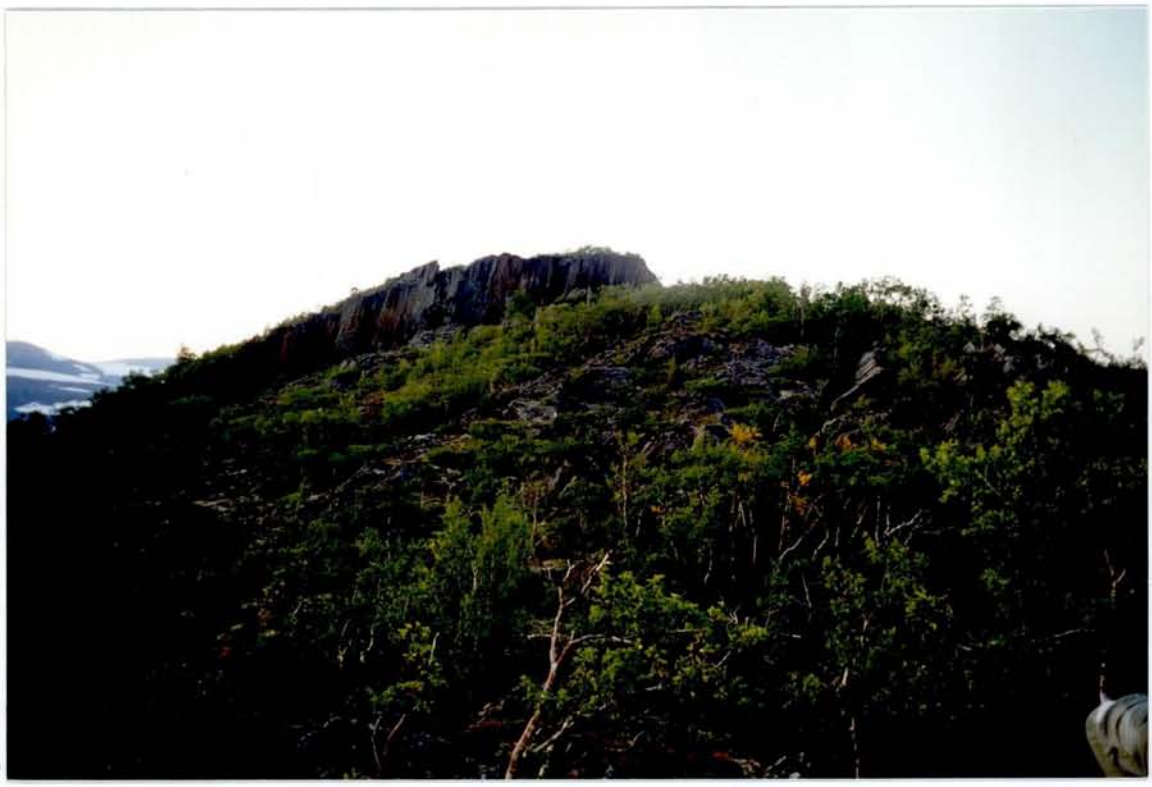

Fig. 2.1.17. Gravity-induced faults at the crest of Kvasshågen in Beiarn have been interpreted as neotectonic faults (Grønlie 1939, Muir Wood 1993). Graben structures are up to 10 metres deep and 20 metres wide. (A, previous pages) Overview photograph from Monsfjellet looking north with Beiardalen to the east and Gråttadalen to the west. The furthermost part of the ridge is called Gråttahaugen while the continuation to the south on the picture is termed Kvasshaugen. (B, previous page) and (C, previous page) Pictures (looking north) of open clefts on Kvasshaugen with Gråttahaugen in the background. Note the scarp edges of the escarpments. (D) Toppling of the steeply dipping mica schists to the east of the escarpment at Gråttahaugen.

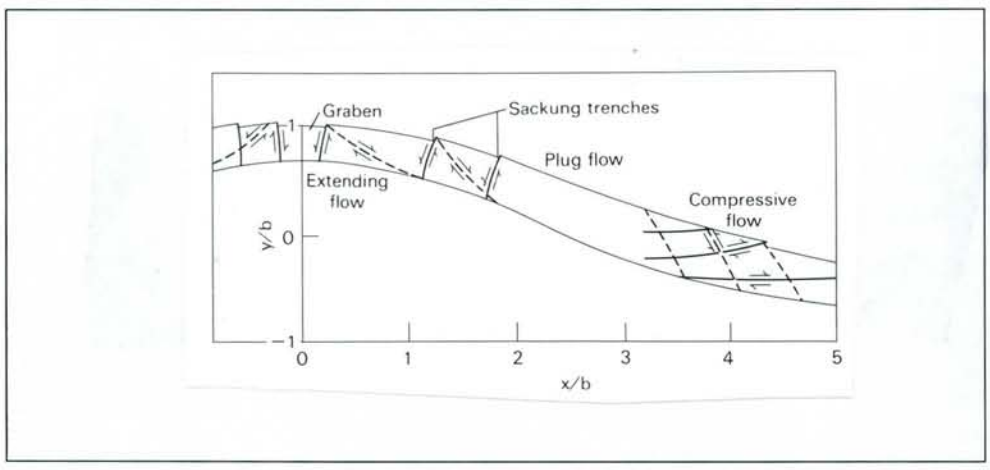

Fig. 2.1.18. Sketch illustrating formation of Sackung features (Savage & Varnes 1987). The potential flow regions and rupture surfaces on a symmetric gravitating ridge are indicated. Inactive rupture surfaces are dashed.

2.1.10 Austerdalsisen, Rana, Nordland

(Map Sheet 1928 II Svartisen, UTM 455.500,7376.500, Zone 32)

A set of north-south trending vertical dipping fractures and faults occur in the Rana area. In the Austerdalsisen area to the NW of Mo i Rana there seems to be a vertical offset of the bedrock surface across these structures. The observations were based on interpretation of areal photographs (Olesen *et al.* 1994). The area has been inspected in the field and Fig. 2.1.19 reveals, however, that these features are most likely of an erosional origin. The foliation of the mica schist is sub-parallel to the bedrock surface. The moving inland ice has most likely been plucking blocks from the bedrock along steeply the dipping N-S trending fractures. This process has produced spectacular escarpments in the bedrock surface.

(A)

(B)

Fig. 2.1.19. Erosional features south of Austerdalsisen, which has been classified as potential postglacial faults from the interpretation of aerial photographs (Olesen et al. 1994). The foliation of the mica schist is sub-parallel to the surface. The moving inland ice has been plucking blocks from the bedrock along steeply dipping N-S trending fractures. This process has produced very spectacular escarpments in the bedrock surface.

2.1.11 Båsmoen Fault, Ranafjorden, Nordland

(Map Sheets 1927 IV Sjona, 1927 I Mo I Rana and 2027 IV Storforshei)

The Båsmoen fault, BF, lies within the regional Ranafjorden lineament and is a potential postglacial fault (Fig. 2.1.20). It consists of SSE-dipping (40-70°) segments of reverse faults and can be traced for 50 km from the head of Sjona in the west, continuing eastwards along Ranafjorden and further into the valley of Dunderlandsdalen to the east (Fig. 5.3.1). The ENE-WSW trending fault zone is locally composed of 2-3 parallel escarpments within a 2 km wide belt. The strike of the individual segments varies between N60°E and N110°E. The heights of the escarpments are 1 - 80 metres. We do, however, believe that a significant portion of these escarpments was formed before the last deglaciation since ice striation is observed locally in the escarpments. Some 1-5 cm thick layers of fault gouge and steeply dipping fractures were identified in the fault escarpments. The appearance of the Båsmoen Fault is similar to that of the postglacial faults reported from the Lapland area in northern Fennoscandia (Lagerbäck 1992, Olesen *et al.* 1992b).

Study of the postglacial overburden in the Ranafjorden area shows that deformations like faulting and slumping occur more frequently here than in the surrounding area (Olsen, this report, section 5.4). The August 31, 1819 earthquake in the Rana area is the strongest historical earthquake known in Scandinavia with an estimated magnitude of 5.8-6.2. Intermediate seismic activity is currently observed in this region (Hicks *et al.,* this report, section 7.1). A zone of earthquakes to the south of the Båsmoen fault is consistent with an active SSE-dipping fault zone.

There is evidence for recent movements along the Båsmoen Fault in (1) A total of 0.89 m uplift of a bladder wrack mark from 1894 to 1990 in Hemnesberget (Bakkelid 1990); (2) Anomalously low uplift of the islands of Hugla and Tomma in the outer Ranafjorden area (0.0, 0.06 and 0.07 m from 1894 to 1990 compared to 0.25 - 0.30 m in the area to the north and to the south (Bakkelid 1990); (3) Associated with the 1819 magnitude 5.8-6.2 earthquake in the Ranafjorden area, an uplift of a shallow sea floor above sea level during an aftershock was reported in the bay Utskarpen (Heltzen, 1834). During the main earthquake a major landslide occurred at the same location. This earthquake is the largest North European near-shore earthquake recorded in historical time (Heltzen 1834, Muir Wood 1989b); (4) An uplift of approximately 1 metre of a farmhouse in the 1870's at Båsmoen (Grønlie 1923). The observation has been made relative to the two neighbouring mountains Snøfjellet and Høgtuva.

There are, consequently, indications of both postglacial and contemporary deformation along the Båsmoen fault (Olesen *et al.* 1994, 1995). It is, however, difficult to find conclusive evidence for both postglacial and present-day movements along specific faults. The Norwegian University of Technology and Sciences (NTNU) established a GPS network in 1994 designed to measure the active geological strain in the Ranafjorden area (Skogseth, this report). Three 15-20 km long profiles are located across outer, central and inner Ranafjorden. The network

was re-measured in 1997 and the calculation of deformations in the three-year period is in progress. The network is expected to give an accuracy of 5-10 mm in the horizontal plane and 15-20 mm in height. If there is any active deformation in the area, as indicated by previously published land uplift observations, this should be recorded by GPS in less than a decade.

Fig. 2.1.20. Oblique aerial photograph of the Båsmoen Fault (Olesen et al. 1994) on Båsmofjellet, looking east, approximately 4 km to the west of the centre of Mo i Rana in the background of the picture. The fault, shown by the arrows, is trending ENE-WSW and cuts the strike of the bedding (c. NE-SW) at an angle of approximately 20°. The southern block seems to be uplifted. The Båsmoen Mine is located along the continuation of the fault immediately behind Båsmofjellet, in the central part of the picture. The continuation of the BF across Loftfjellet to the east of Båsmoen can be seen in the background.

2.1.12 Conclusions

Field checking of neotectonic reports and claims has shown that the majority of these can be attributed to other effects than tectonic faulting. In northern Norway there are now documented postglacial crustal deformation in Rana, Beiarn, Kåfjord and Masi. The extensional faults in Beiarn are, however, gravity-induced and classified as a sackung feature, which has earlier been reported from mountainous areas in western US and Canada, Alps and New Zealand. It is a matter of debate if these features are caused by slow creep or triggered by earthquake shaking. The normal NW-SE trending fault in Kåfjord is interesting since it may represent a perpendicular extensional fault to the system of NE-SW trending reverse faults in northern Fennoscandia. No conclusive evidences for postglacial faulting in Rana have yet been found, but there are numerous indications of both present and postglacial deformation along this zone. Olsen (this report) has also found additional sites of liquefaction along the fault scarp. The Rana, Kåfjord and Masi areas will be studied in more detail in 1998. A NW-SE trending fault in the Sodankylä area in northern Finland will also be subject for ground penetrating radar (GPR) studies to check if it also represents a normal fault similar to the Nordmannvikdalen fault in Kåfjord.

The locations of neotectonic claims (Appendix 2.1) that have not been studied in 1997 will be subject for field checking in 1998. The Northern North Sea area does also look interesting for further neotectonic studies, since the results by Riis (this report, section 5.4) are very promising.

The present study of neotectonic claims in Norway suggest that they can be classified into five groups:

(1) Neotectonic faults (examples: Stouragurra in Masi, Nordmannvikdalen in Kåfjord and possible Båsmoen in Rana)

(2) Gravitationally induced faults (examples: Beiarn and Vassdalfjellet)

(3) Erosional along older zones of weakness (examples: Skipskjølen, Nordreisa, Skjomen and Austerdalsisen)

(4) Overburden draping of underlying bedrock features (example: Gæssagielas in Karasjok)

(5) Stress release features (examples: Lebesbye and Kobbelv).

No work was carried out at the two latter localities during the 1997 field season.

2.2 NEOTECTONIC PHENOMENA IN SOUTHERN NORWAY

By John Dehls and Alvar Braathen, NGU

2.2.1 Introduction

Seven sites of reported neotectonic activity were visited in southern Norway during the 1997. Two sites were inaccessible due to weather conditions and will be revisited in 1998. The remaining five sites (Fig. 2.2.1) are described below.

Fig. 2.2.1. Locations of five reports of neotectonic activity visited in southern Norway.

2.2.2 Ringja, Tysvær, Rogaland

(Map Sheet 1213 I Vindafjorden, UTM 322.000, 6588.000, Zone 32)

Long, deep fractures, sub-parallel to the fjord, are described by Anundsen and Gabrielsen (1990)(Fig. 2.2.2). They are given as evidence of Vindafjord being an active semi-graben.

Our investigation revealed two orthogonal sets of vertical fractures, all open at least 0.5 metres (Fig. 2.2.3). The Cambro-Silurian schists that are cut by the fractures are characterized by a very strong, shallow foliation, dipping 15º towards the fjord. We believe that these are gravity-induced faults, with movement of large blocks occurring along the reactivated foliation (Fig. 2.2.4).

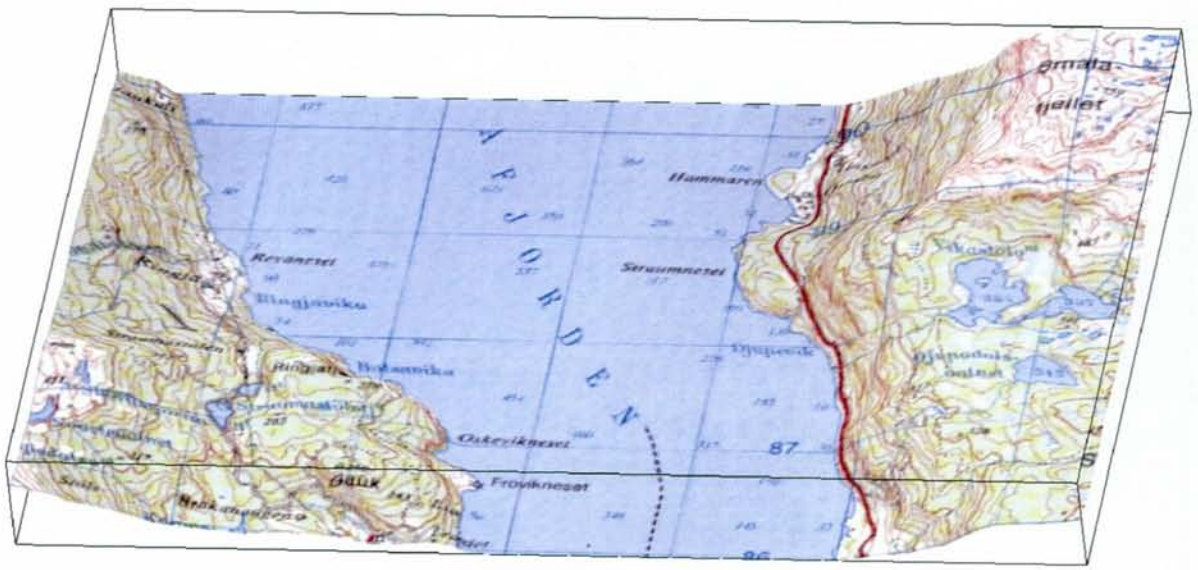

Fig. 2.2.2. Open clefts at Ringja are located on the west side of Vindafjorden, which Anundsen and Gabrielsen (1990) have suggested is an active semi-graben.

Fig. 2.2.3. Left: Open clefts are abundant throughout the area, and are often covered by vegetation. Two orthogonal sets can be found. Right: Offsets can often be measured across the fractures and are usually on the order of 1 metre.

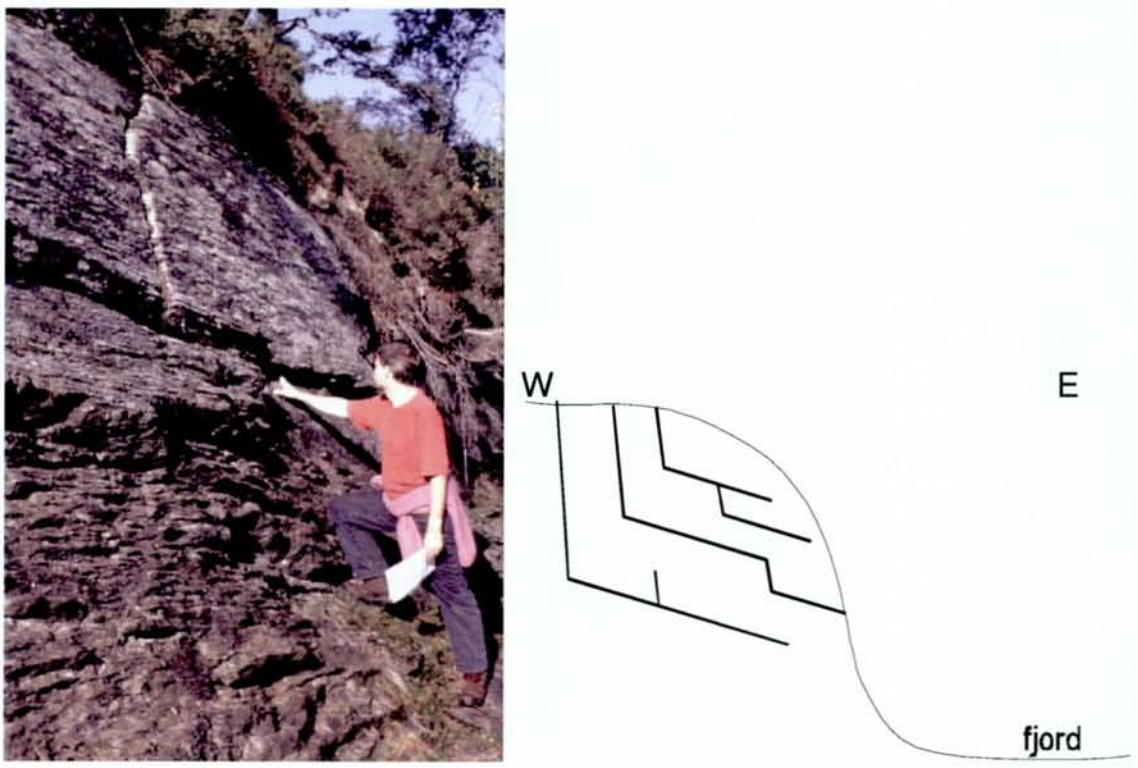

Fig. 2.2.4. Left: The Cambro-Silurian schists have a very strong, shallow foliation, dipping 15° towards the fjord. Right: Schematic diagram of the fracture system at Ringja. Large blocks appear to be sliding along the schistosity surface towards the fjord.

2.2.3 Lygre, Kvinnherad, Hordaland

(Map Sheet 1215 III Fusa, UTM 322.200, 6666.000, Zone 32)

Reusch (1888) describes a north-south trending scarp along Lygrefjord as possibly being a postglacial fault (Fig. 2.2.3).

The scarp is approximately 1.5-km long and 10-50 metres in height, and may be part of a longer (20 km?) lineament. There is no evidence of neotectonic movement along the scarp. There are abundant fractures parallel to the scarp, increasing in density towards the scarp. There are numerous large blocks fallen from the scarp. The feature is probably a 2nd order fracture zone, and can be classified as an erosional feature.

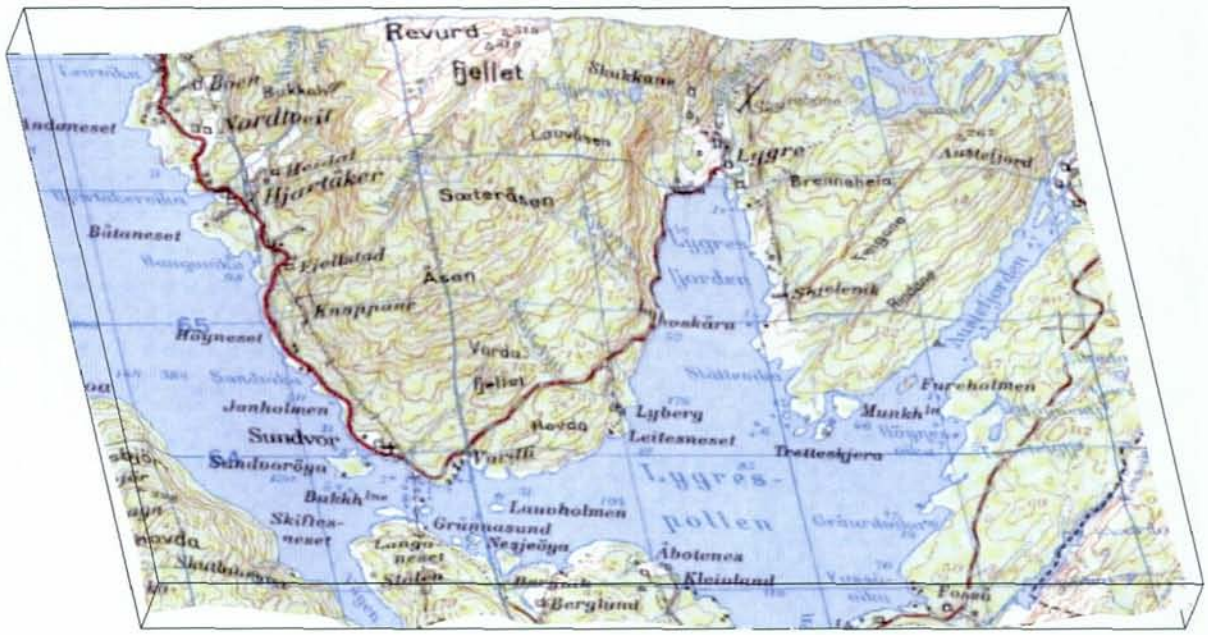

Fig. 2.2.5. Location of the scarp at Lygre.

2.2.4 Mosvatnet, Suldal, Rogaland

(Map Sheet 1314 II Suldalsvatnet, UTM 378.500, 6604.700, Zone 32)

In a photograph in the Stavanger Turistforening Årbok, Anundsen (1988b) shows a 1-5 metre wide, 5-10 metre deep fissure, with a stream flowing through it (Fig. 2.2.6). This fissure is described as a possible postglacial fault. It is suggested that one side of the fissure was raised with respect to the other.

Since 1988, a dam has been constructed upstream, and the bottom of the fissure is clearly visible in several places. It is now apparent that the fissure is the result of weathering out of a fine-grained amphibolitic dyke (Fig. 2.2.7). There is no evidence that one side of the fissure is consistently higher than the other. This feature can be classified as an erosional feature.

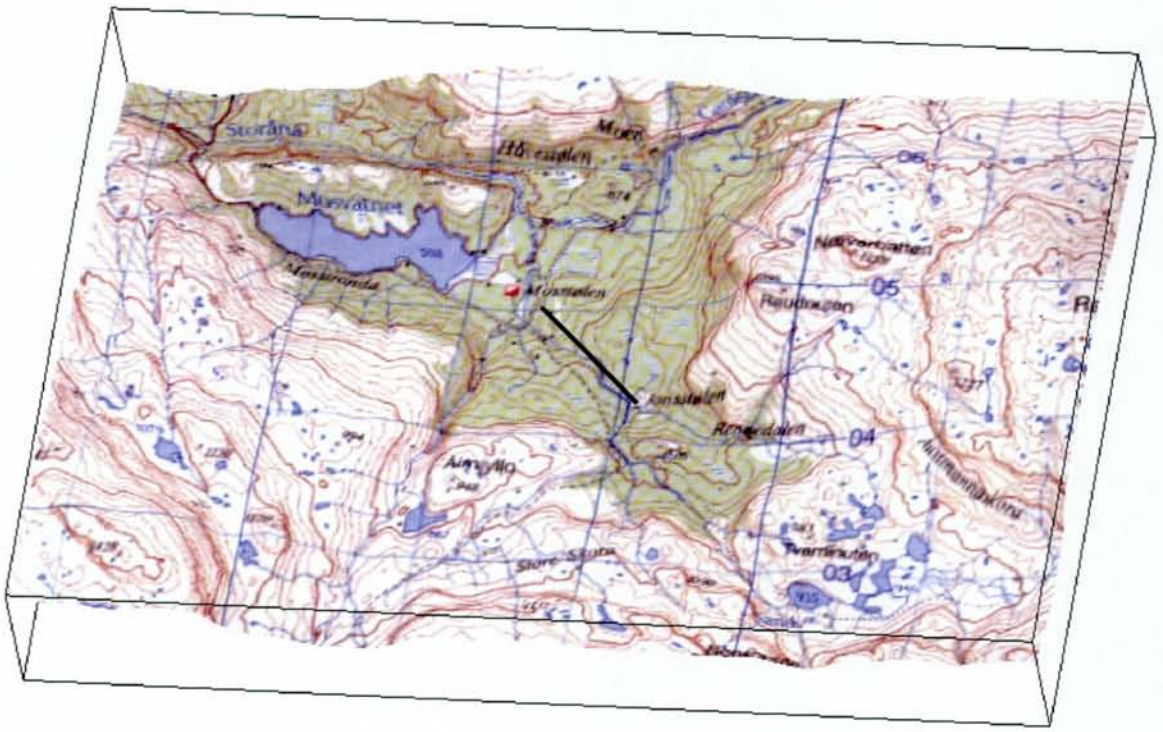

Fig. 2.2.6. Location of the fissure at Mosvatnet (black line).

Fig. 2.2.7. Since the original report in 1988, a dam has been constructed upstream, allowing the bottom of the fissure to be seen (left). A fine-grained amphibolitic dyke can be seen at the bottom (right).

2.2.5 Ragnhildnuten, Sandnes, Rogaland

(Map Sheet 1212 IV Stavanger, UTM 313.500, 6526.250, Zone 32)

Feyling-Hanssen (1966) reports a 'mountain' that has been split in two by a postglacial fault, with dip-slip and sinistral offsets of 30 metres each. This 'mountain' is Ragnhildnuten, a popular hiking spot SE of Sandnes (Fig. 2.2.8)

The hill has a 50-metre escarpment along the western side, due to erosion along a fracture zone. There is no evidence that any movement has taken place. The escarpment is part of a NNW-SSE lineament that can be seen in the next 2 ridges, about 3-4 km away.

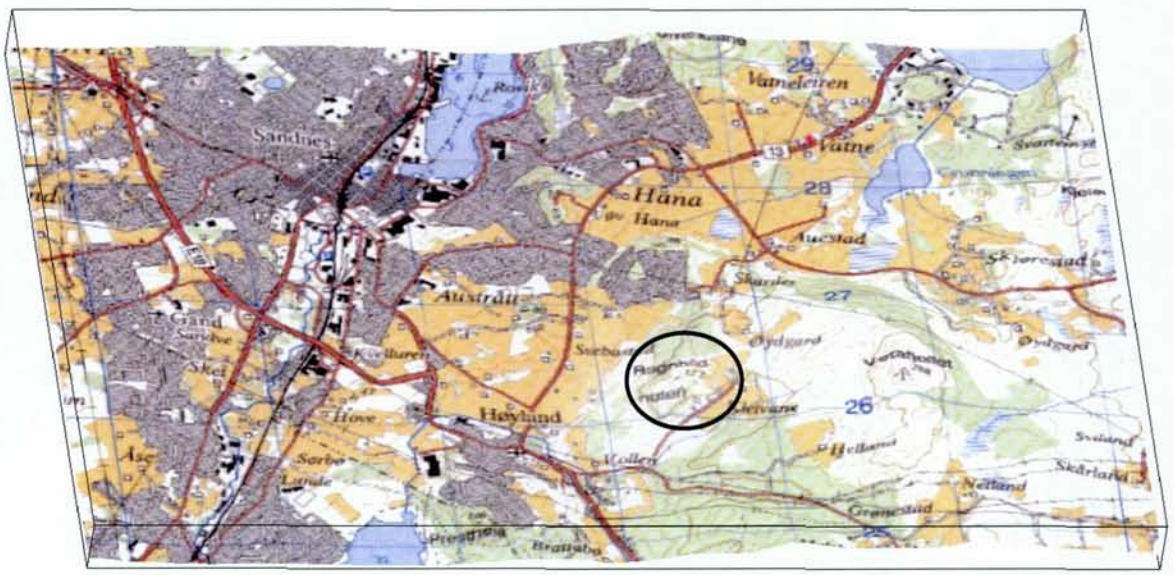

Fig. 2.2.8. Location of Ragnhildnuten, near Sandnes. 1.5X vertical exaggeration.

2.2.6 Ulvegrovene, Forsand, Rogaland

(Map Sheet 1312 IV Frafjord, UTM 348.000,6536.000, Zone 32)

Anundsen (1988a) describes a narrow zone of active subsidence parallel to the valley of Røssdalen (Fig. 2.2.9). The turf along the escarpments is described as being torn apart.

Ulvegrovene is a small hanging valley above Røssdalen. The structure is fairly straight and approximately 500 m long, running across the valley. It is up to 4 m wide and 1.5 m deep (Fig. 2.2.10). Neither side seems to be vertically offset. Both ends of the structure abut the valley walls, and there is no indication of a fault continuing in the bedrock. The structure is perpendicular to the slope of Ulvegrovene, which seems at odds with an explanation of gravity sliding. Ulvegrovene is a hanging valley, however, and the glacial sediments on the south side of the fissure are probably moving downwards, sliding towards Røssdalen, We conclude that the feature almost certainly a result of gravitational forces.

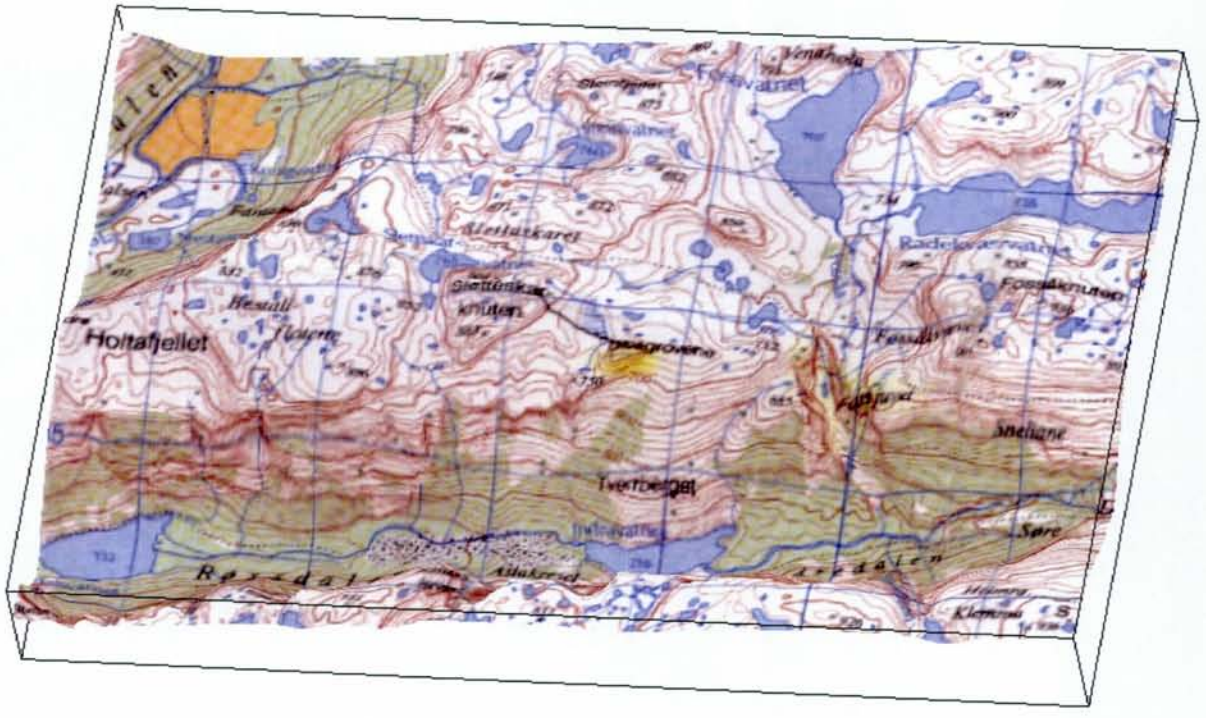

Fig. 2.2.9. Location of the 'fault' at Ulvegrovene.

Fig. 2.2.10. Left: The structure at Ulvegrovene is approximately 500 m long, perpendicular to the valley walls and parallel to the valley of Røssdalen. Right: The fissure is up to 4 m wide and 2 m deep.

2.2.7 Conclusions

Examination of reports of neotectonic features in southern Norway have ruled out tectonic faulting in five locations. Gravitationally induced faults were found at Ringja and Ulvegrovene. The features at the remaining locations can all be explained by erosion along zones of weakness. These zones of weakness include regional fracture zones (Lygre and Ragnhildnuten) and a mafic dyke (Mosvatnet).

Several reports remain unchecked and will be visited in 1998.

Appendix 2.1. Reported evidences of neotectonics in Norway. A tentative assessment of the additional claims is also included. Criteria for classification of postglacial faulting have been presented earlier by Fenton (1991, 1994) and Muir Wood (1993). The following grading system (Muir Wood 1993) has been utilised: (A) Almost certainly neotectonics, (B) Probably neotectonics, (C) Possibly neotectonics, (D) Probably not neotectonics and (E) Very unlikely to be neotectonics. Muir Wood (1993) reported 10 claims of neotectonics in Norway in a review of neotectonics in Fennoscandia. We have added 31 more accounts to the list.

NO.	LOCATION AND REFERENCE	OBSERVATION	COMMENT	GRADE
1	Bjørnøyrenna, Barents Sea margin Fiedler (1992), Muir Wood (1995)	Offset of shallow reflectors along the southern Barents Sea margin has been interpreted as effects from sea floor instability and postglacial strike-slip faulting by Fiedler (1992) and Muir Wood (1995), respectively.	There is no offset of the reflectors below the scarp at the sea floor. We do therefore favour the gravity-induced mechanism.	D
2	Malangsdjupet, offshore Malangen, Troms Fanavoll & Dahle (1990) and Fanavoll & Dehls (this report)	An offset of Quaternary reflectors can be observed on IKU shallow sparker line IKU-C84-306. A step at the sea floor marks the shallow termination of the fault. Multi-beam data reveal a bulge in the bathymetry corresponding to the fault on the seismic line. The extent of the fault as expressed on the sea bottom is limited to ~0.5 km.	The limited extent of the fault (0.5 km) reduces the grade of this claim. It is, however, a possibility that the short fault scarp is a secondary structure to strike-slip movements along the NW-SE trending Bothnian-Senja Fault Complex	C
3	Lebesby, Laksefjord, Finnmark Roberts (1991).	A road-cut drillhole penetrating cleaved phyllites has been observed to be offset in a reverse fault sense by 5.8 cm along a 40° dipping fault surface. This displacement occurred at some time during the period 1986 to 1989.	This feature is according to Fenton (1994) typical for stress release phenomena and is of surficial character.	E
4	Tanafjord, Finnmark (no exact location) by J.E. Rosberg according to Tanner (1907).	Postglacial fault (no published description).		

NO.	LOCATION AND REFERENCE	OBSERVATION	COMMENT	GRADE
5	Skipskjølen, Varanger peninsula, Finnmark Olesen et al. (1992b)	WNW-ESE trending 4 km long escarpment within the Trollfjord-Komagelv Fault Zone has been observed from aerial photographs. The northern block seems to be downfaulted.	The scarp has been sculptured and rounded by the moving inland ice. The height of the scarp is varying considerable along the scarp.	E
6	Gæssagielas, Karasjok, Finnmark Olsen (1989).	E-W trending 1.5 km long assumed Late Quaternary fault. The northern block is depressed.	The scarp is interpreted to represent a till draped escarpment in the underlying bedrock.	E
7	Masi-Iešjav'ri area, Finnmark Olesen (1988), Muir Wood (1989a), Olesen *et al.(1992a, 1992b, 1992c)*, Bungum & Lindholm (1997) Roberts *et al.* (1997).	The NE-SW trending postglacial Stuoragurra Fault extends for 80 km in the Masi-Iešjav'ri area in the Precambrian of Finnmarksvidda. The fault is manifested in the surface as a fault scarp up to 7 metres high and is situated within the regional Proterozoic Mierujavri-Sværholt Fault Zone. The Stuoragurra Fault is a southeasterly dipping reverse fault. A c. 1 m thick zone containing several thinner (a few cm wide) zones of fault gouge represents the actual fault surface. Report of 2.3 mm relative subsidence of the footwall block from 1987 to 1991. The January 21 earthquake (M 4.0) in the Masi area was most likely located along the Stuoragurra Fault at a depth of c. 10 km.	The age of the SF is constrained in that it crosscuts glaciofluvial deposits northeast of Iešjav'ri and an esker northeast of Masi. Thus it formed after the deglaciation which is estimated to 9,000 yrs. BP.	A

NO.	LOCATION AND REFERENCE	OBSERVATION	COMMENT	GRADE
8	Storslett, Nordreisa, Troms Wontka (1974)	An up to 150 m high scarp to the southeast of Storslett is interpreted in terms of a postglacial reactivation of the Caledonian Jyppyrä fault which has an apparent accumulated displacement of approximately 700 m.	The height of the scarp varies considerably and also appears to be rounded by glacial erosion. The scarp is most likely formed by plucking of the moving inland ice along a Caledonian fault.	D
9	Lyngen, Troms and Øksfjord-Alta, Finnmark Holmsen (1916)	Postglacial uplift has been estimated from levelling of shore-lines in northern Troms and western Finnmark. The uplift shows negative anomalies from the regional trend in the order of 5 metres in the Lyngen and Øksfjord areas. This effect has been attributed to gabbro massifs.	The interpretation is hampered by poor age control on the formation of the shorelines.	C
10	Nordmannvikdalen,Kåfjord, Troms Tolgensbakk & Sollid (1988), Sollid & Tolgensbakk (1988).	NW-SE trending postglacial faults in the Kåfjord area, North Troms. The eastern block is depressed compared to the western.	No detailed description of these faults exists, but they appear to show many similarities to the postglacial faults in the Lapland region (Kujansuu 1964, Lagerbäck 1979, Olesen 1988). The sense of movement and vergence are of particular interest. These faults may constitute the NW-SE strike-slip faults, which have been postulated by Talbot & Slunga (1989).	B

NO.	LOCATION AND REFERENCE	OBSERVATION	COMMENT	GRADE
11	Tjeldsundet, Troms Grønlie (1922), Vogt (1923)	Displacement of Holocene shorelines (an offset of c. 2.2 m down to the west). Lower shorelines appeared to be unbroken indicating that the inferred faulting occurred immediately after the deglaciation. Vogt (1923) pointed at the striking coincidence of the young faulting occurring in an old regional fault-zone along Tjeldsundet.	Multibeam echo sounding data and marine seismic profiling (Longva & Dehls, this report) do not reveal any fault scarps in the sediments or bedrock at the sea floor of Tjeldsundet. The different altitudes of the shorelines may therefore be due to variations of the currents through the sound during deposition of the shorelines.	D
12	Vassdalfjellet, 4 km east of the E6 in Kvanndalen north of Bjerkvik, Nordland Bargel *et al.* (1995)	A series of parallel east-west-oriented open fractures can be observed on the western part of the top of the ridge. Some of these are over 1 m wide and many are so deep that their depth is difficult to assess. There have been vertical movements along some of the fractures	The longest fault is 600 m. They are situated close to a steep 600 m high wall along the southernmost slope of Vassdalfjellet. We infer that the faults are gravity-induced.	E
13	Reinneset, Skjomen, Nordland Bargel *et al.* (1995)	A 1.5 to 10 m high escarpment on the headland between Skjomen and Sørskjomen is interpreted in terms of a reverse postglacial fault dipping to the north. The fault continues to the west on the other side of Skjomenfjorden. Foliated granite can be observed in a few dm wide zone at the foot of the escarpment. The high, sharp-edged fault wall facing the direction of the moving inland ice points to a young age.	An inspection of the locality shows that the top of the escarpment is rounded and that the height of the escarpment varies considerable over short distances along the fault. These observations point towards a formation due to erosion along an older zone of weakness.	D
14	Tysfjord-Kobbelv area, Nordland Myrvang (1993)	Large-scale rock bursting and even buckling at the surface due to high horizontal stress in the order 30-40 MPa.	Stress release phenomena of superficial character	E

NO.	LOCATION AND REFERENCE	OBSERVATION	COMMENT	GRADE
15	Steigen, Nordland Atakan *et al.* (1994)	The earthquake swarm occurred in 1992 and contained 200 shocks but no main shock was recorded. The magnitude of the shocks was up to 3.6.	Earthquake swarms usually occur in volcanically or tectonically active areas such as plate boundaries but have also been reported from passive continental margins surrounding the northern part of the Atlantic Ocean and the Arctic Sea.	A
16	NW of the island of Røst, Nordland Rokoengen & Sættem (1983)	The sea floor relief shows several abrupt changes in level and slope that were interpreted in terms of postglacial faults. The main escarpment is located 1.2 km beyond the steep boundary between the crystalline basement and deformed sedimentary sequences.	An alternative model also suggested by Rokoengen & Sættem (1983) is that the sea floor jumps are formed by wave cut cliffs and tidal current erosion at a sea level about 125 m lower than the present one.	E
17	Continental slope, Røst Basin, Nordland Mokhtari (1991) and Mokhtari & Pegrum (1992)	Evidence of recent downslope gliding along the continental slope.	This fault is most likely not caused by a deep-seated tectonic process but rather by gravity gliding.	D
18	Fulla Ridge, Vøring Basin Muir Wood (1995)	Muir Wood (1995) interpreted seismic data by Granberg (1992) in terms of a mid-late Quaternary reverse fault, activating Miocene faults along the Fulla Ridge.	The Pliocene reflectons beneath the potential offset Quaternary refletor do not seem to be offset, contraticting the hypothesis of a young faulting	D
19	Meløy, Nordland Bungum *et al.* (1979)	The spectacular earthquake swarm on Meløy was located within the seismicity zone of the Nordland coast. The swarm occurred in 1977/1978 and contained 10,000 shocks, but no main shock was recorded. The magnitude of the shocks was up to 3.2.	These swarms may be interpreted to be related to the formation of new zones of weakness in relatively competent bedrock (R. Muir Wood, pers. comm. 1993).	A

NO.	LOCATION AND REFERENCE	OBSERVATION	COMMENT	GRADE
20	Kvasshaugen mountain between the valleys of Beiardalen and Gråtådalen, Nordland Grønlie (1939), Johnsen (1981)	NNE-SSW trending clefts occur along an approximately 5 km long NNE-SSW trending zone. These clefts are up to 4 m wide and 10 m deep and the eastern sides are down-faulted.	These faults are suggested to be of postglacial age. They may relate to a WNW-ESE oriented extension. The faults are classified as some of the most reliable claims of neotectonic surface fault rupture in Scandinavia (Muir Wood 1993) but are probably of superficial character.	D
21	Austerdalsisen, Rana, Nordland Olesen *et al.* (1994)	Interpretation of aerial photographs unveiled a set of north-south trending, vertical dipping fractures and faults in the Austerdalsisen area to the NW of Mo i Rana. There seems to be a vertical offset of the bedrock surface across these structures. The foliation of the mica schist is sub-parallel to the bedrock surface.	Field inspected revealed that the features are most likely of an erosional origin. The moving inland ice has most likely been plucking blocks from the bedrock along steeply dipping N-S trending fractures.	E

NO.	LOCATION AND REFERENCE	OBSERVATION	COMMENT	GRADE
22	Ranafjord area Helzen (1834), Grønlie (1923), Muir Wood (1989b), Bakkelid (1990), Olesen et al. (1994, 1995) Hicks *et al.* (this report). The Båsmoen Fault can be traced for 50 km from the head of Sjonafjorden along Ranafjorden and further east into the valley of Dunderlandsdale n. Olesen et al. (1995)	The Båsmoen Fault consists of SSE-dipping (40-70°) reverse-fault segments within a 2-km wide zone. The maximum accumulated displacement is in the order of 5-10 m. A study of the postglacial overburden in the area has shown that deformation apparently occur more frequently than in the surrounding areas. There is evidence for recent movements along the Båsmoen Fault at the locations Utskarpen, Straumbotn and Båsmoen on the northern shore of Ranafjorden close to the fault. Hemnesberget is situated in the hanging wall block 7 km to the south of the escarpment. An extension of the BF may continue in the sound immediately to the north or to the south of the Hugla and Tomma islands. All these locations show anomalous land uplift. A new seismic mini-array have registered numberous earthquakes which can be attributed to the Båsmoen fault.	The appearance of the fault is similar to that of the postglacial faults reported from the Lapland area of northern Fennoscandia. It has not yet been found any conclusive evidences for postglacial movements along specific fault scarps. In order to reach a final conclusion a Global Positioning System (GPS) network designed to measure the active geological strain in the area has been established. We do believe that significant portions of the fault movement, as indicated by the escarpments, were formed before the last deglaciation since ice striae are observed locally along the escarpments.	B
23	Southern end of the Klakk Fault Complex, about 100 km to the west of Hitra island Muir Wood & Forsberg (1988)	On a NW-SE regional seismic reflection profile a faulted offset of Tertiary reflectors appears to pass up through the youngest base Quaternary (?) reflector. The fault involves downward displacement to the west and the reflector offset is several tens of metres. The underlying fault appears to be near vertical in dip and probably trends approximately N-S.	The displacement does not affect the sea-bed, and the quality of the regional seismic line on which the offset is observed makes it impossible to observe any detailed structure in the uppermost part of the sedimentary section (Muir Wood 1993).	C

NO.	LOCATION AND REFERENCE	OBSERVATION	COMMENT	GRADE
24	Breisunddjupet, Møre og Romsdal Holtedahl (1959)	The elevation of the strand flat to the north of the NW-SE trending Breisunddjupet seems to be lower than the strand flat to the south.	Later, more detailed studies by H. Holtedahl (pers. comm. 1995) have questioned this observation.	D
25	Northern Østerdalen, Hedmark Holmsen (1916)	Postglacial uplift has been estimated from levelling of shorelines left by ice-dammed lakes. Gabbro massifs (Tron and Klettene) have been subject to separate upheaval on the order of 3 metres.		C
26	Gnedden, Kvam, and Rudihø, Heidal, Oppland Werenskiold (1931)	Up to one metre wide open NNE trending fractures. One side seems to be down-faulted. The turf is hanging down into the fracture at Rudihø.	The fractures on the Rudihø mountain are most likely gravity-induced.	D
27	Øygarden Fault Rokoengen & Rønningsland (1983), Muir Wood & Forsberg (1988)	The northern half of the N-S trending Øygarden Fault (between 61° and 61°45'N) runs parallel with the coast of western Norway and marks a significant change in the depth of the bedrock surface beneath the thick Quaternary sedimentary cover. The major scarp that has developed along the fault has some of the appearance of a fault-scarp (with vertical offset up to 150m), and although offsets have not been observed in the overlying sedimentary section itself, sediments onlap the scarp, with some suggestion of dips steeping towards the fault (Muir Wood 1993).	The fault now bounds crystalline basement in the east from relatively soft Cretaceous sediments in the west (Muir Wood 1993). The key to the origin of this scarp remains the age of the basal sequence above the unconformity. If, as claimed, this comprises marine sands of probable Pliocene age then a faulted origin of the scarp is preferred. However, if the basal sediments formed immediately following intense glacial scouring then an erosional origin is indicated.	D

NO.	LOCATION AND REFERENCE	OBSERVATION	COMMENT	GRADE
28	Grytehorgi and Vøringfossen, Hordaland Reusch (1901)	NNE-SSW trending fault on Grytehorgi .The down-faulted block is to the west. Ice-striation seems to be offset by 1 metre (normal fault). Other N-S sharp escarpments in the Vøringsfossen area are also suggested to be effects of postglacial faulting.	Løset (1981) questioned the postglacial age of the Grytehorgi fault since it is filled with till and erratic blocks. Neotectonic movements along the N-S trending faults are, however, possible.	D
29	Hjeltefjorden, 30 km northwest of Bergen Unpublished commercial report from NGI/NORSAR	At the northern end of Hjeltefjorden a boomer seismic survey was undertaken in the mid-80's for a possible tunnel crossing. Several E-W lines between Seløy and Uttoska, appeared to show a consistent offset of the superficial sediments in the floor of the fjord, along a NNW-SSE trending dislocation, involving down to the west displacement of 5-10m (Muir Wood 1993).	Statoil has collected multi-beam echo sounding from the area for the planning of a pipeline across the sound. These data will be subject for closer investigations in the NEONOR project.	C
30	Lygre, northern side of the mouth of Hardangerfjord Reusch (1888)	Potential postglacial fault occurring as a N-S trending escarpment. The western block seems to be down-faulted. The length of the escarpment is not reported, but an accompanying drawing indicates a length of approximately 1 km.	There is no evidence for displacement. The scarp is an erosional feature along a fracture zone, which may be part of a regional lineament.	E
31	Yrkje Anundsen *et al.* (submitted)	Levelling in combination with repeated triangulations between concrete pillars, showed that both horizontal and vertical displacements in the order of 0.1-0.9 mm/year take place along the Yrkjefjord fault zone. Annual measurements during a period of 10 years indicate that movements change, i.e. are reversed in some periods.		D

NO.	LOCATION AND REFERENCE	OBSERVATION	COMMENT	GRADE
32	Vindafjorden - Ølen area, Rogaland, Anundsen (1989)	A 7 km wide and c. 30 km long N-S trending active half-graben has been reported. Along the eastern slope of Vindafjord, and on the mountain plateau to the east of the fjord, a series of long subparallel crevasses is observed. A present subsidence is supported by precision levelling (20 mm movement over 19 years)	The subparalles crevasses, along with an orthogonal set, can be – explained by gravitational sliding along a very strong foliation dipping towards the fjord. The step-like nature of the fjord walls appears to be an erosional feature.	D
33	Etne, Rogaland Karpuz *et al.* (1991)	The 4.25 (±0.25) magnitude Etne earthquake (29 Jan. 1989) occurred as a result of predominately normal faulting on a NW-SE trending fault. Secondary effects of the earthquake were observed as surface fissures in Quaternary sediments. The basement and walls of a farmhouse were damaged as a result of this slope instability.	The structure is most likely caused by ground shaking and not a deep-seated tectonic fault.	D
34	Ulvegrovene, north of Røssdalen, Rogaland Anundsen (1988a)	Active subsidence of a narrow zone. The turf along the escarpments seems to be torn apart. The structure is parallel to the valley of Røssdalen.	Most likely a gravity induced structure.	E
35	Mosvatnet Anundsen (1988b)	The sides of open fractures in the bedrock are located at different levels indicating vertical movements along the fractures.	Erosion of a fine-grained amphibolitic dyke.	E
36	Karmøy, Rogaland and Fjøsanger, Hordaland Mangerud *et al.* (1981) and Sejrup (1987)	A considerable long-term neotectonic uplift, 10-40 m, of western Norway during the last 125,000 years is based on investigations of marine sediments from interglacials.		C

NO.	LOCATION AND REFERENCE	OBSERVATION	COMMENT	GRADE
37	Karmsundet, 20 km northwest of Stavanger, Rogaland Bøe *et al.* (1992)	The Karmsundet Basin is a small half-graben bounded to the east by the major Kvitsøy Fault and filled with sediments of assumed Jurassic age. Overlying Quaternary sediments show plentiful evidence of instability including slump scars, rotated sedimentary units and superficial fault structures.	The majority of these superficial features do not correspond with underlying faults and hence cannot be considered as direct evidence of outcropping fault-rupture (Muir Wood 1993). Deformation accompanying glacial readvance cannot be discounted.	D
38	Gannsfjord lineament, Jæren, Rogaland Abandoned clay pit at about 10-30 m above sea level at Gann, on the western side of the Sandnes Harbour. Opstad and Høgemork at about 200 above sea level to the east of the Gannsfjord lineament. Feyling-Hanssen (1966), Fuggeli & Riis (1992)	Subsurface boreholes revealed a NE-SW trending boundary, steeper than about 60 degrees, between mostly marine clay to the west and sand to the east. The clay is overlain by Weichselian till. Glaciomarine clays of Weichselian age to the east of the Gannsfjord fault appear to uplifted by recent tectonic movements.	Work by E. Larsen (pers. comm. 1996) indicates that the N-S trending escarpment separating 'Høg-Jæren' from 'Låg-Jæren' is formed by the northwards moving Skagerrak glacier.	D
39	Egersund-Flekkefjord area, Rogaland Anundsen (1989), Anundsen *et al.* (submitted)	The Egersund Anorthosite-Gabbro Province shows a subsidence of 2-2.5 mm/yr. The zone of maximum subsidence coincides with a zone of maximum gravity anomaly.		C

NO.	LOCATION AND REFERENCE	OBSERVATION	COMMENT	GRADE
40	Finse - Geilo area, Hordaland - Buskerud and Haukeligrend, Telemark Anundsen *et al.* (submitted)	Anomalous uplift in the Finse - Geilo area and anomalous subsidence in the Haukeli area from repeated levelling.		C
41	Ødegården, Bamle, Telemark Brøgger (1884)	Approximately 0.2 metre sinistral offset of a 0.5 by 0.6 m pothole along a WNW-ESE trending fault. The pothole is estimated to be of Quaternary age.	Probably blasted away, not possible to find today (Løset 1981, Selnes 1983).	D

3 OFFSHORE FAULTING (TASK 2)

3.1 INTERPRETATION OF SEISMIC DATA FROM THE KARMSUNDET BASIN

By Leif Rise and Reidulv Bøe, NGU

3.1.1 Introduction

The Karmsundet Basin is a recently discovered sedimentary basin (approximately 28 x 5 km) located on the innermost continental shelf of SW Norway, southeast of the island of Karmøy (Bøe *et al.* 1992). The sedimentary rocks are down-thrown along the N-S trending Kvitsøy Fault (Fig.3.1.1), and are preserved in a half-graben with reflectors dipping towards the east-southeast. Precambrian and Cambro-Silurian metamorphic rocks are located to the east of the Kvitsøy fault, and the sedimentary rocks rest unconformably upon Caledonian igneous rocks at the western margin of the half-graben. The age of the sedimentary rocks is unknown, but a Triassic-Jurassic age is suggested based on comparison with sedimentary basins along the coast of southern Norway showing similar geometry.

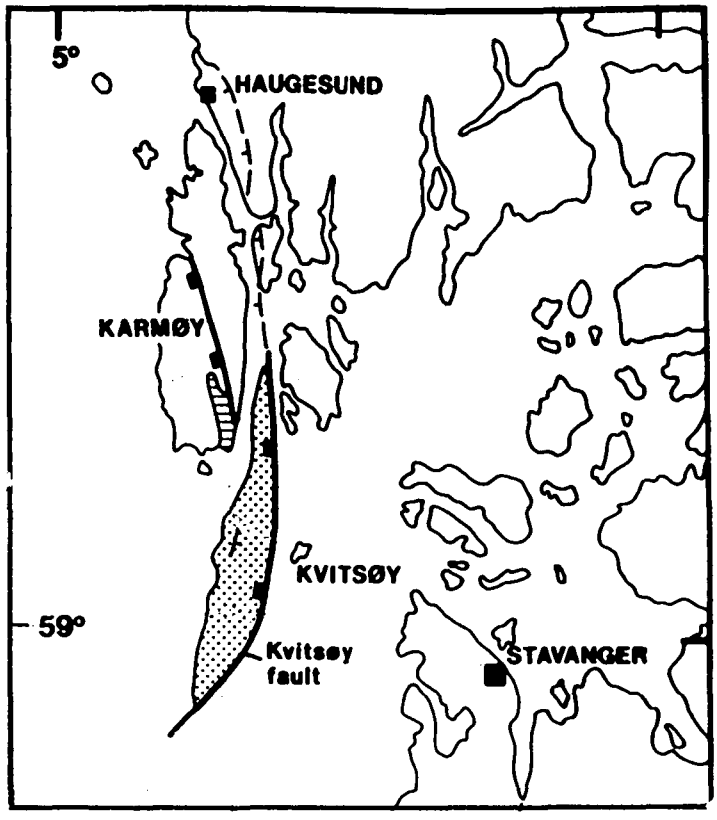

Fig. 3.1.1. Map showing the location of the sedimentary rocks in the Karmsundet Basin and the Kvitsøy Fault.

During the Quaternary period glaciers eroded more strongly in the sedimentary rocks than in the surrounding metamorphic and igneous rocks, and in particular close to the Kvitsøy Fault. This has formed a Quaternary basin, which after the last deglaciation approximately 13.000 years ago, has been filled with a thick succession of glaciomarine and post-glacial clays. To the west of Kvitsøy the clays reach a thickness of almost 300 ms TWT (250 m). During the

interpretation of the sedimentary rocks, Bøe et al. (1992) also observed faults, slide scars and slump deposits in the Quaternary clays. The authors suggested that these features could be related to reactivation of the Kvitsøy Fault and earthquake activity.

3.1.2 Seismic database

The interpretation in Karmsundet and in the offshore area south of Karmøy is based upon shallow seismic lines collected by NGU in 1989 and 1990 (Bøe 1990). A 20 cubic inch air gun was used as an acoustic source, with single channel analogue recording of the received signals. A total of 350 km was interpreted, with a distance between the individual lines in the order of 1-2 km (Fig.3.1.2). The quality of the seismic lines is good, but the detailed interpretations are limited by the pulse length, which is 10-12 ms.

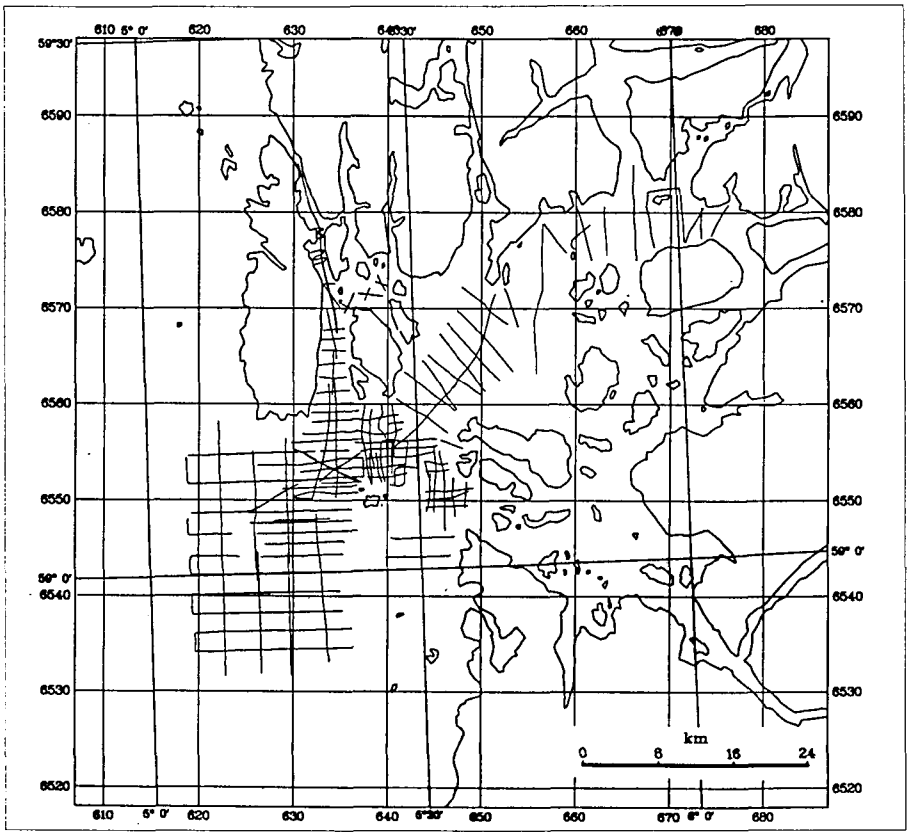

Fig. 3.1.2. NGU's shallow seismic data grid used during the interpretation.

3.1.3 Bathymetry

In Karmsundet (east of Karmøy) and the southerly extension of Karmsundet there is a trench, with a maximum depth of ca. 380 m west of the threshold to Boknafjorden. This trench can be traced along the eastern margin of Karmsundet, past Kvitsøy, and as far south as approximately 59°N. The trench is situated almost directly above the position of the Kvitsøy fault (Bøe *et al.* 1992). From the trench there is a gradual shallowing in westerly direction, while towards the east of the Kvitsøy Fault, the water depth decreases abruptly.

3.1.4 Quaternary sediments

Based on the available data the outcropping strata have been divided into three groups; soft clay, till and exposed bedrock (Fig. 3.1.3). The Kvitsøy fault is located beneath the eastern-most part of the area with soft clay, very close to where till or bedrock are mapped. The soft clay is dominantly acoustically layered and consists predominantly of normally consolidated glaciomarine clays similar to those found in the Norwegian Trench (cf. Troll Field).

The clay thickness varies within the area. In the northern part of the mapped area it is thickest in the trench close to the Kvitsøy Fault (150 m)(Fig. 3.1.4). At the outlet of Boknafjorden and further south the thickness of the clay is largest west of the trench (100-250 m), and is often less than 100 m in the trench itself (Figs. 3.1.5 and .6).

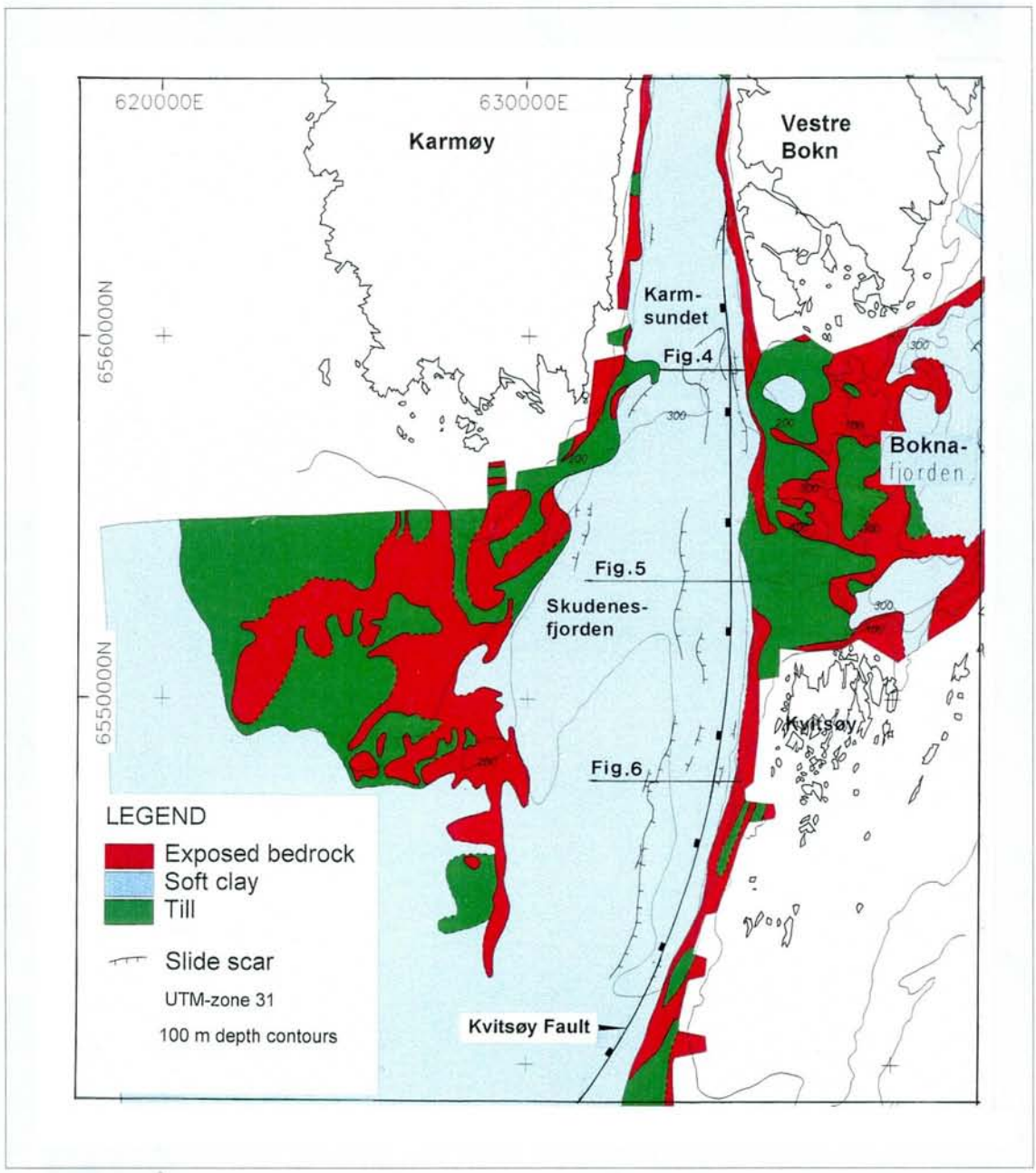

Fig. 3.1.3. Outcropping crystalline bedrock and sediments, and the location of the Kvitsøy Fault in the easternmost part of the soft clay basin. The location of the seismic sections (Figs. 3.1.4, .5 & .6) across the main slide scars are shown.

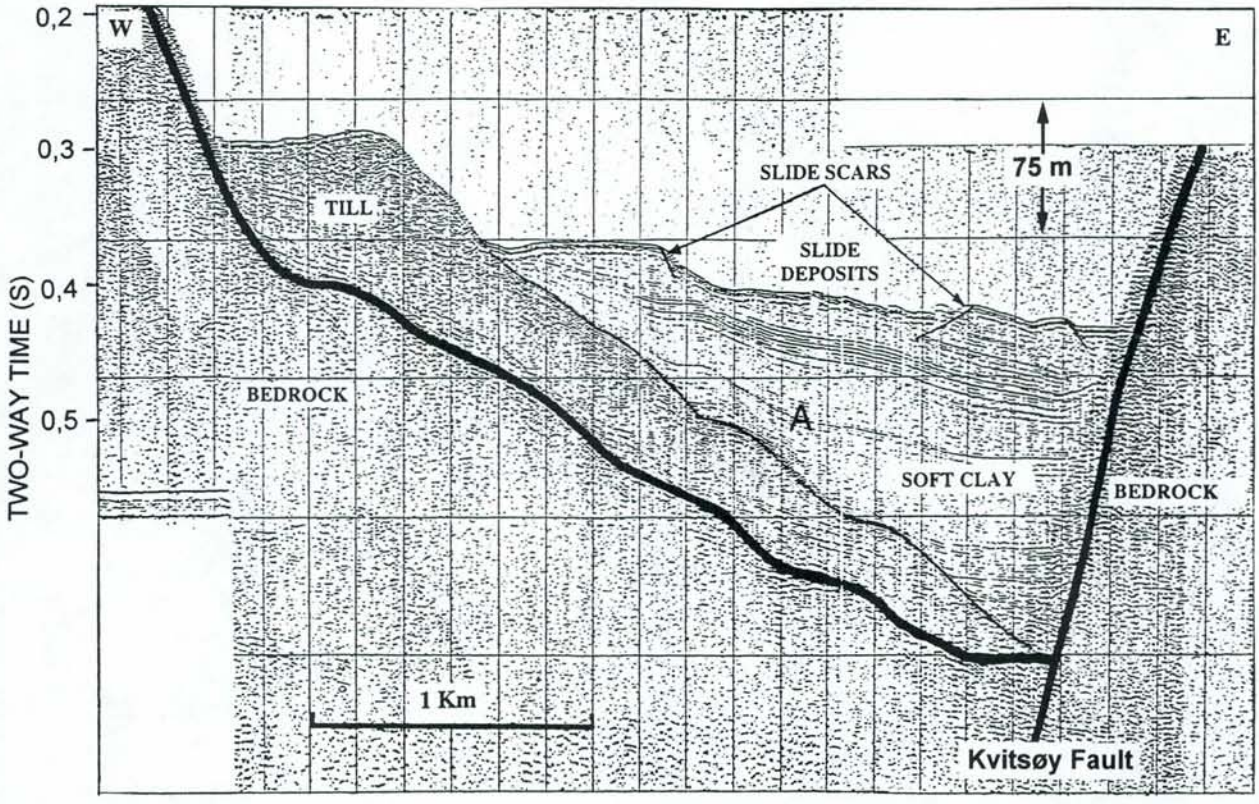

Fig. 3.1.4. Seismic profile P02 across the northernmost slide southwest of Vestre Bokn. Reconstruction of the seafloor before the sliding indicates a general easterly slope gradient of approximately 1:30 (2 degrees).

The change in deposition of sediments in the trench from north to south seems to a large degree to have been caused by an abrupt change in the oceanographic current pattern at a certain time during the glaciomarine deposition (at reflector A in Figs. 3.1.4, .5 & .6). The resulting depositional pattern will be further commented below, as it seems to be important for evaluation of the sliding activity after time "A."

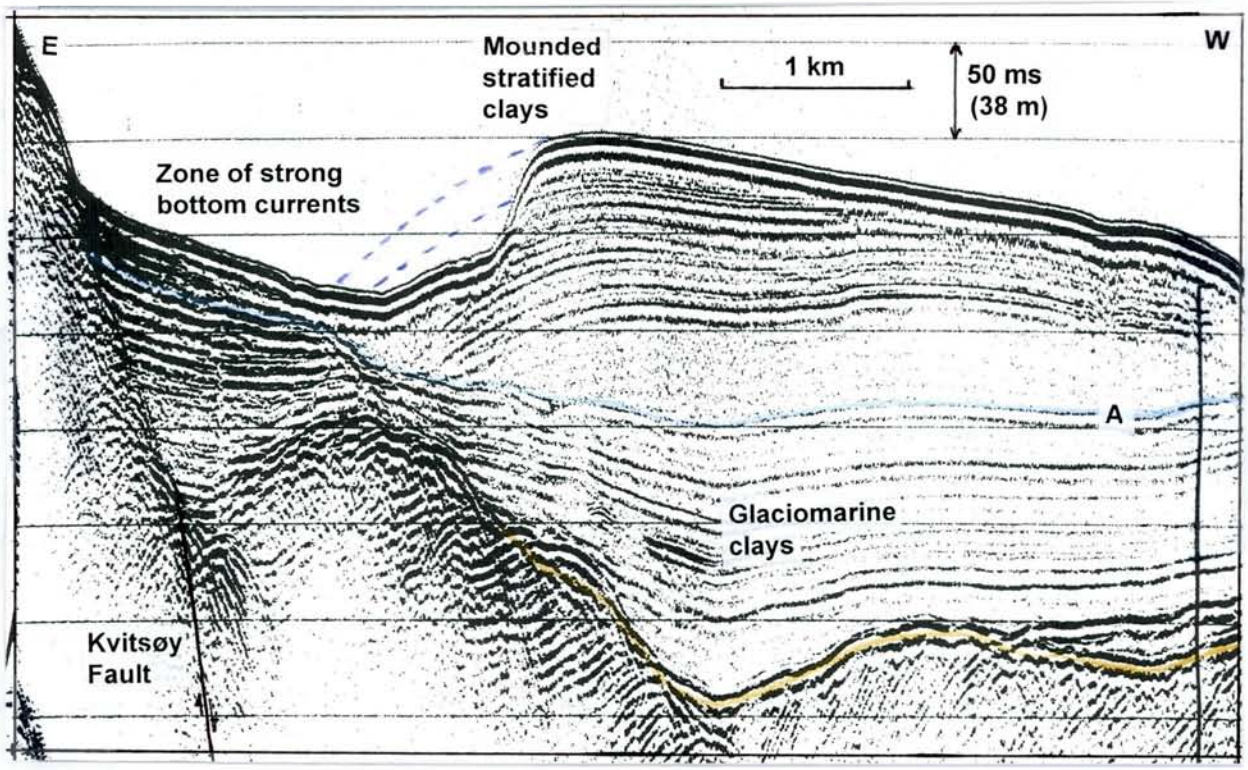

Fig. 3.1.5. Seismic profile P34 across the slide northwest of Kvitsøy. Note the downfaulted sedimentary rock succession along the Kvitsøy Fault. Note also the abrupt change in the oceanographic current pattern occurring at reflector A, which has resulted in mounded stratified clays being deposited above this level.

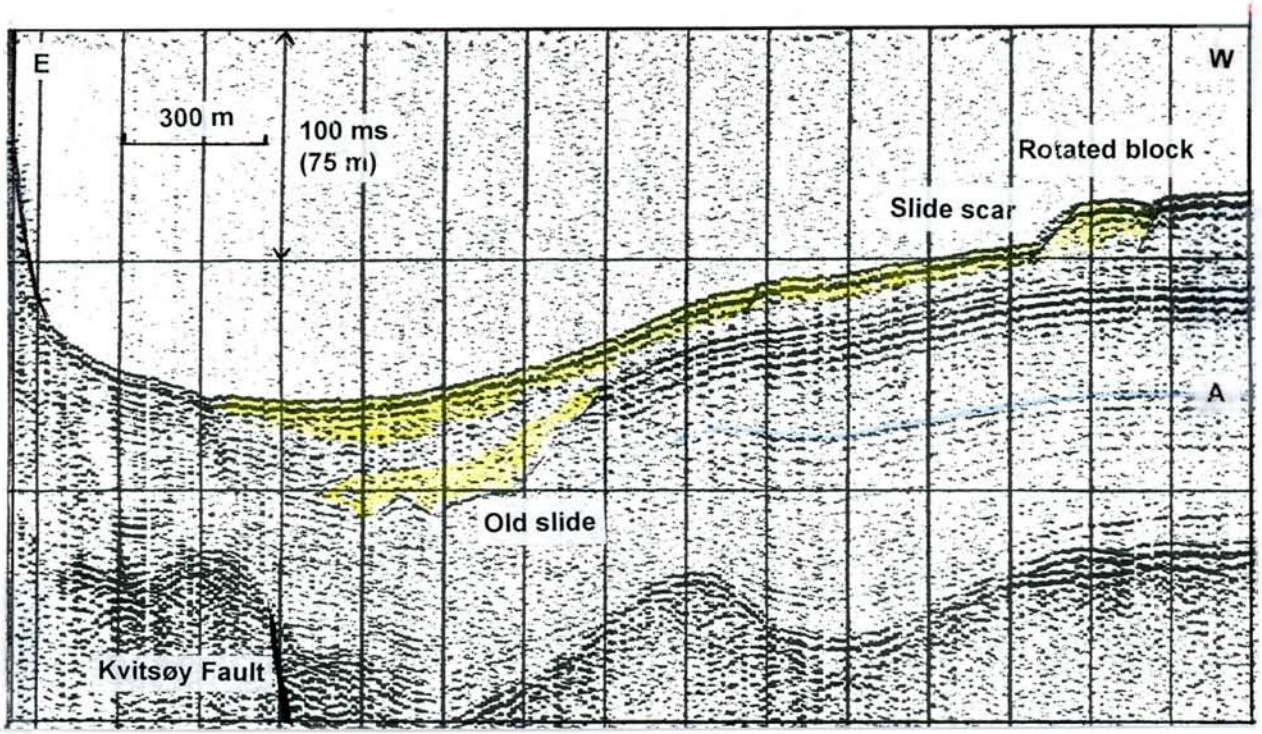

Fig. 3.1.6. Seismic profile P08 across the slide southwest of Kvitsøy. Note the partly rotated, approximately 200 m wide sediment block, and the interpretation of an old slide.

3.1.5 Assessment of sediment instability

The occurrence of slide scars has been thoroughly mapped in Karmsundet and in the southern extension of Karmsundet west of Kvitsøy (Skudenesfjorden). Three large, N-S trending slide scars and several small ones occur from the latitude of the southwestern tip of Vestre Bokn and southwards (Fig. 3.1.3). Buried old slides also exist. In general the sliding occurs on the western slope of the trench, and shows a direction of mass movement/sliding towards the east and southeast. As the bathymetry and the distribution of sediments vary, the three main slide scars will be commented separately.

Slide scar southwest of Vestre Bokn

The northernmost of the large slide scars is a cirque-shaped feature (Fig. 3.1.3), almost 20 m deep, where the slide deposits can be recognised east and southeast of the slide scar due to the seismic signature and a rugged seafloor topography (Fig. 3.1.4). In this area there is no apparent change in the sedimentary environment at reflector A, indicating a stable current regime. On the seismic records we see no indication of current erosion of the seafloor. The eastern boundary of the slide scar is located only 200-300 m from where the Kvitsøy Fault is mapped. Reconstruction of the seafloor along the E-W seismic line before the sliding indicates a general easterly slope gradient of approximately 1:30 (2 degrees). The other seismic lines crossing this slide scar indicate that the original slope in N-S direction is less than 2 degrees. As a rule of thumb in soil engineering, slopes in normally consolidated glaciomarine sediments should be carefully evaluated with respect to instability if the gradient exceeds 1:4 or 1:5, if extra loading is planned or expected (H. Brennodden, Geopartner a/s, pers. com.).

Although we have no access to detailed bathymetric data in the area (Statoil, confidential data), and we can not exclude the possibility that the sediments may be under-consolidated (causing reduced undrained shear strength), we conclude that it is very likely that an earthquake caused an extra loading of the sediments and triggered this slide.

Slide scar northwest of Kvitsøy

This N-S trending slide scar has a length of about 4 km with a steep back wall up to 40 m high. In this area, at the outlet of Boknafjorden into Skudenesfjorden, the seismic records clearly show that the oceanographic current pattern changed at a certain time during the glaciomarine deposition. The sediments below reflector A onlap the underlying till or bedrock (starts to fill the entire basin created by the glacial erosion). Above level A, it is evident that there is a zone of enhanced bottom currents in the trench extending southward from Karmsundet. The strong current caused non-deposition close to the steep slope, and the middle of the basin came in a "backwater" environment with weak currents. In this area a thick succession of glaciomarine and marine clays accumulated (Fig. 3.1.5). Extrapolation of the present reflectors in the sediments into the space that has been subject to sliding indicates that a trench with increasing relief (in the order of 50 m) was formed through the time.

Assessment of the original slope angle before the sliding is very uncertain, but a gradient of 1:20 to 1:15 (3 to 4 degrees) is inferred based on the available data. Under normal conditions this should not cause gravitational sliding of the sediments. Based on the available data, however, we can not exclude the possibility that the present slide scar is the end result of several slides or a progressive slide, which was first caused by local instability due to strong current erosion in the eastern slope of the trench. Present strong NE-SW tidal currents to the north of Kvitsøy are reported by Gade (1986).

Although current erosion in the eastern slope of the trench may be an important factor for the instability in this area, we cannot exclude the possibility that an earthquake has triggered the main slide, using the existing data.

Slide scars and old slump deposits southwest of Kvitsøy

This N-S trending slide scar has a length of about 7 km with a back wall 10-20 m high (Fig. 3.1.6). Most of the E-W seismic lines across the slide show a low seafloor gradient in front of the slide. The southernmost part of the trench is deeper, with a more pronounced relief. It is difficult to estimate the morphology before the most recent sliding activity, but the present data do not indicate any large and steep relief of the trench. The seismic data show that two 100-200 m wide blocks of sediments have been partly rotated directly west of the slide scar (Fig. 3.1.6). This indicates that the present slide scar possibly has been developed through several minor slides. Local current erosion may have caused the minor slides.

Abrupt cutting of reflectors and uneven surfaces show that several older slides have occurred in the area. The present data do not indicate that steep and high slopes existed before the slumping.

3.1.6 Deformation and faulting in the glaciomarine sediments

We have seen some examples of features indicating faulting and deformation of the Quaternary sediments, but due to the limited resolution and other factors influencing the seismic appearance, the interpretation is unsure. Most of the features are probably connected to recent or old sliding activity and deformation of sediments below the slide scars or below the slump deposits. Local infilling of current grooves may also have caused particular seismic reflections giving a false indication of sediment displacement.

The observed possible tectonic features are in glaciomarine sediments, and we have found no connection to displacements at the till or bedrock surface. None of the observed features have been recognised on the neighbouring profiles, so if the observed features represent faults, the offset/length ratio of them is high.

3.1.7 Conclusion

Based on the very low slope gradient and no indication of extraordinary strong bottom currents/erosion southwest of Vestre Bokn (northernmost site), we believe that an earthquake triggered the northernmost slide in the studied area.

Increased accumulation of sediments west of the trench combined with strong bottom currents/erosion in the trench northwest/southwest of Kvitsøy has decreased the stability in the western slope of the trench. We cannot rule out, however, that reactivation of the Kvitsøy Fault has been the triggering mechanism for the sliding in this area.

3.2 SEISMIC INVESTIGATIONS IN THE NORTH SEA

By Fridtjof Riis, Norwegian Petroleum Directorate

3.2.1 Identification of neotectonic features in the eastern parts of the North Sea.

The objective of the study is to identify and evaluate possible neotectonic features in the areas offshore Norway. In 1997, the work has been focussed at the north-eastern parts of the North Sea, where there is a good seismic coverage and where the seismicity is high.

Interpretation of 2D and 3D seismic surveys in the Norwegian channel indicates that Quaternary fault movements can be resolved in the 3D data in the Troll area, and in the single channel seismics acquired by the NPD in the coastal areas. In the Troll area, a reactivation of a fault west of the Øygarden Fault Zone is indicated. Several lineaments of probable tectonic origin show WNW-ESE and NE-SW trends.

3.2.2 Data, data selection, data resolution

Recent fault throws are likely to be in the order of a few meters or less. Such throws will normally not be identifiable in conventional 2D seismic profiles with a 4 ms sampling interval. In areas which are presently seismically active, a good 3D seismic coverage is available mainly in the northern part of the Norwegian Channel. The two surveys NH9101 and SG9202, which cover the Troll Field (Fig. 3.2.1), were selected for the study. These surveys were shot with a 12.5 m CDP distance and a 12.5 m line distance. The sampling interval was 4 ms. The surveys were loaded on a Charisma workstation from Petrobank. The Petrobank version of SG9202 is not properly scaled, and several lines are missing. However, the Quaternary part could be interpreted with confidence, although deeper reflectors have very low amplitudes.

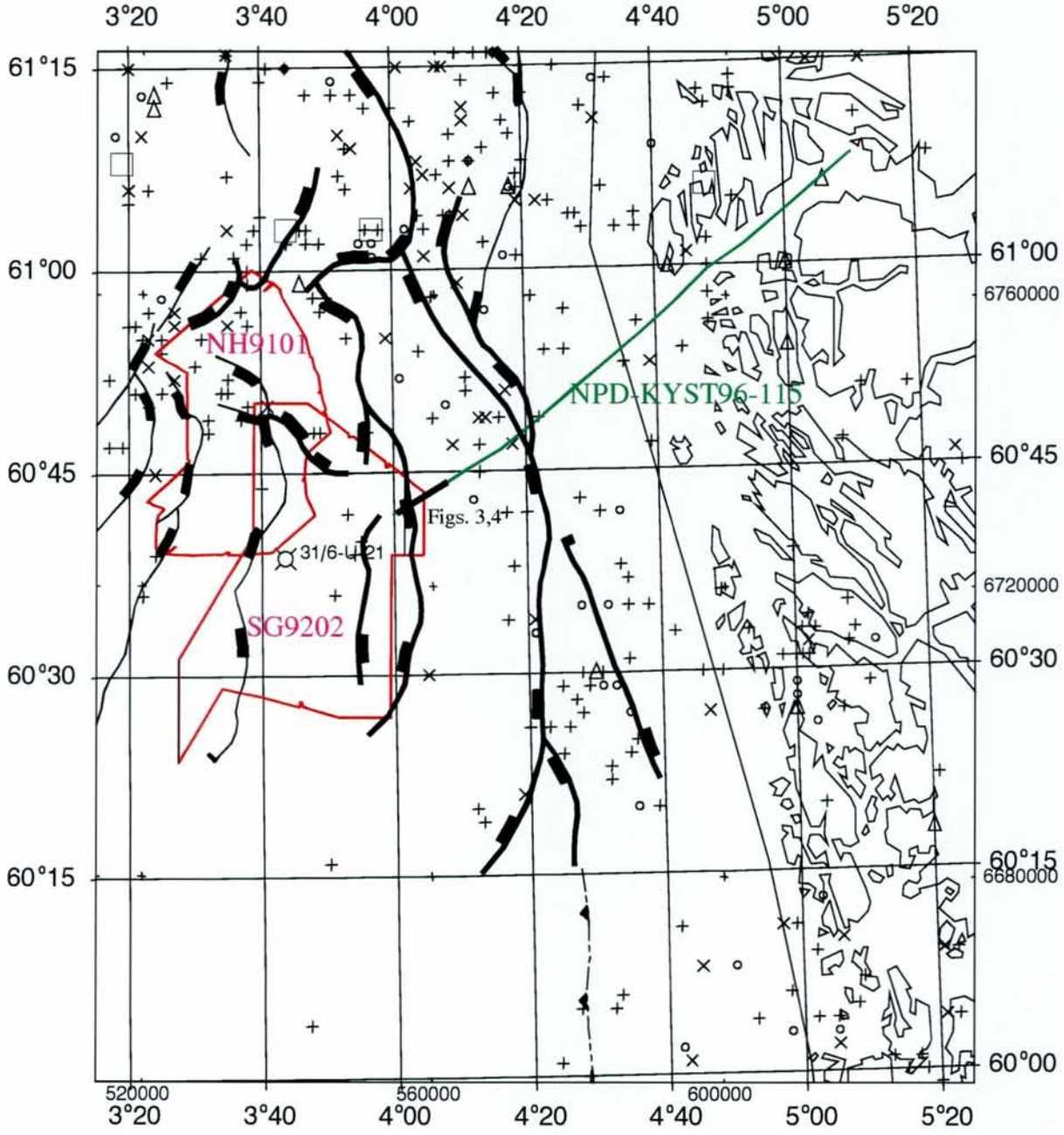

Fig. 3.2.1. Map showing location of the interpreted data in the Troll area. Major faults at the Jurassic level are shown as heavy barbed lines. Earthquakes (+, ×, o) are plotted from the NORSAR database. Note relation between Mesozoic faults and earthquakes.

The 2D surveys NPD-KYST-96 and NPD-SK-95 were selected to search for possible neotectonic phenomena along the coast. These lines exist in two versions: A deep version with 3 seconds recording time and a shallow, single channel version with 1 second recording time and a 1 ms sampling interval. The single channel version yields sufficient resolution to identify recent faulting. However, small-scale static shifts are common along the lines. Such shifts may be mistaken for real faults with vertical fault planes.

3.2.3 Identification and evaluation of neotectonic features

The Quaternary section encountered in the Norwegian Channel has been cored in well 31/6-U-21 (Sejrup *et al.* 1995). It is built up of alternating glacio-marine sediments and tills, which can be readily correlated from the well to seismic sections. In general, the glacio-marine sediments are characterized by continuous, parallel reflectors with moderate to low amplitudes. The reflection patterns of the tills are more variable, often with irregular, high amplitude reflectors defining the boundaries and with an interior of low reflectivity or chaotic reflections. Time slices and dip maps at the bases of the tills typically show pronounced linear patterns of grooves. The grooves trend parallel to the glacier motion, and in the Troll area they are commonly oriented along the main axis of the Norwegian Channel. The tops of the tills have an irregular morphology.

In a glacial environment, many depositional features like slumping and glacio-tectonics may easily be interpreted as tectonic movements caused by stresses in the crust. The best way of identifying "true" tectonic movements is to interpret glacio-marine layers in areas where glacio-tectonics is not likely to happen. It should be noted that the glacio-marine beds often show a conspicuous draping of irregularities in the underlying surfaces. Such draping may be caused by a large input of ice-dropped material, and it may penetrate sections with a thickness of several tens of meters, thus simulating faults with vertical throws.

As noted above, errors in the data such as small scale static shifts, may be erroneously interpreted as real offsets in the bedding. In the 3D surveys, the static shifts between the lines are sufficiently large that small scale offsets parallel or close to parallel with the shooting direction will have a low chance to be detected.

Data on offshore neotectonics are very sparse, and it is not evident what kind of structural expressions one should look for. Well-documented neotectonic faults would be the most obvious evidence for recent activity. Other features such as regional tilting or gentle folding should also be looked for, although they are more difficult to document.

3.2.4 Description of the Troll area

The Troll area is situated in the southern part of the zone of high seismicity in the northern North Sea (Fig. 3.2.1). It is completely covered by 3D surveys, and detailed bathymetric data exist. The Quaternary stratigraphy is well known from 31/6-U21. Major faults trending NS and NW-SE involve the basement and penetrate the Mesozoic section. Many of the faults were reactivated in the Tertiary. Commonly, major faults with a single fault surface at depth are represented in the Tertiary and upper parts of the Cretaceous sections as more complex sets of synthetic and antithetic faults with small throws.

2D interpretation

Evidence of fault reactivation is shown in line KYST-96-115 across a major fault trending parallel to the Øygarden Fault (Fig. 3.2.1). The fault bounds a large Triassic basin at its downthrown western side, and the fault continues into the basement. It was re-activated in the Tertiary, and the drags may indicate a component of reverse motion (Fig. 3.2.2). The Quaternary section above the fault is disturbed, and a plot of line Kyst-96-115 in large scale shows that the disturbance is not due to static shifts (Fig. 3.2.3). A vertical zone has been developed in the Quaternary sediments above the fault, where layers have been slightly flexed and faulted. The deformation zone can be traced almost to the sea floor, which indicates a recent age. The sense of motion is difficult to infer from only this line.

Interpretation of other lines in the survey has revealed additional candidates for tectonic faults, which will be analyzed further in 1998.

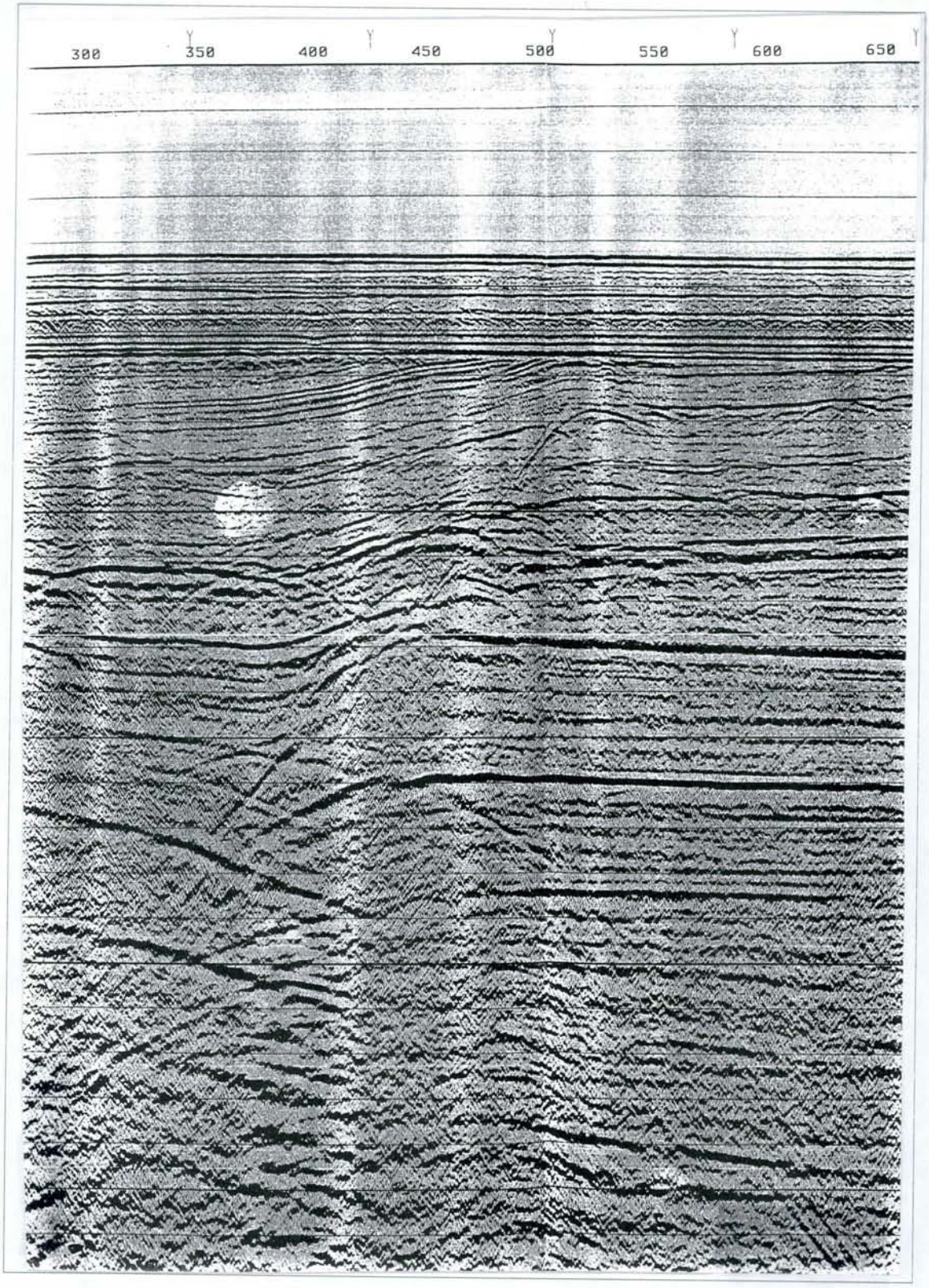

Fig. 3.2.2. Seismic line KYST-96-115 crossing the fault east of Troll. 100 ms between horizontal lines. The location is shown in Fig.3.2.1. West is to the left.

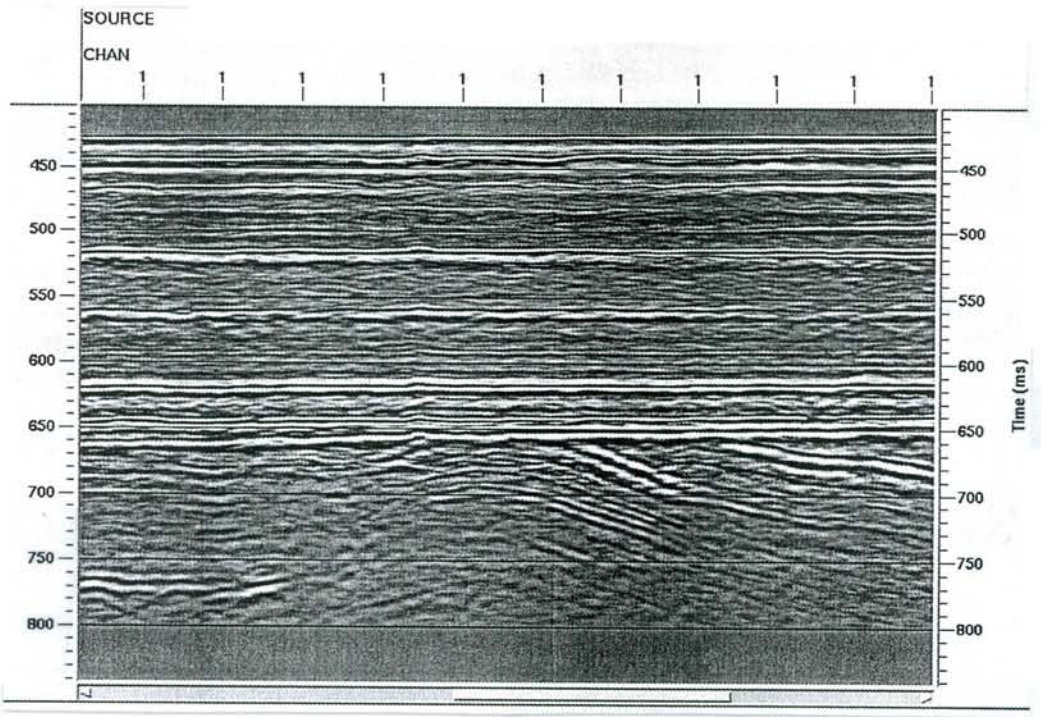

Fig. 3.2.3. Close-up of the Quaternary section in Fig. 3.2.2, above the fault at approximately shot point 530. The Quaternary layering is disturbed where the fault is intersected by the Base Quaternary unconformity at 650 ms, and the disturbance propagates almost to the seafloor. West is plotted to the right.

3D interpretation

The 3D interpretation revealed several candidates for neotectonic faults, but there are many pitfalls in the interpretation, as described above. The faults shown in Fig. 3.2.4 were picked by using the following set of criteria:

- Faults should be recognizable in the time slices and in the mapped surfaces.
- One fault should be recognized in a number of time slices.
- Fault orientations should be oblique to the line direction (because of static shifts).
- Glacially induced structures, such as grooves or plough-marks must not be interpreted as faults.

Fig. 3.2.4 shows the interpreted fault lines from the two Troll area surveys. The tie between the seismic data and the shallow well is shown in Fig. 3.2.5. Reflectors in the well-bedded, glaciomarine sediments have been used as reference to identify faults. Note that the shooting directions is different in the two surveys. Fault trends parallel to the line direction are very unlikely to be interpreted. The throws of the faults are probably less than 5 m. The amounts of throw are difficult to determine exactly because of the limits in vertical resolution. Because the faults can rarely be directly observed in the seismic lines, their character (normal, reverse or lateral) must be inferred from time slices or mapped horizons. Figs. 3.2.6 and 3.2.7 show how the fault lineaments are expressed on a time slice and a map of a Lower Pleistocene glacio-marine horizon in the SG9202 survey.

As shown by Figs. 3.2.8 and 3.2.9, the trends of the interpreted faults correlate quite well with the deeper Tertiary and Mesozoic faults. There are not always connections to deep-seated faults. This may be due to a branching geometry of the basement-involving faults.

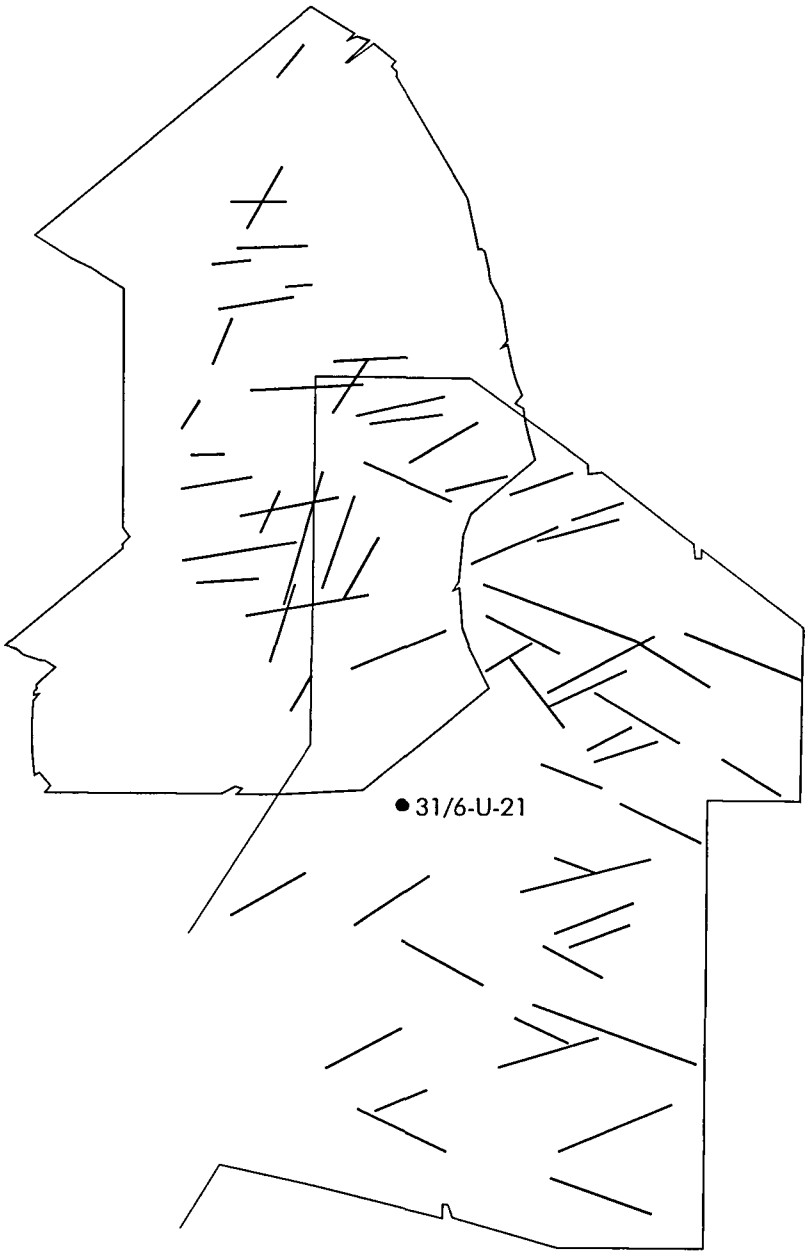

Fig. 3.2.4. Interpreted Quaternary lineaments of the Troll area. For location, compare with the outlines of the 3D surveys shown in Fig. 3.2.1.

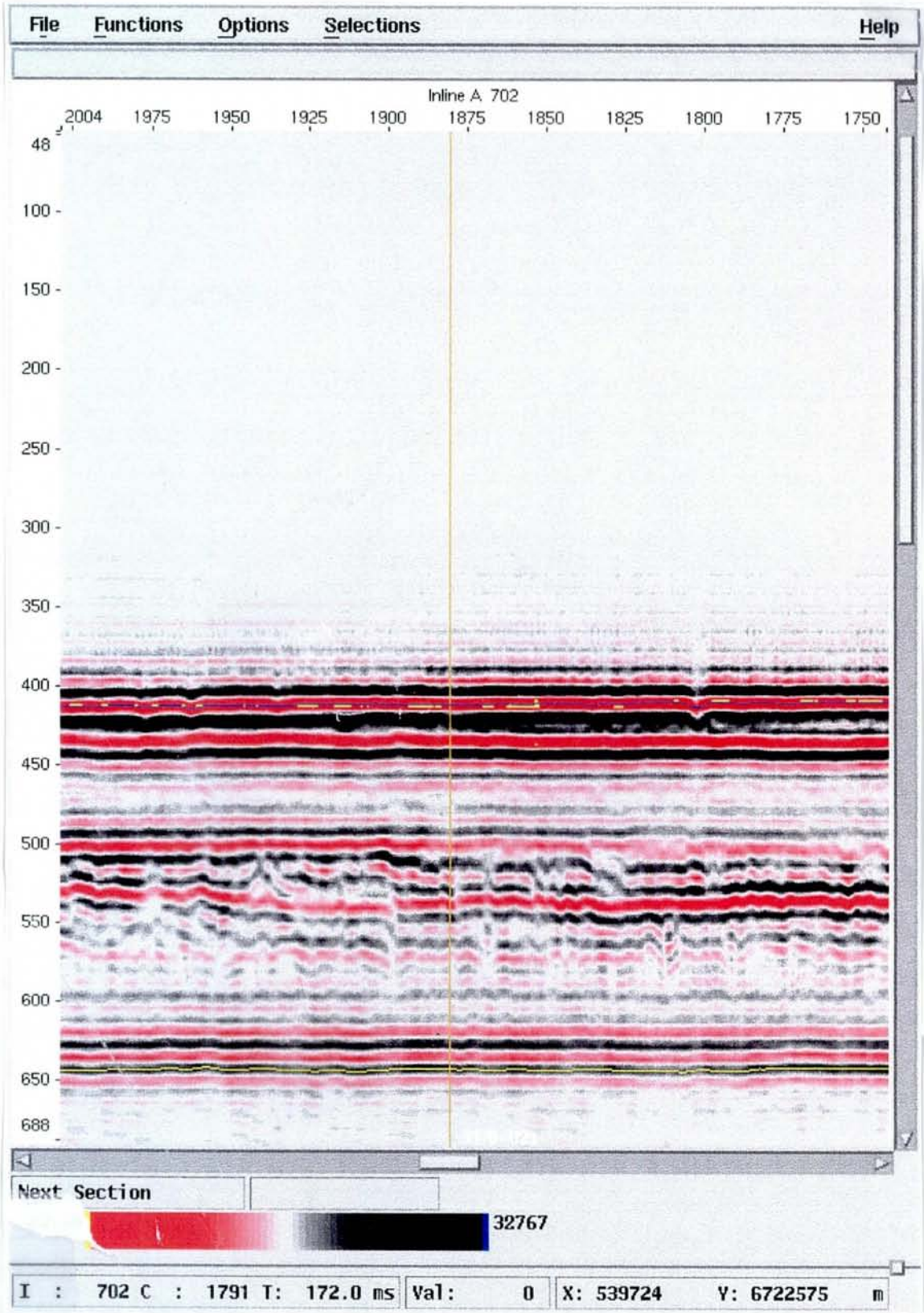

Fig. 3.2.5. Seismic section through well 31/6-U21 which penetrates the Quaternary. The uppermost, Weichselian till is interpreted to be located between approximately 420 and 500 ms. A Middle Pleistocene (possibly Saalian) till is interpreted between 540 and 570 ms. The lowermost 20-30 ms above the basal unconformity at 660 ms represent intercalated diamicton and glaciomarine sediments dated by Sejrup et al. (1995) to the Lower Pleistocene. Glaciomarine sediments occur between the tills, and the Lower Pleistocene section between 580 and 630 ms has been used for automatic interpretation and fault identification.

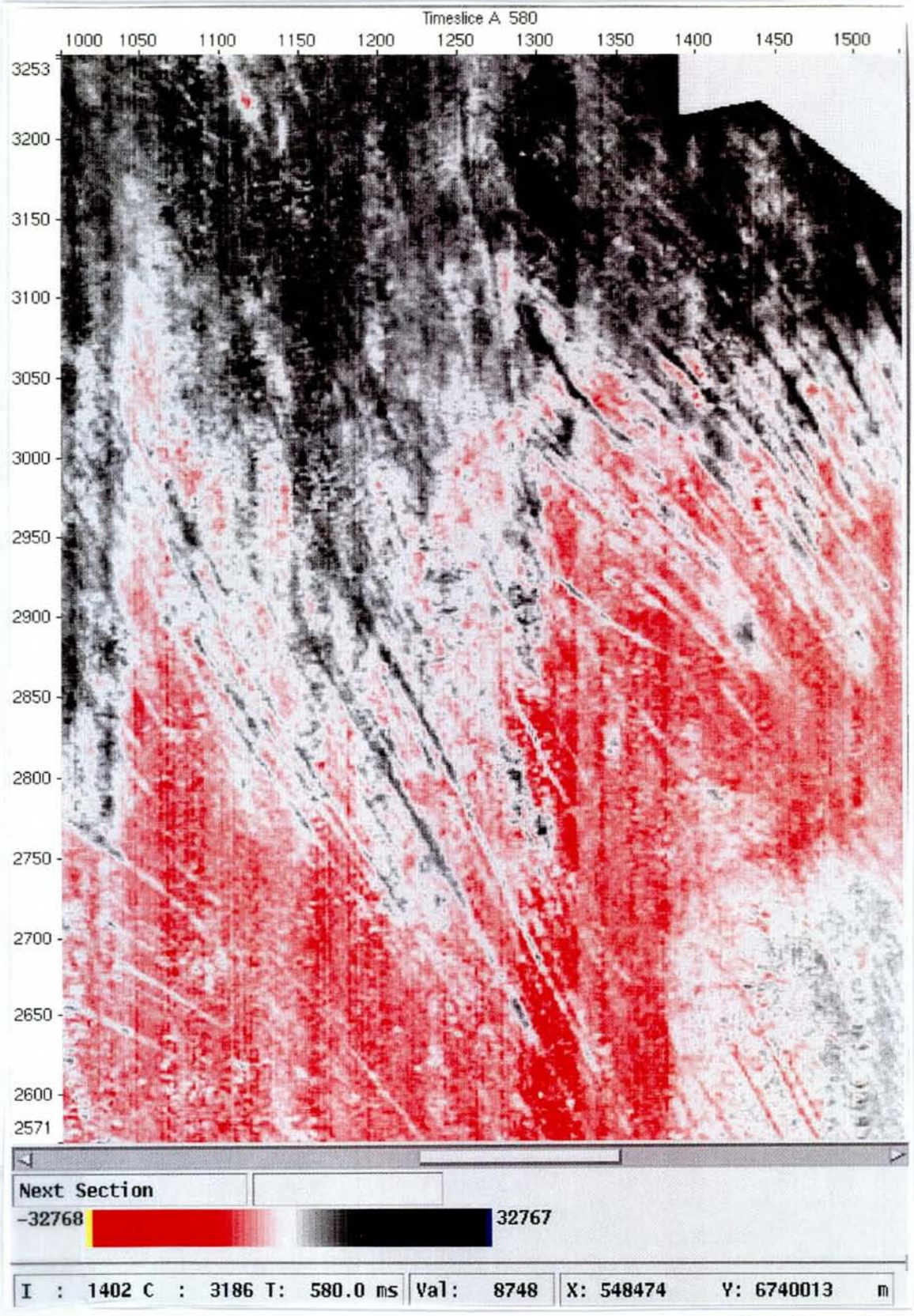

Fig. 3.2.6. Time-slice at 580 ms from the SG9202 survey indicating NE-SW trending tectonic lineaments crosscutting glacial forms (upper central part of figure).

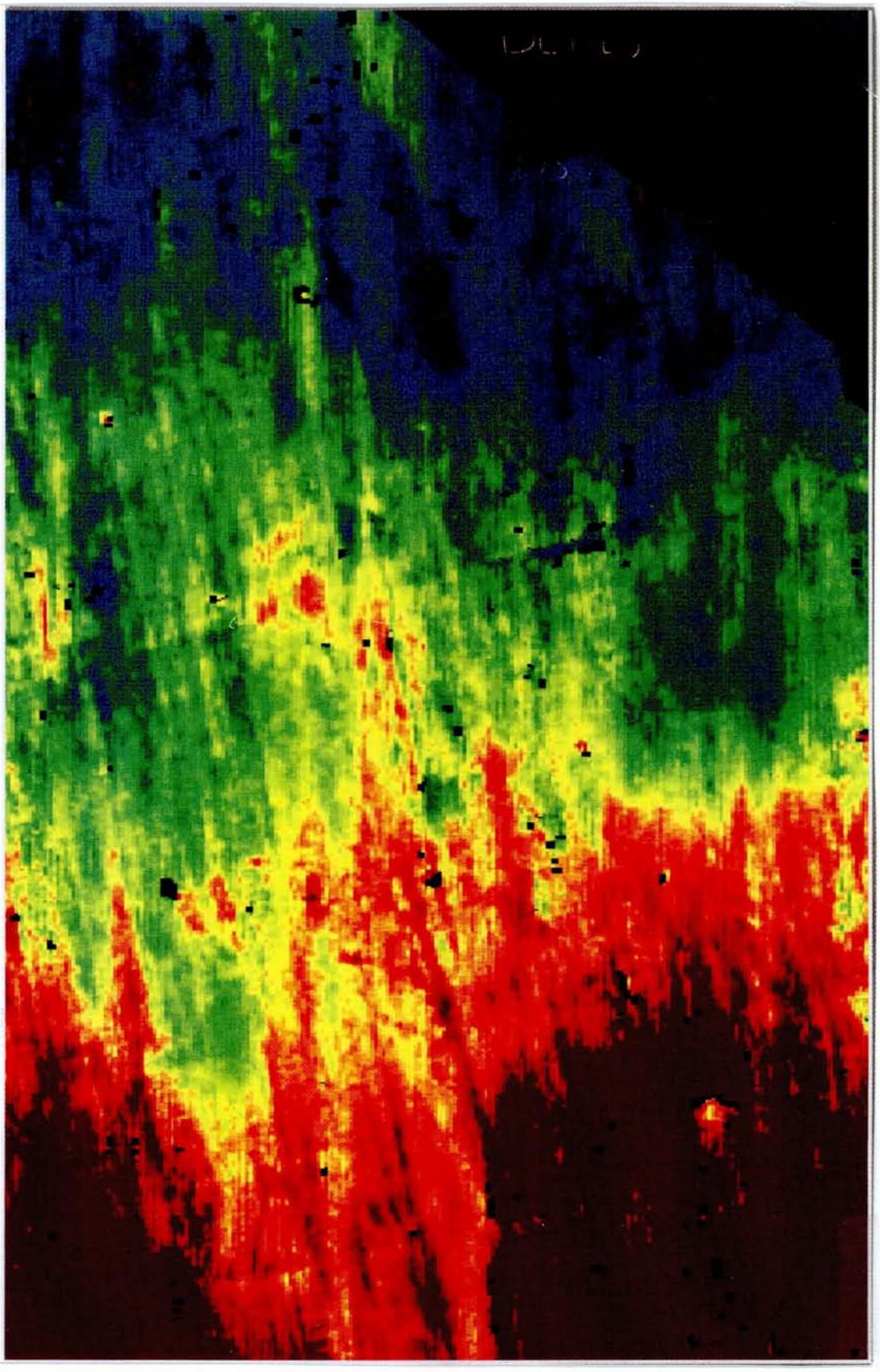

Fig. 3.2.7. Automatic time interpretation of Lower Pleistocene reflector, SG9202 survey. Glacial grooves trending mainly NNW-SSE and tectonic lineaments trending ENE-WSW are indicated. The N-S oriented stripes are caused by static shifts within the 3D survey.

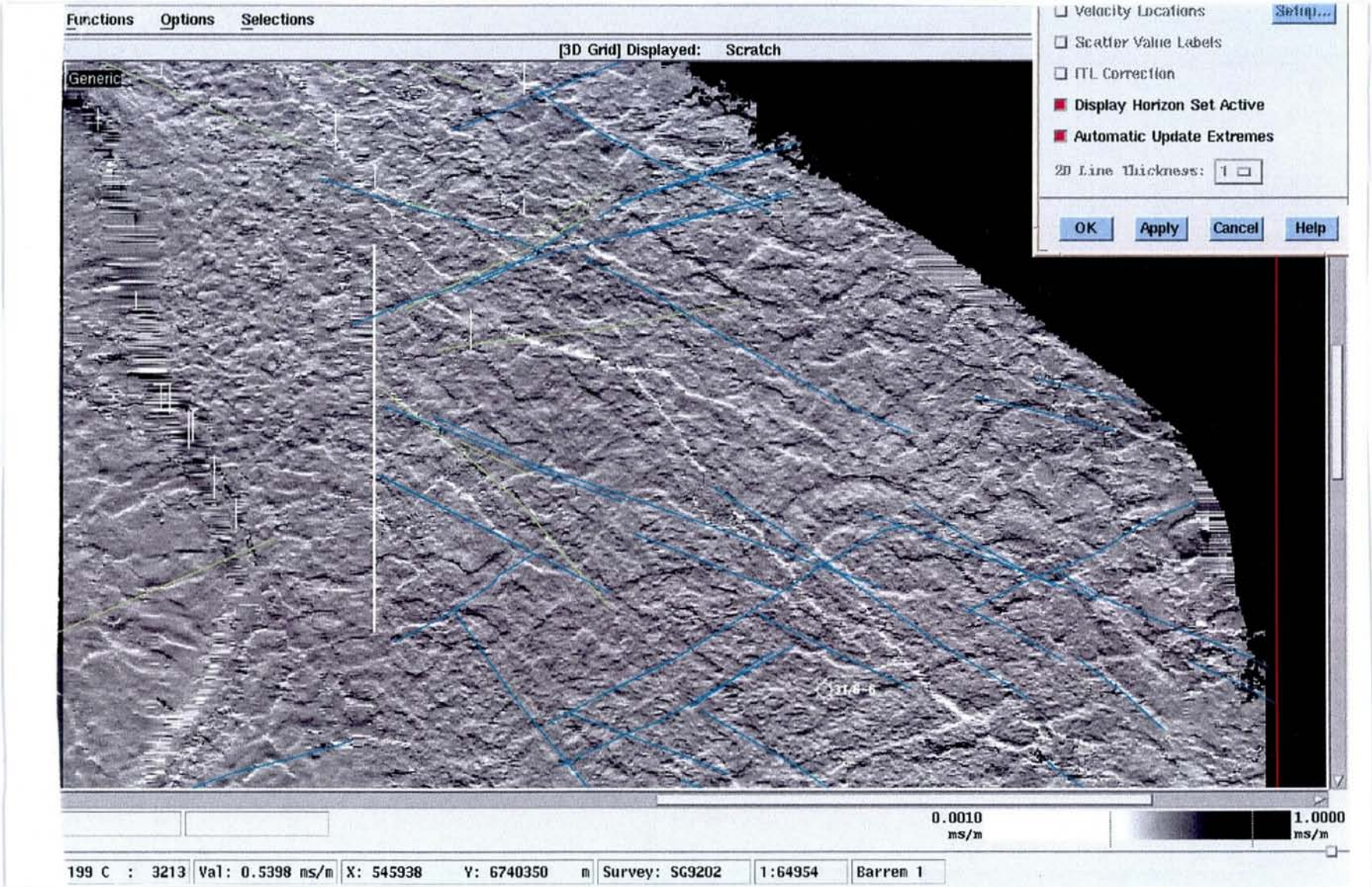

Fig. 3.2.8. Dip map of an automatically interpreted Lower Cretaceous reflector (Barremian unconformity), overlain by the interpreted Quaternary lineaments (blue and green lines). SG9202 survey. The dip map shows a major fault to the west and is dominated by small scale faults with two NW-SE trends (approximately N45°W and N60°W) and a more subtle ENE-WSW trend (N60°E). The dip map is illuminated from the north.

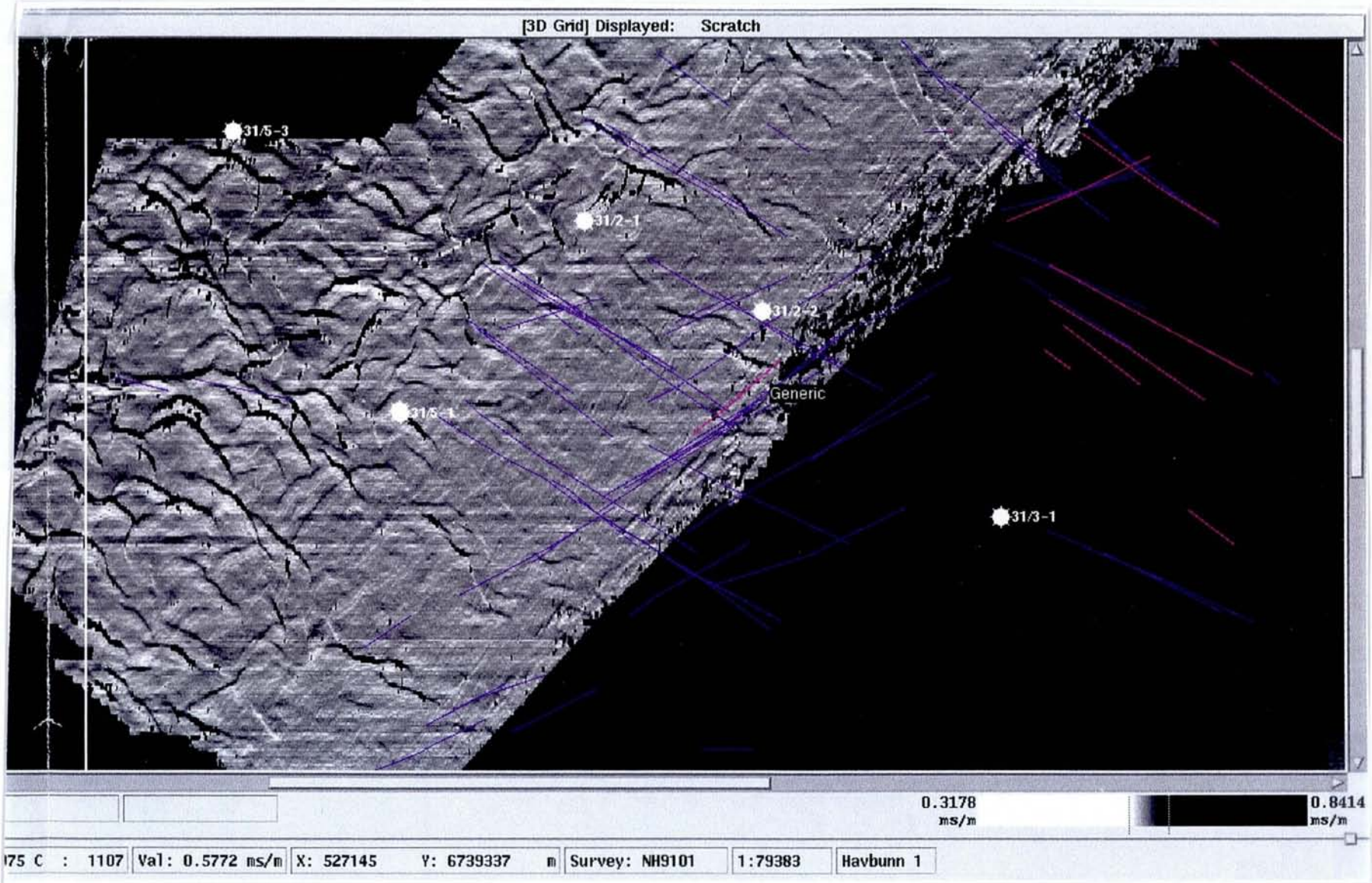

Fig. 3.2.9. Dip map of the Base Tertiary reflector, overlain by the interpreted Quaternary lineaments. NH9101 survey. The reflector is truncated and does not appear to the right. The orientation of the map is such that the truncation boundary trends approximately NS. Two fault trends are apparent, one trend WNW-ESE and one NNE-SSW.

3.2.5 Conclusions

Seismic interpretation in the Troll area indicates recent reactivation of a NS-trending basement fault. A set of NW-SE and NE-SW trending tectonic lineaments were formed in the Quaternary sediments, but they cannot be traced to the sea floor. These structures are interpreted as tectonic because they are linear features which cut glacially formed structures and they have similar trends as tectonic structures in the underlying Mesozoic and Cenozoic sections. More data are needed to interpret the stress system that may have formed the structures.

3.2.6 Plans for 1998

The aim is to study 3D surveys in areas with high seismicity: the Lofoten area and the eastern and north-eastern part of the North Sea. The study will be complemented by a review made by IKU of regional shallow seismic data. IKU will also interpret 3D surveys. The neotectonic features will be evaluated, classified and entered into the database at NGU.

1st - 2nd quarter: loading of surveys from Petrobank. Study of survey SG9603 north of Troll.

3rd – 4th quarter: Lofoten area. Possible surveys are ST9404 and NLGS95. Integration with IKU interpretation.

3.3 MULTIBEAM ECHO-SOUNDING DATA IN THE MALANGEN AND LOFOTEN AREAS

By Stein Fanavoll, IKU, and John Dehls, NGU

Multibeam echo-sounding data was collected in the areas west of Kvaløya ('Malangsdjupet') and west of Røst in Lofoten by Statens Kartverk/Sjøkartverket. The objective was to do a closer investigation of two areas of reported possible neotectonic activity, reported on IKU shallow seismic data.

Data was collected using a multibeam sounder EM100 manufactured by Simrad of Norway, on the Norwegian Mapping Authority vessel "M/S Sjømåleren." The EM100 operates at 95 khz and provides bottom coverage along a swath that is 1.7 times the water depth across track, using 32 beams. The shallow water in Tjeldsundet was covered using wide mode (80°), while the deeper and rougher waters offshore Røst and in Malangsdjupet were covered using narrow mode (40°). Raw data was gridded in *Geosoft* using a minimum curvature method and processed using *ER-Mapper 5.5*, an image processing software package.

3.3.1 Malangsdjupet

A possible neotectonic fault can be observed on IKU shallow sparker line IKU-C84-306 (Fig. 3.3.1) (Fanavoll & Dahle 1990). A clear offset of the base Quaternary can be observed, as well as of the lower horizons within the Quaternary. In the upper part, horizons are terminated against the fault and converts into a chaotic reflection pattern on the downthrown side of the fault. A deflection of the sea-bottom marks the termination of the fault.

Because of the resolution of the sparker data, limited by the width of the signal, it is not possible to verify how shallow the fault goes. Use of boomer data with higher resolution does not contribute significantly to answer this question, even though a slight disruption can be seen through the 'ringing' of the upper layers (Fig. 3.3.2).

Multi-beam data was acquired in an area of approximately 4x3 km (Fig. 3.3.3). The main feature on the data is the stepwise deepening into the Malangen Trench, marked with an 'A' on the figure. The position of the seismic line is plotted together with the multibeam data, and approximately in the middle of the investigated area one can observe a bulge of limited extent which corresponds to the fault seen on the seismic line ('B' on the figure).

Plotting the data as a gradient plot (Fig. 3.3.4), we can observe three different features: the deepening into the Malangen Trench (A), the fault (B) which appears with an angle to A, and the wave noise (C), appearing as the NE-SW high frequent gradients.

The extent of the fault as expressed on the sea-bottom is limited and can be measured to ~0.5 km. Plotting the observation onto an earthquake map (Fig. 3.3.5), we see that the fault is positioned in the trend of the Senja-Bothnia Fracture Zone. The very limited extent of the fault may be explained by its being a normal fault positioned perpendicular to a transverse zone, where strike-slip movements are expected to occur

Another interesting observation is the earthquake cluster forming a NE-SW trend corresponding to a fault zone extending from the Haltenbanken area to Troms. Brekke & Riis (1987) refer to this as the Andøya-Vøring Lineament. The abundance of earthquakes decreases abruptly when crossing the Senja Fracture Zone, which indicates that this corner is an area where stresses are likely to be released.

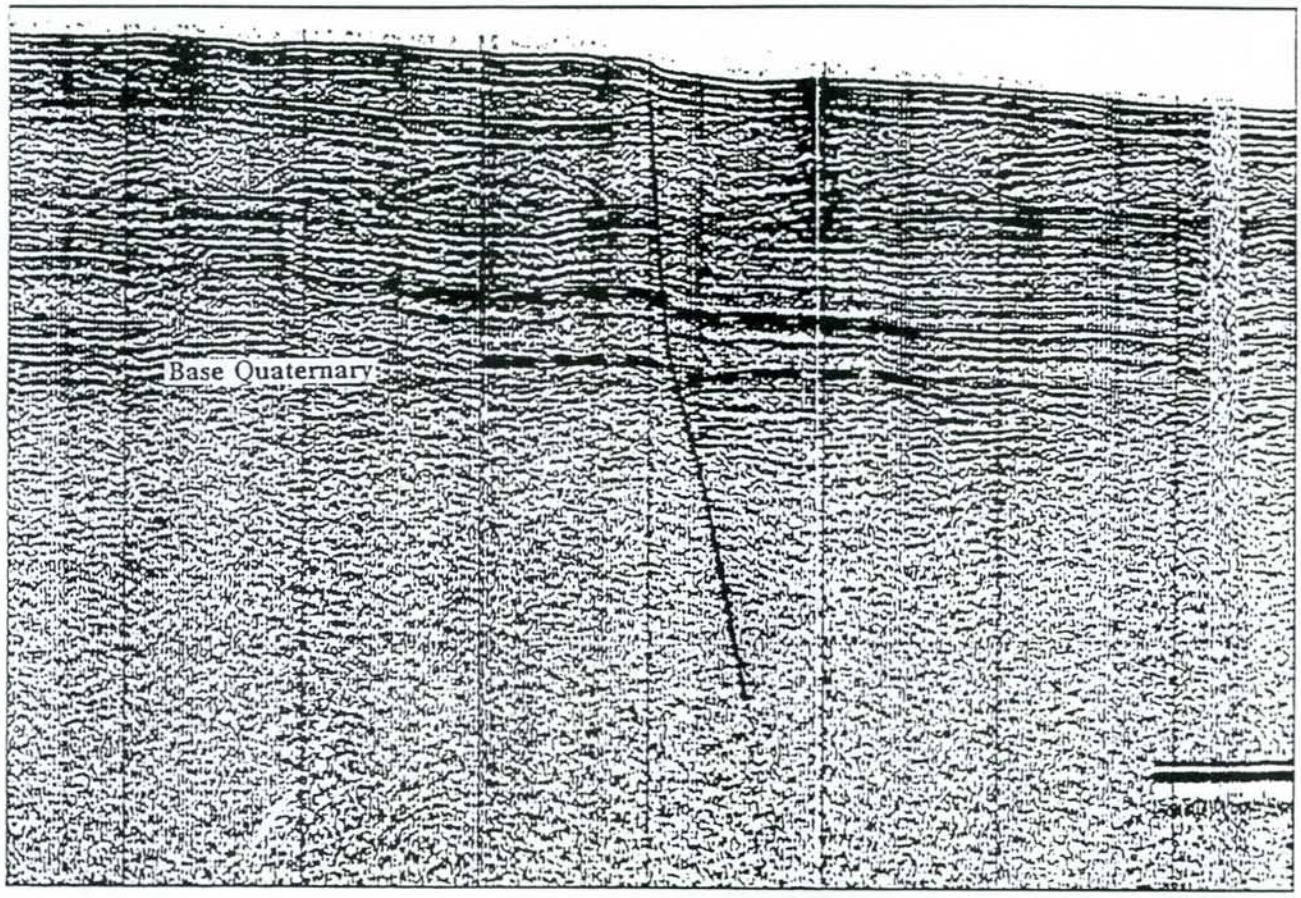

Fig. 3.3.1. Part of seismic line IKU-C84-306, from Malangsdjupet, showing a young fault cutting the Base Quaternary and younger horizons. The seabottom is offset by flexuring.

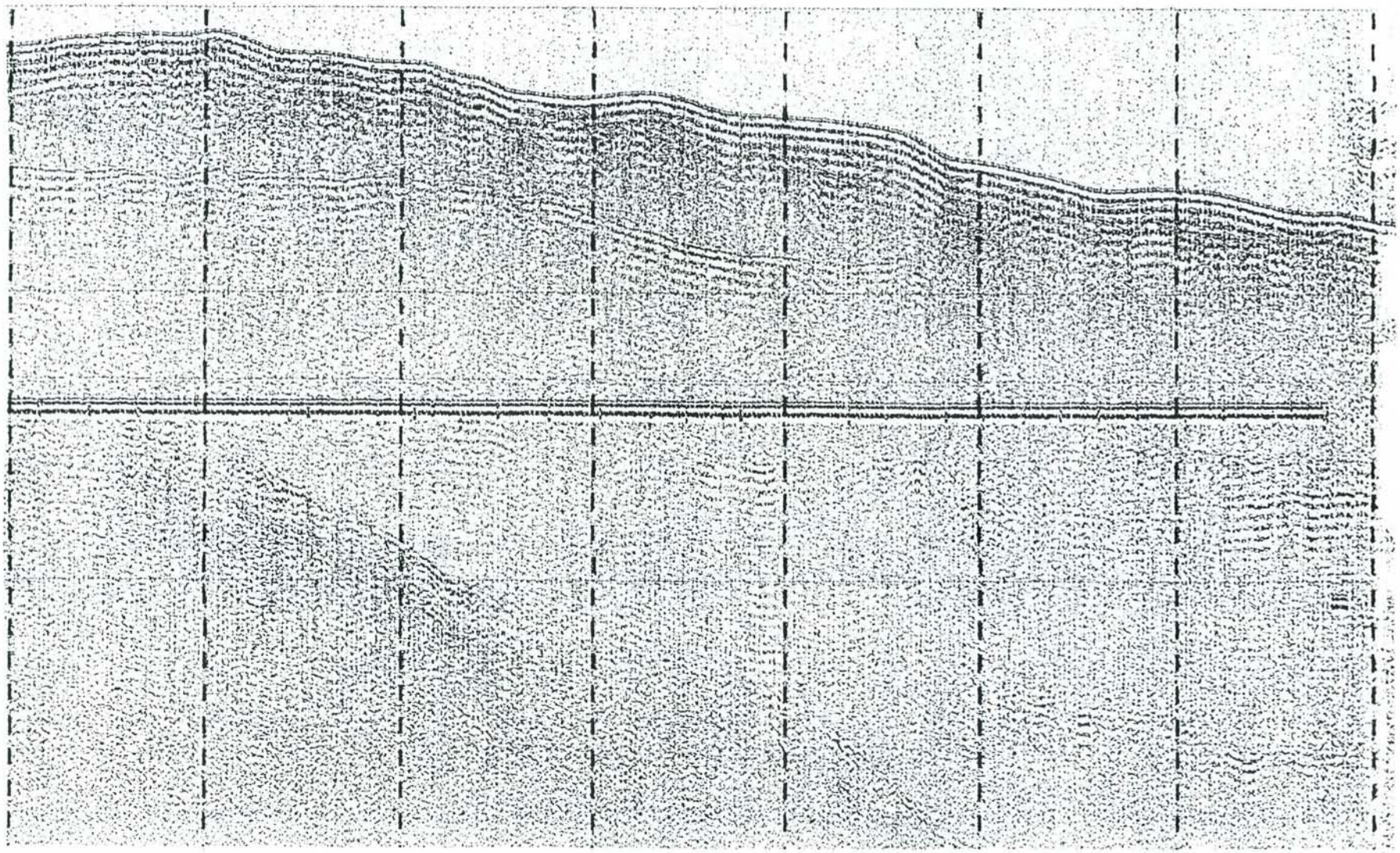

Fig. 3.3.2. Boomer data across the fault in Fig. 3.3.1.

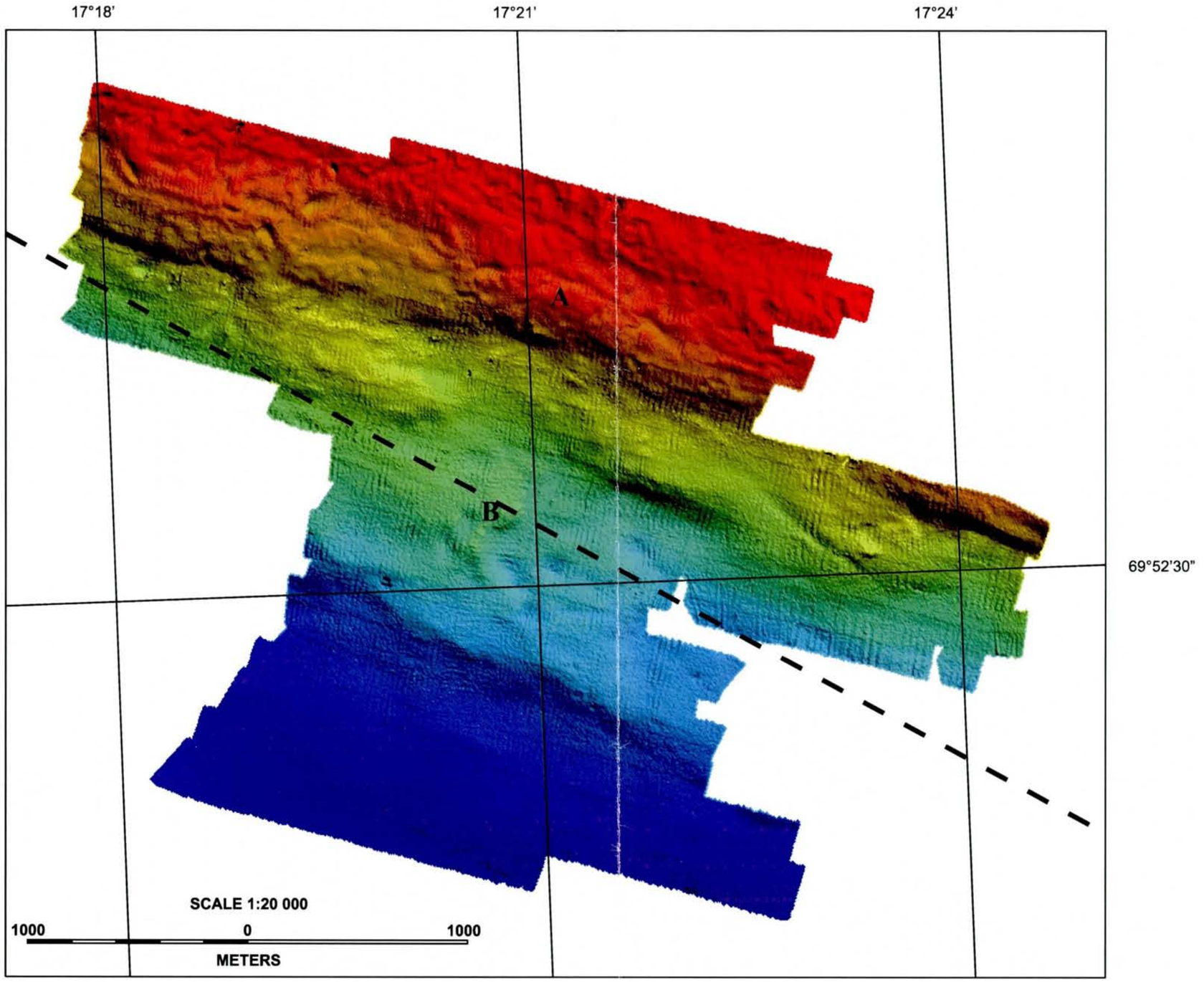

Fig. 3.3.3. Coverage of multibeam data in the area of the fault in Fig. 3.3.1. The position of the seismic line is shown by the dashed black line, and the fault is seen just west of the 17° 21' line. Data collected by the Norwegian Mapping Authority vessel "M/S Sjømåleren."

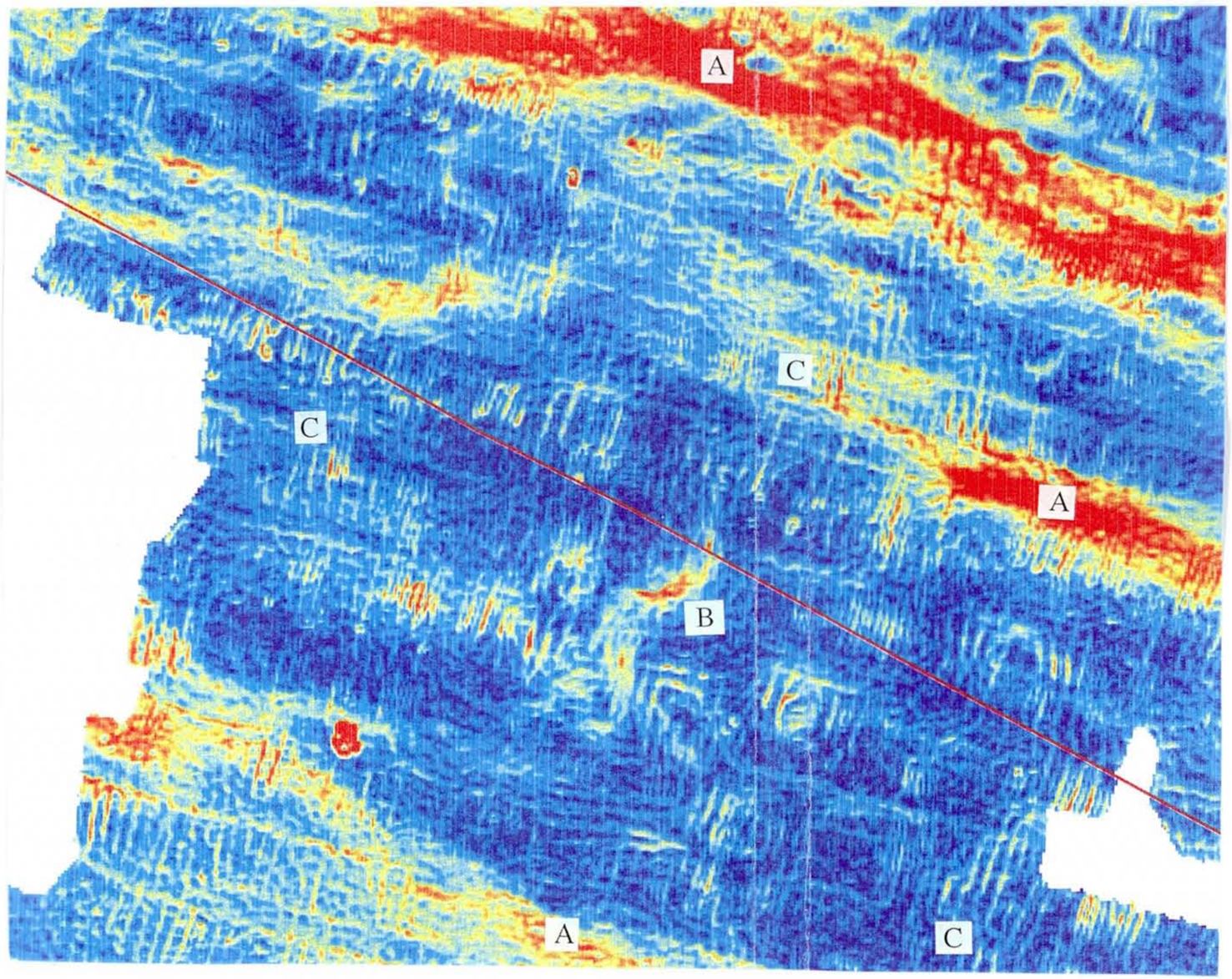

Fig. 3.3.4. Gradient plot of the multibeam data in Fig. 3.3.3. The fault (B) is seen as a different feature than the deepening into the Malangen Trench (A) and the wave noise (C).

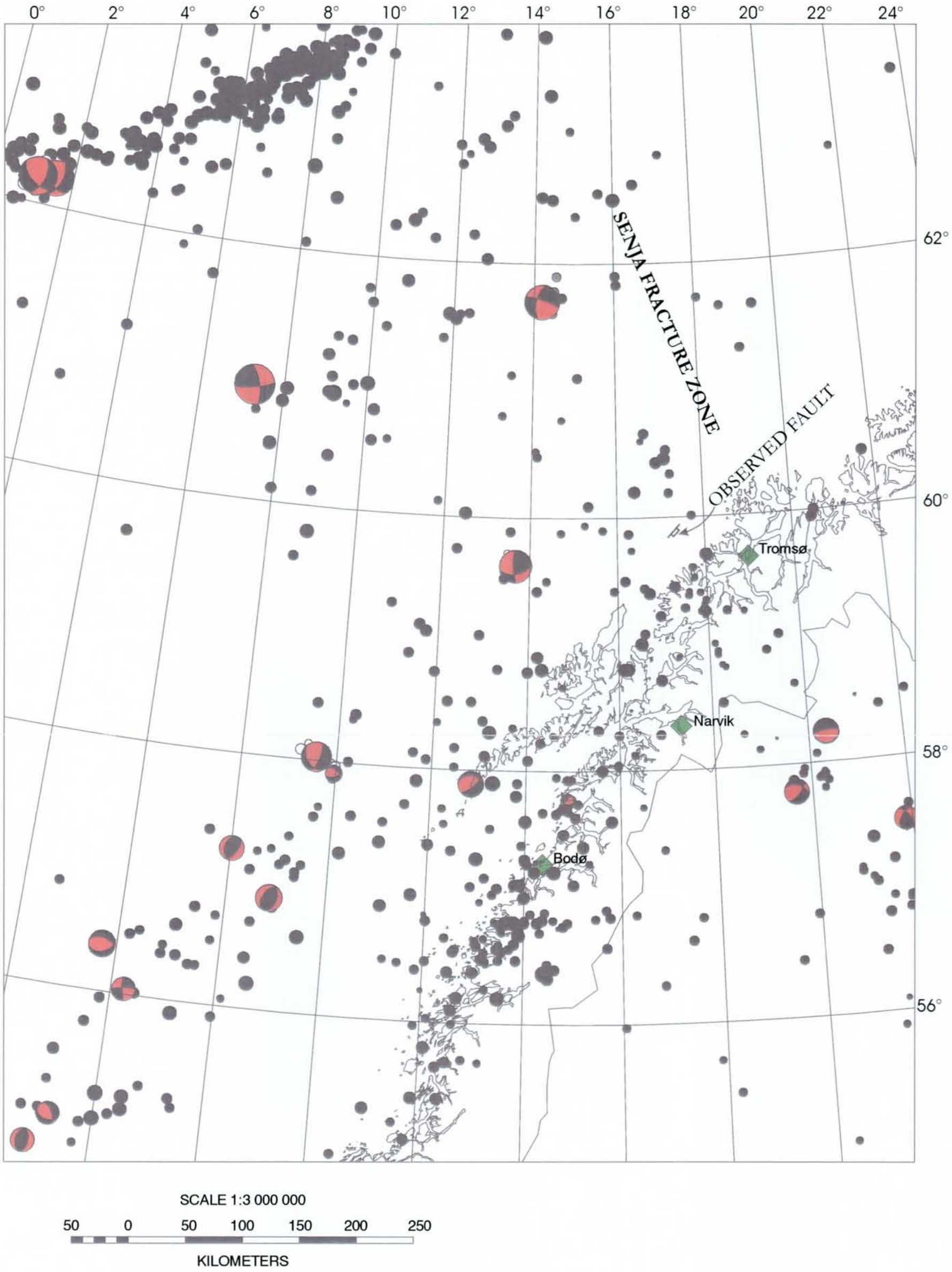

Fig. 3.3.5. Earthquake map of the area offshore northern Norway. Courtesy of NORSAR. Black circles represent earthquake epicenters and are scaled proportional to magnitude. Where focal plane solutions are available, the compressional quadrant is black and the extensional quadrant is red.

3.3.2 The Lofoten area

On line IKU B82-130 (Rokoengen & Sættem 1983), west of Røst Island, several observations of escarpments on the sea-bottom is related to faults (Fig. 3.3.6). However, these data has a much poorer quality than the IKU C84-306 line, and from seismic, there can not be drawn any conclusions as to whether these escarpments are caused by neotectonic activity. Data of higher resolution, like boomer, was not acquired along the line.

The multibeam echo-sounding data cover an area of 8 by 0.5 km (Fig. 3.3.7). Unfortunately, the acquisition was terminated prior to the plan due to bad weather. The navigation on the seismic line is regarded as rather uncertain, and it is possible that the seismic line and the multibeam data do not overlap. However, it is possible to recognise the main features from the seismic on the multibeam data. On Fig. 3.3.7, the position of the three faults and the basement scarp are marked with A, B, C, and D, respectively. Even though not conclusive, our opinion is that the observations represent erosional features rather than neotectonic activity. This is most certain for the basement scarp and the eastern fault (C), while the western faults (A and B) are more uncertain.

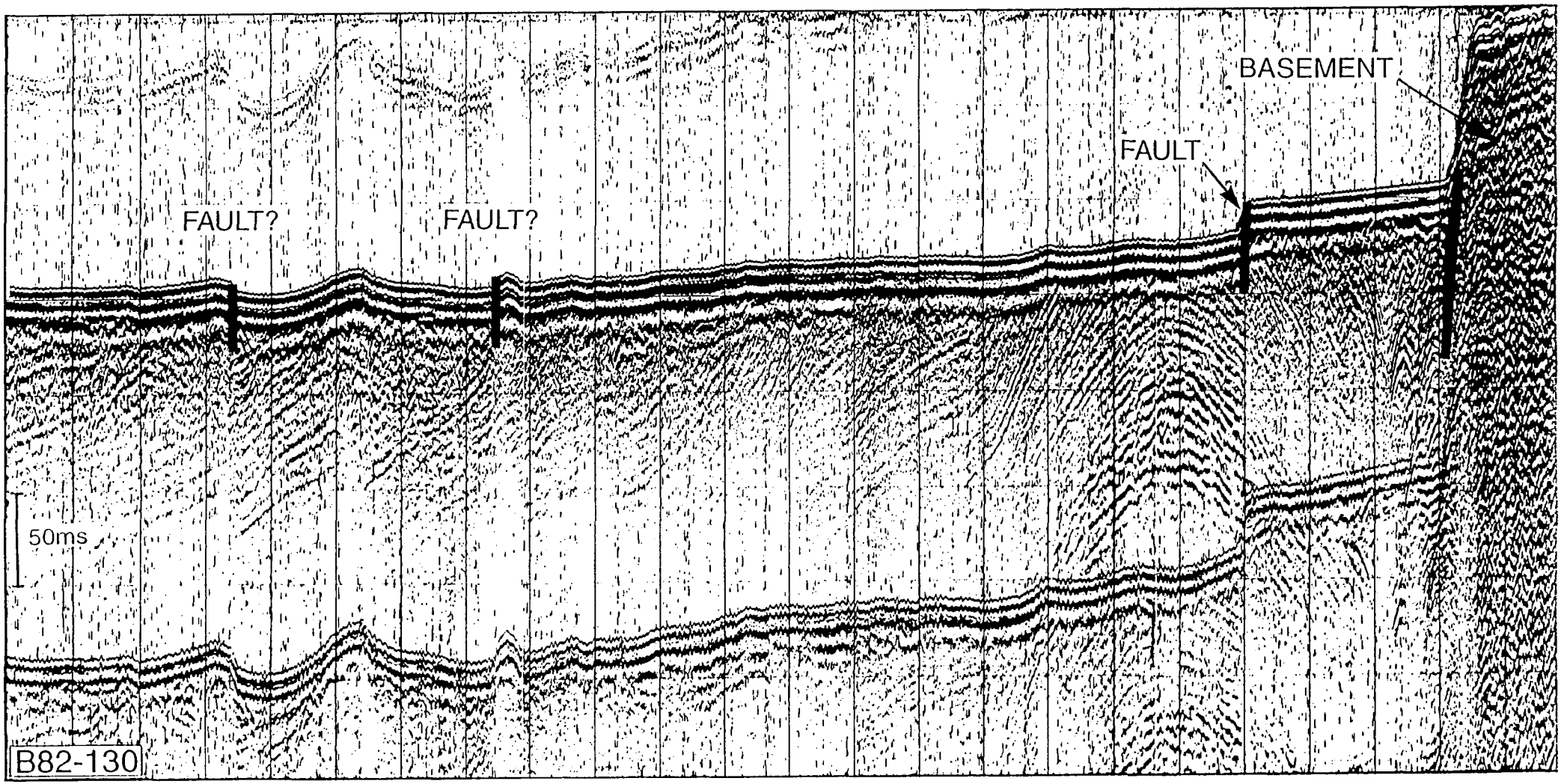

Fig. 3.3.6. Observed offsets of the seabottom on line IKU-B82-130 offshore Røst. The data do not show whether these are the result of erosion or neotectonic activity.

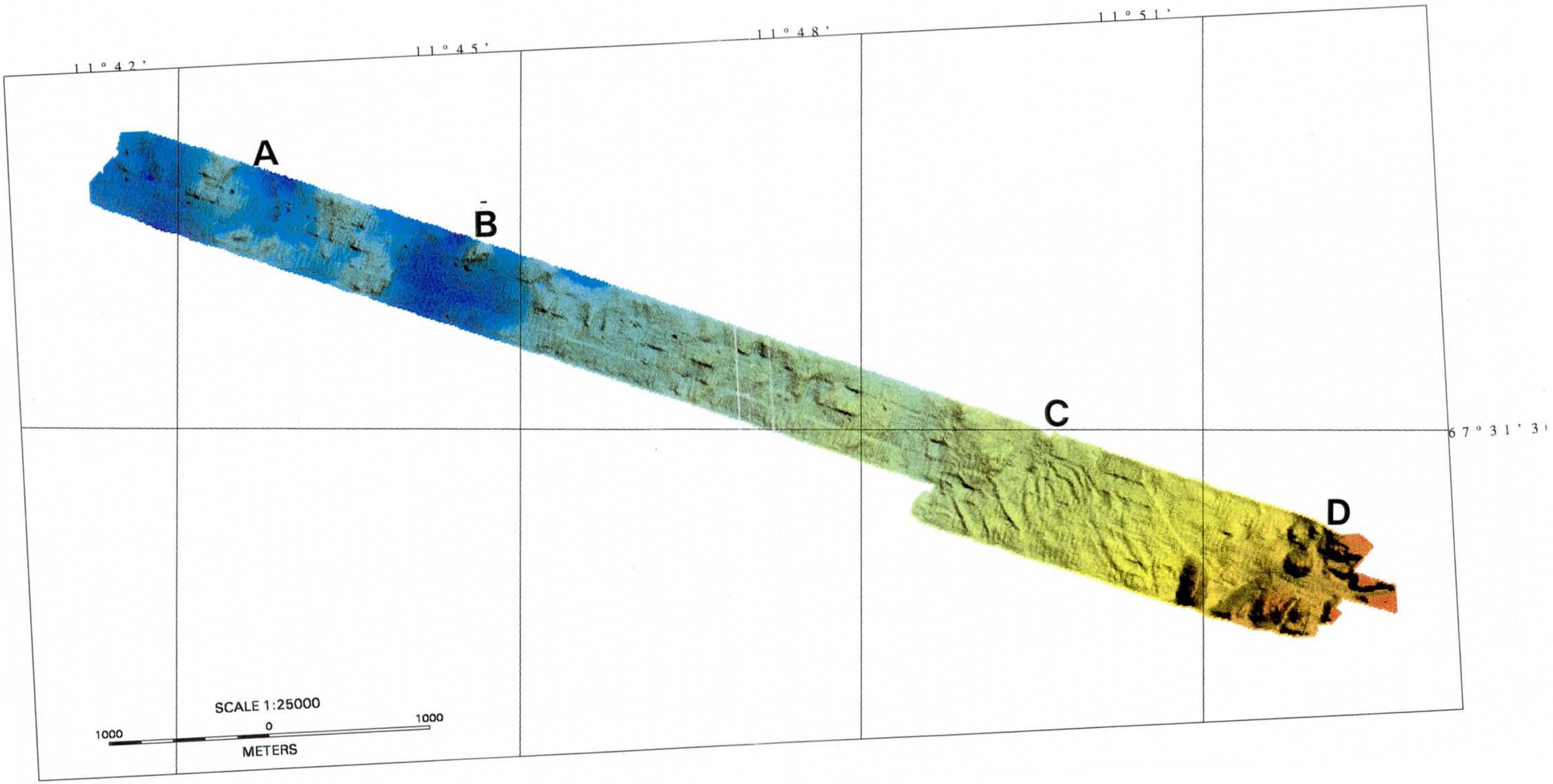

Fig. 3.3.7. Coverage of multibeam data west of Røst. Approximate position of observed faults are indicated.

4 1:3 000 000 NEOTECTONIC MAP AND DATABASE (TASK 3)

4.1 PRELIMINARY NEOTECTONIC MAP OF NORWAY

By John Dehls, NGU

Accompanying this report is a preliminary version of the 1:3 000 000 neotectonic map of Norway. It is an initial attempt at integrating many different types of information, and will probably change considerably before the final map is produced. It is very easy to plot many types of information on one map. It is a challenge to develop a symbology that makes the information understandable. Any comments concerning the map are welcome. Fig. 4.1.1 is the legend to the map.

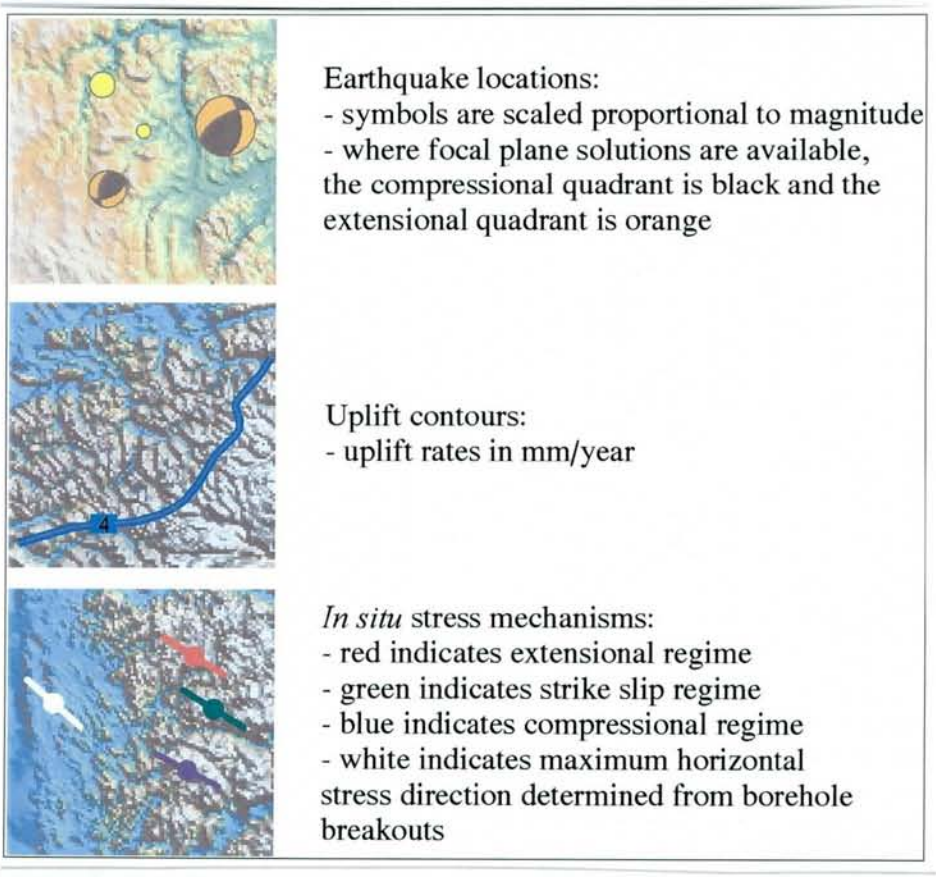

Fig. 4.1.1. Legend for the accompanying neotectonic map of Norway. The underlying image is derived from world bathymetry data from NOAA and digital elevation data from Statens Kartverk.

The NEONOR database is composed of point data (earthquake activity from NORSAR, in situ stress measurements from NTNU), line data (neotectonic faults, coastlines, uplift contours from the Norwegian Mapping Authority), polygonal data (national outlines) and gridded data (bathymetry and elevations, potential field data). Parts of this dataset are being published in 1:3 million scale maps by Lindholm *et al.* (in press) and Fejerskov *et al.* (in press). The point data is stored in a Microsoft Access database that is linked to Arc/Info, and can be accessed by other programs, including Web queries. All line and polygon data is stored in Arc/Info. Gridded data is stored as BIL files that can be accessed from Arc/Info or image analysis software such as ER-Mapper. The database will be continuously updated when new data are produced during the project period. The compiled dataset constitutes a firm foundation for the inte-

grated neotectonic analysis, which is scheduled for the second half of the NEONOR Project period. The database will be made accessible to all project participants.

Several interesting patterns can immediately be noticed on the neotectonic map.

- There is a close correlation of areas with increased seismicity and areas of known petroleum reservoirs in the Central Graben, Viking Graben, Halten Terrace and Dønna Terrace. Seismic pumping (Sibson 1981, Muir Wood & King 1993) may consequently be an active mechanism for the migration of hydrocarbons from the source rocks to potential reservoir formations.
- A deflection of the land uplift pattern near Nordfjord, corresponding to an area of increased seismicity.
- A zone of increased seismicity occurs along the continental margin of Mid-Norway (e.g. Bungum *et al.* 1991).
- There is a linear trend of earthquakes along the Senja fracture zone that extends inland, suggesting present deformation along an onshore extension of the fracture zone.

5 GEOLOGY & GEOPHYSICS (TASKS 4 & 9)

5.1 OFFSHORE AND ONSHORE STUDIES OF THE JÆREN AREA, SOUTHWEST NORWAY

Eiliv Larsen, NGU, Fridtjof Riis, Norwegian Petroleum Directorate and Leif Rise, NGU

The Jæren area is covered by a thick section of Quaternary sediments covering a long period of time in the Middle and Upper Pleistocene (Janocko *et al.* 1997, Janocko *et al.* 1998).

A marked terrain boundary at Jæren, south of Stavanger separating Høgjæren ("High Jæren") with elevations around 200 m asl. from Lågjæren ("Low Jæren") with elevations from sea level to ca. 100 m.asl. has been suggested by many to be of a possible tectonic origin (e.g. Andersen *et al.* 1987, Fugelli & Riis 1992). This relatively steep break in slope is running in a NNE-SSW direction from Gandsfjorden in the north to Brusand in the south. The main reason for suggesting a tectonic origin has been the occurrence of glaciomarine clays at Høgjæren at elevations almost 200 m above the Late Glacial marine limit. The idea has been that one should expect the strongest glaciotectonic depression after the last (maximum) Weichselian glaciation, and thus that earlier glacier advances should result in even lower marine limits and accordingly marine sediments at correspondingly lower elevations.

During the last few years, new evidence from a stratigraphic project at Jæren (Larsen 1992) has given new insights into the Quaternary development in the area. Drilling on both sides of the terrain boundary has revealed till deposited by the last ice sheet stratigraphically on top (Janocko *et al.* 1998). At Høgjæren, this surface till is underlain by *in situ* glaciomarine clays dated to approximately 30.000 years BP, whereas the underlying sediments at Lågjæren are of varying origin, but consistently Early Weichselian or older (Janocko *et al.* 1998). This demonstrates events of erosion or non-deposition in Lågjæren, i.e. in the areas immediately below the marked terrain boundary. In Høgjæren all evidences of former ice movements show directions towards the west, whereas both western and northern directions are found at Lågjæren, the northern one being the oldest (Sejrup *et al.* 1997).

The ice movement towards the north originated from a fast flowing ice stream along the Norwegian Channel, which had its eastern flank along the terrain boundary across Jæren (Sejrup *et al.* 1997). Strong evidence for this ice stream is also found in the sediments of the Norwegian Channel itself and on the shelf break beyond the mouth of the channel (Sejrup *et al.* 1995, King *et al.* 1996, Longva & Thorsnes 1997). This ice stream caused the erosion that has been documented at Lågjæren, and the formation of the break in slope between Lågjæren and Høgjæren. Calculations show that the thickness of the ice stream was sufficient to cause a glacio-isostatic depression large enough to explain the transgression and formation of Weichselian glaciomarine clays at Høgjæren.

Offshore Jæren, the surveys NPD-SK-95 and KYST-96 (see Fig. 5.1.1 for a coverage map) have an improved resolution compared to previous conventional seismic lines, and they are well suited to study the relations between the Quaternary cover and the deeper faults. A preliminary study of the NPD-SK-95 survey is reported here. In addition, one high-resolution seismic line has been shot in Gandsfjorden (NGU 9206010). The eastern slope of the fjord is steep, and a thick succession of glaciomarine clays is deposited in the fjord basin. The till on top of the bedrock is probably thin. No features indicating neotectonic activity have been found.

Although the model of Sejrup *et al.* (1997) seems to explain all their observations, it does not rule out the possibility of an additional tectonic component for the uplift of the interior. Some observations may indicate such a component:

A short seismic section across the Gandsfjorden lineament (Mauring & Rønning 1990) suggests possible Quaternary faulting (Fig. 5.1.2).

Fugelli and Riis (1992) pointed out that the distribution of highly elevated supposedly Weichselian marine clays is not limited to the Jæren area, and glacio-marine clays have later been found at a high elevation close to Hjelmeland (Figure 1).

Riis (1996) suggested a significant Pliocene-Pleistocene uplift of southern Norway and a corresponding subsidence of the North Sea, based on the relations along the offshore Base Quaternary angular unconformity.

The new offshore seismic lines indicate that the basement surface topography south of Karmøy is controlled by Late Paleozoic to Early Triassic normal faults which may have been reactivated later in the Mesozoic. Between Jæren and Lista, the main faults trend NW-SE. The thick Quaternary deposits of the lowlands of Jæren and Lista seem to fill basins which were formed by exhumation of pre-existing narrow Paleozoic/Mesozoic tectonic basins (line NPD-SK95-6, Fig. 5.1.3). A direct correlation between these Quaternary deposits and the Quaternary sediments of the Norwegian Channel is very difficult when based on seismic data alone, and any post-depositional vertical movements would be difficult to prove.

No obvious tectonic deformation of the Quaternary sediments has so far been observed in the seismic lines, although many seismic lines show conspicuously tilted layers along the eastern boundary of the Norwegian Channel (Fig. 5.1.3). In Fig. 5.1.3, the basement horst between sp. 3550 and 3700 has a surface dipping towards the Norwegian Channel. The surface is interpreted to be an originally horizontal surface which has been subsequently tilted, and where the Mesozoic sedimentary cover has been stripped off. The slope of the Quaternary sediments adjacent to the horst is parallel to the tilted basement surface. This slope could be explained as a recent tectonic tilt, while alternative explanations would be sediment draping of the underlying surface, possibly combined with glacio-tectonic deformation.

At the present stage, sedimentary draping is thought to be the simplest and best explanation. It is possible that a more detailed investigation along the inner margin of the Norwegian Channel, e.g. the onlap patterns on the basement horst, may reveal features with a probable tectonic origin.

In conclusion, the data can be fitted into a model where both the terrain boundary itself and the highly elevated marine clays are explained in terms of glacier erosion and glacio-isostatic depression and rebound. The pattern of erosion was controlled by Paleozoic and Mesozoic basins and basement horsts. However, this model does not exclude the possibility of a neotectonic component in additional to the major glacio-isostatic events which caused the main vertical motion of the region.

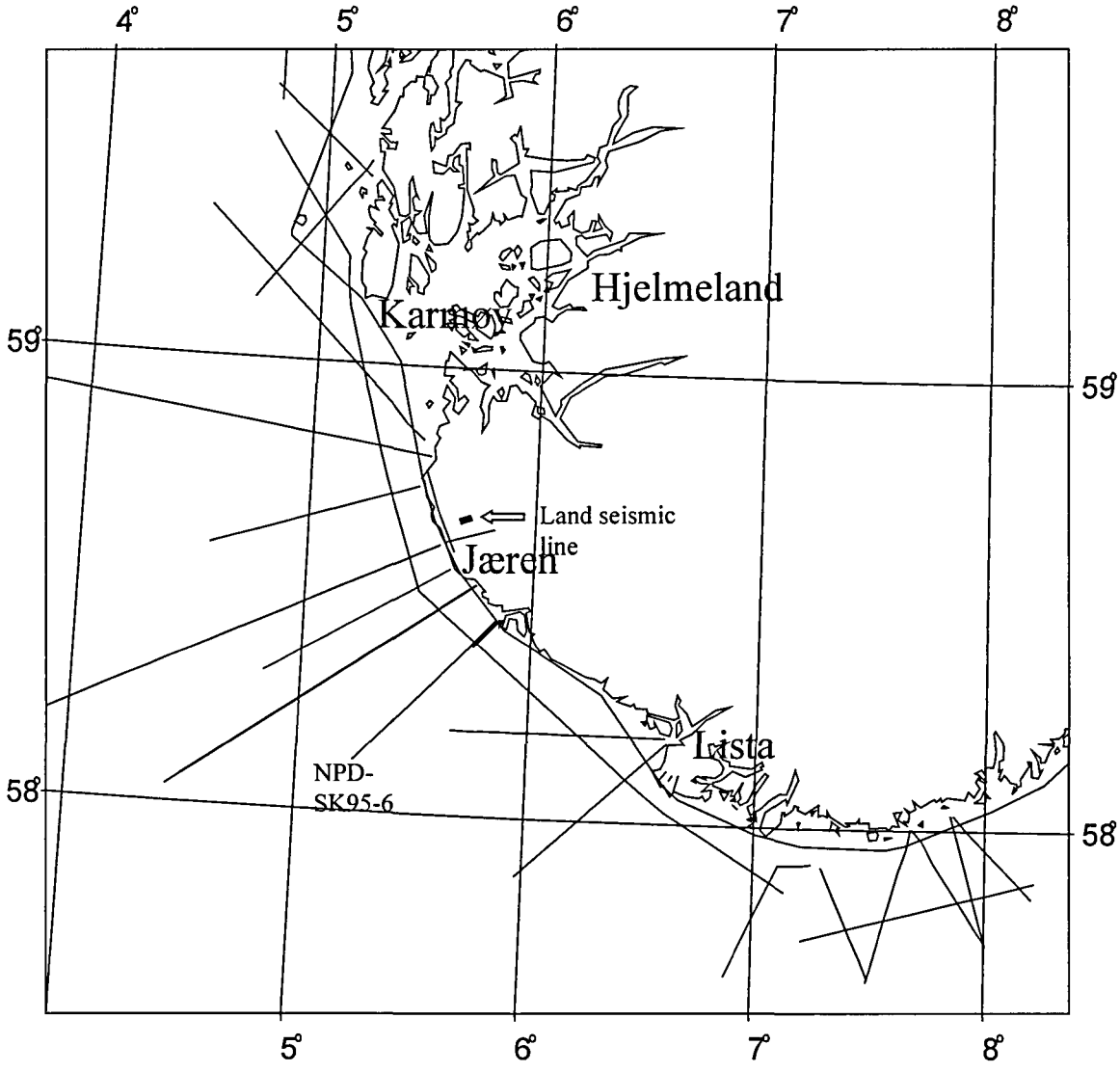

Fig. 5.1.1. Data coverage of NPD-SK95 survey, Jæren area, including land seismic lines. Locations of Figs. 5.2.2 and 5.2.3 are indicated by heavy lines.

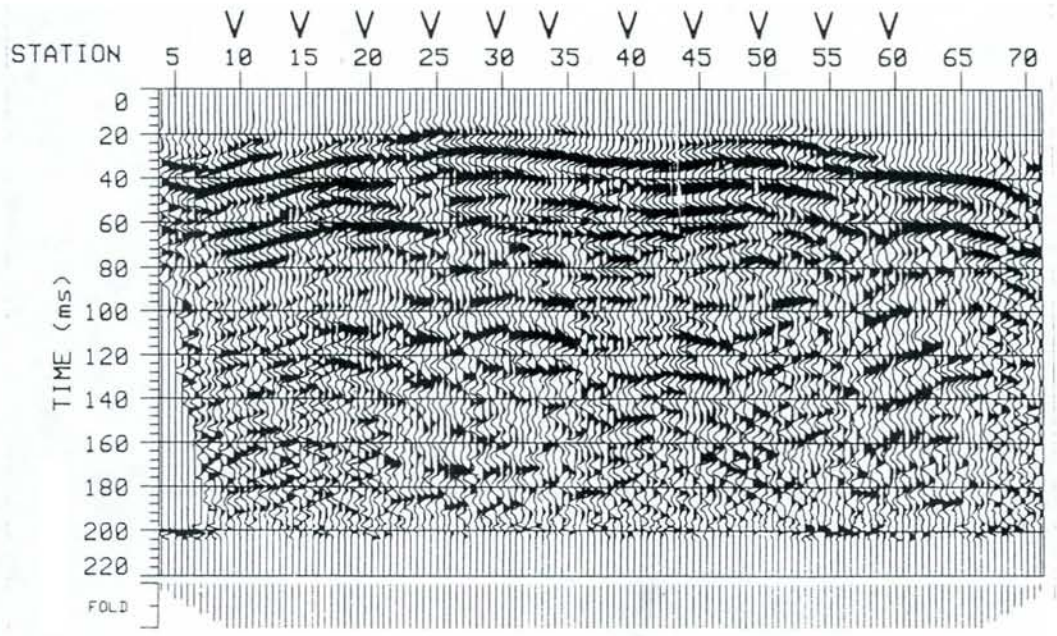

Fig. 5.1.2. Seismic line crossing the onshore lineament between Låg-Jæren and Høg-Jæren. The location is shown in Fig. 5.1.1. The basement is interpreted at approximately 120 ms, and a fault in the lower part of the Pleistocene section is indicated between stations 55 and 60.

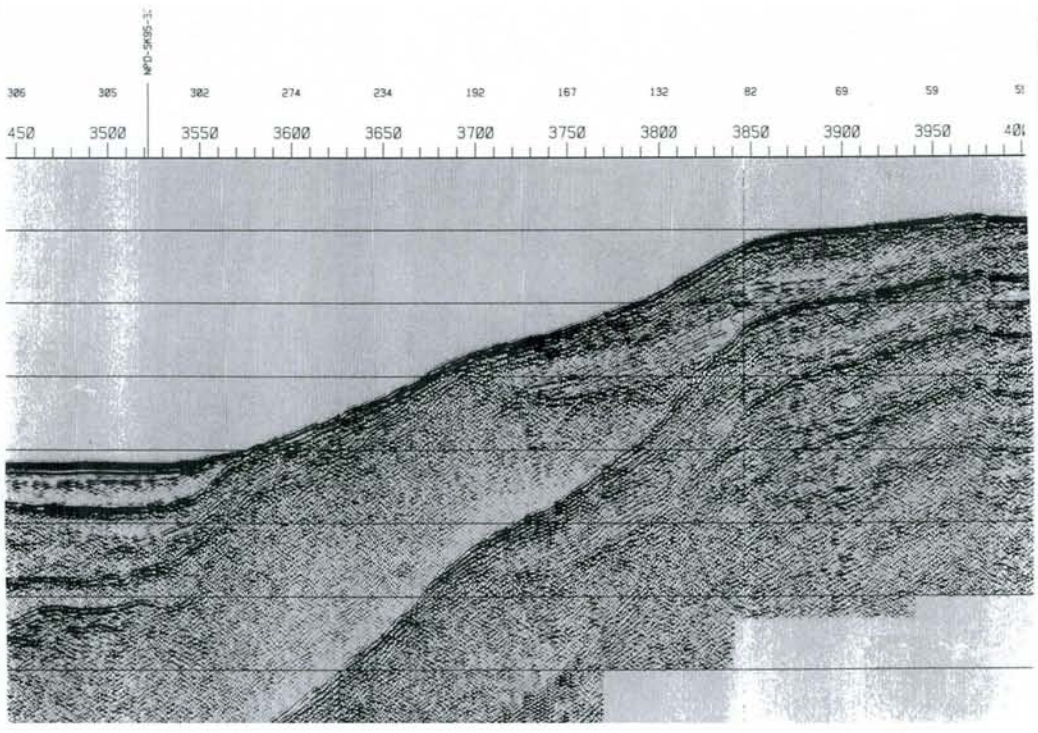

Fig. 5.1.3. Seismic line (NPD-SK95-6) south of Jæren indicating exhumation and Quaternary infill of a Paleozoic or Mesozoic basin. The location is shown as a heavy line in Fig. 5.1.1. A tilted basement horst is located between shot points 3560 and 3710. The landward basin is filled with Quaternary sediments with a conspicuous dip away from the coast. The fault at SP 3560 could be interpreted with a Quaternary reactivation, but other explanations are possible.

5.2 GROUND-PENETRATING RADAR PROFILES ACROSS POSTGLACIAL FAULTS AT KÅFJORD, TROMS AND FIDNAJOHKA, FINNMARK

By Eirik Mauring, Odleiv Olesen, Jan Steinar Rønning and Jan Fredrik Tønnesen, NGU

5.2.1 Introduction

Ground-penetrating radar (GPR) measurements have been carried out across presumed postglacial faults at Kåfjord, Troms and Fidnajohka, Finnmark, Norway. The work is a part of the NEONOR (Neotectonics in Norway) project, which is financed by NGU, Amoco, Phillips, Norsk Hydro, Statkraft, Oljedirektoratet, Statens Kartverk, Norges Forskningsråd and NORSAR.

The purpose of the measurements was to map the subsurface extension of the faults, and to clarify whether the Nordmannsvik fault (Kåfjord) is a gravitational induced fault or a true tectonic postglacial fault. The measurements were carried out by Jan Steinar Rønning (Fidnajohka, 7/7-1997) and Jan Fredrik Tønnesen (Kåfjord, 29/9-1997). Processing was carried out by Eirik Mauring. Interpretation of GPR records was done by Odleiv Olesen, Jan Fredrik Tønnesen and Eirik Mauring.

5.2.2 Instrumentation and data acquisition

GPR measurements were carried out along three profiles at Kåfjord and one profile at Fidnajohka. Common mid-point (CMP) records were obtained for velocity analysis and depth conversion of the GPR records. Measurements were carried out using pulseEKKO IV GPR system at Fidnajohka and pulseEKKO 100 GPR system at Kåfjord (both manufactured by Sensors & Software Inc., Canada). Transmitter frequency and voltage were 50 MHz and 1000 V respectively. The antennae separation was 1 m and the station interval was 0.5 m. Profile information and additional acquisition parameters are listed in Table 1.

Table 1: Profile information and acquisition parameters.

Location	Profile #	Profile length (m)	Sampl. Int. (ns)	Recording time (ns)	Stacks
Kåfjord	1	125.5	1.6	1200	16
Kåfjord	2	210.5	1.6	1200	16
Kåfjord	3	200	1.6	1200	16
Fidnajohka	807	175.5	1.6	1000	32

5.2.3 Processing

CMP measurements were carried out for velocity analysis. At Kåfjord, the correct CMP stacking velocity seems to be c. 0.11 m/ns, while it is 0.10-0.11 at Fidnajohka. A velocity of 0.10 m/ns was selected for depth conversion at the latter locality.

After data acquisition, the GPR records were terrain corrected. At Kåfjord, elevations were read from a map in scale 1:50 000. Small terrain variations were corrected for using elevation information from comments on the GPR records. At Fidnajohka, levelling of the profile has

previously been performed. During plotting, a stepwise linear gain was applied to the data in addition to 5-point stacking along traces to reduce high-frequency noise. This report also offers alternative presentations of the records using trace difference. In trace difference, the differences of neighbouring traces are presented in order to enhance dipping reflectors.

5.2.4 Results

Kåfjord

As mentioned earlier, one of the objectives of the investigations at Kåfjord is to try to determine whether the Nordmannsvik fault is a gravitational induced fault or a true tectonic postglacial fault. Varnes et al. (1989) suggest that gravity induced sliding is most likely to occur when the elevation difference is greater than 300 m. At Kåfjord, the slope of the terrain is 10-12°, and the elevation difference between the fault scarp and the valley bottom is 150-200 m. Thus, gravitational sliding seems less likely, but still has to be considered.

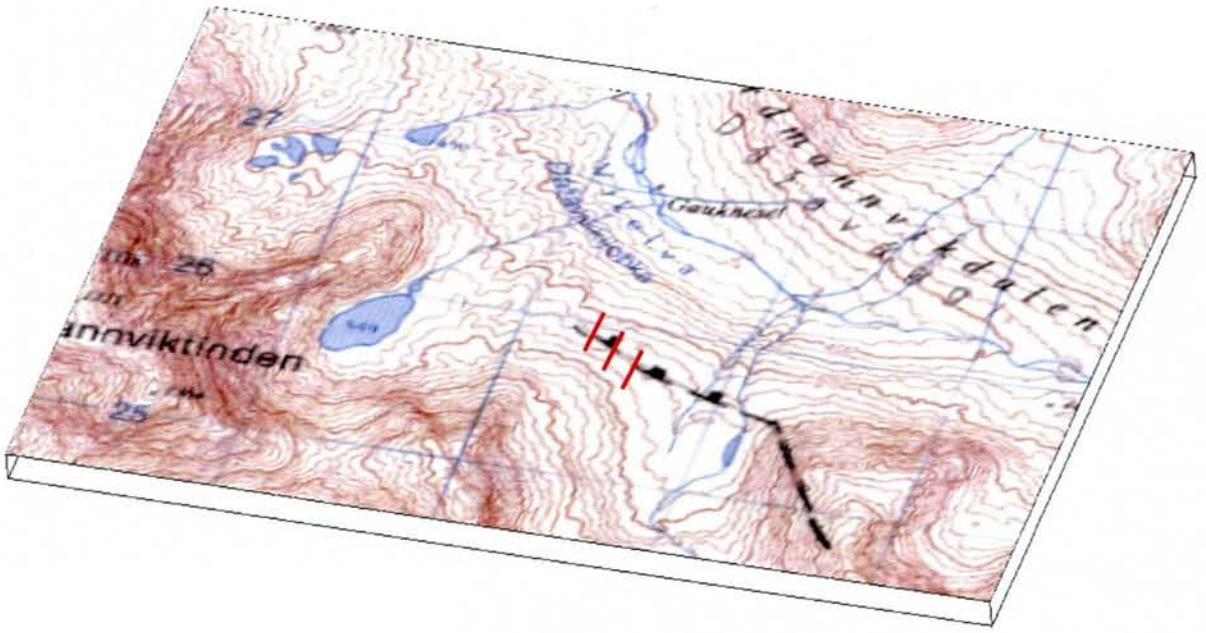

Figure 5.2.1. Location of the three GPR profiles across the Nordmannsvik fault. Shown in red from NW to SE are profiles 1, 2 and 3.

P1

The record is shown in Fig. 5.2.2. Possible bedrock surface can be seen as a reflector subparallel to the terrain surface at depths of 5-10 m. The reflector is not very distinct, due to small contrasts in permissivity between bedrock and the overburden, which in turn indicates that the water saturated zone lies deeper than the overburden/bedrock interface. There is normally a large permissivity contrast between water-saturated overburden and bedrock.

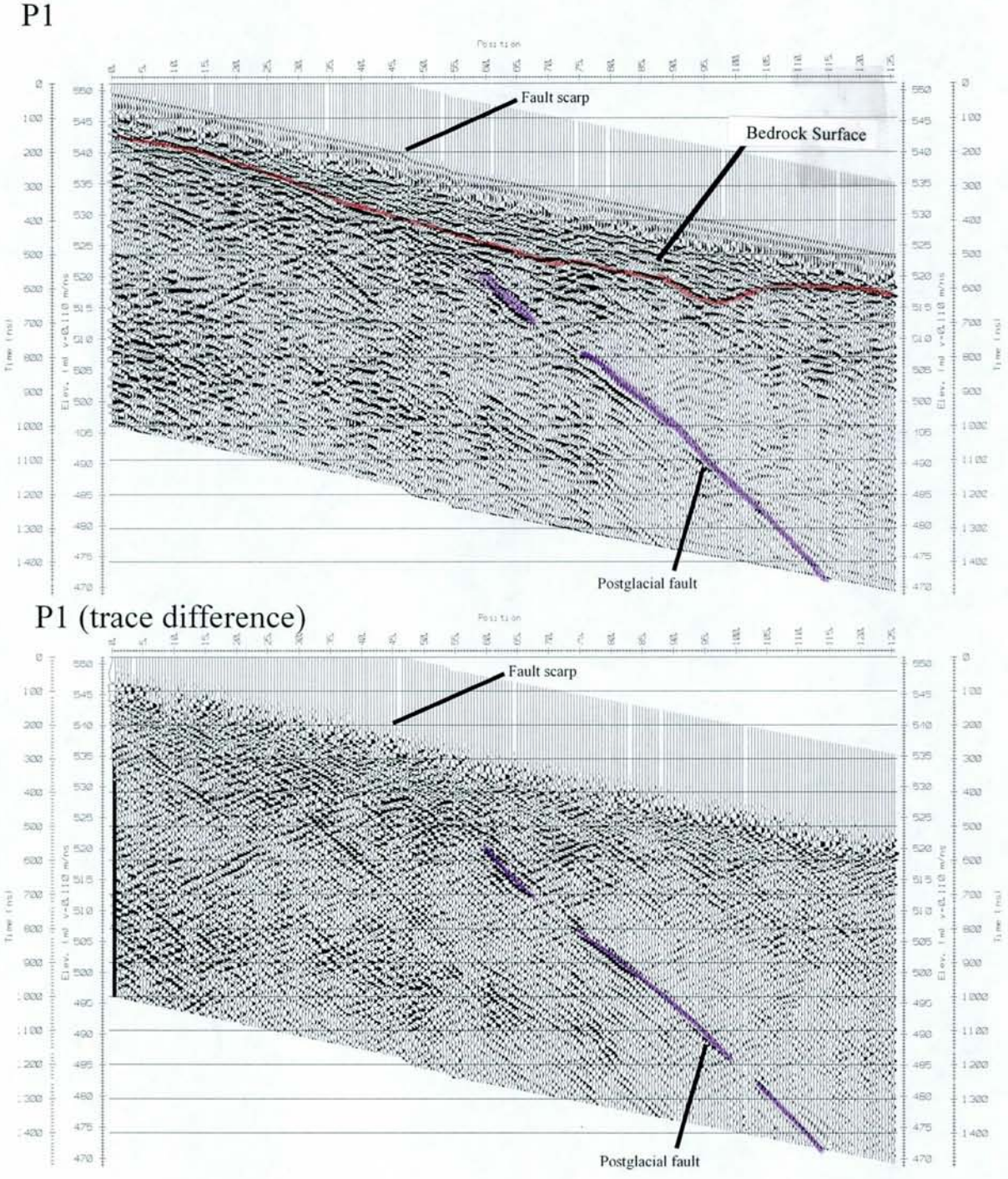

Fig. 5.2.2. Terrain corrected GPR profile 1 at Kåfjord. Top: GPR record, 'normal' presentation. Bottom: GPR record with trace difference applied.

Several dipping reflectors can be seen in bedrock. These could represent foliation or fracturing. The former is less likely, since structural observations in a small stream c. 500 m to the east show that the dip of foliation is c. 10° towards the north-east. This is much gentler that can be observed on the record (see below). An abrupt offset in the terrain surface between position 45 and 50 corresponds with the position of the up-dip extrapolation of the most prominent reflector between position 55 (525 m.a.s.l.) and 115 (471 m.a.s.l.). This could indicate that the dipping reflector represents a structure that has been active during Holocene (i.e. postglacial activation). The dip is fairly constant towards depth (a migrated dip of c. 48° to-

wards the north-east). This is in favour of tectonic faulting, since a gravitational induced slip interface is expected to become more gently dipping towards depth (Varnes *et al.* 1989). Still, the profile should be extended towards the valley bottom to the north-east to see whether the structure can be followed back up towards the terrain surface. This would be the case of a gravitational induced slip. A preliminary interpretation of the structure is that it represents a normal, listric, postglacial fault.

The trace difference record enhances the dipping reflectors. On this record, several dipping reflectors can be seen. Some of them can be followed across just a few traces and should be considered as artefacts of the trace difference processing. Others could represent fractures/faults that have not been activated after the last deglaciation. An example of these could be a reflector that can be followed from position 25 (530 m.a.s.l.) to position 85 (480 m.a.s.l.).

P2

The 'normal' and trace difference records are shown in Fig. 5.2.3. Top of bedrock can be seen as a reflector at depths of 5-10 m in the upper record ('normal' presentation). Two dipping reflectors are prominent. Both have a migrated dip of c. 50° towards the north-east. The one farthest to the north-east (position 125 to 180) probably has a terrain surface expression in terms of an elevation offset between position 120 and 125 which corresponds to the surface feature discussed for profile 1. In fact, the feature can be followed continuously between the two profiles. The corresponding dipping reflector is interpreted to have a postglacial activation. The dip is fairly constant towards depth, again indicating tectonic faulting. The prominent, dipping reflector to the south-west (position 50 to 105) does not have a surface expression, indicating that this structure has not been activated during Holocene.

A gently dipping reflector can be followed more or less continuously from position 25 (538 m.a.s.l.) to position 180 (505 m.a.s.l.). The reflector seems to cut through steeper dipping events, and the most plausible interpretation is that it represents the groundwater table. The undulating appearance can in some places be due to insufficient topographical correction. A possible hydraulic head drawdown can be seen between position 135 and 145 (514 m.a.s.l.). This could be an effect of a very permeable fault zone.

The trace difference record shows distinctive diffraction patterns from the upper termination of the presumed postglacial fault. This is further evidence for abrupt offset of the bedrock surface due to fault movement.

P2

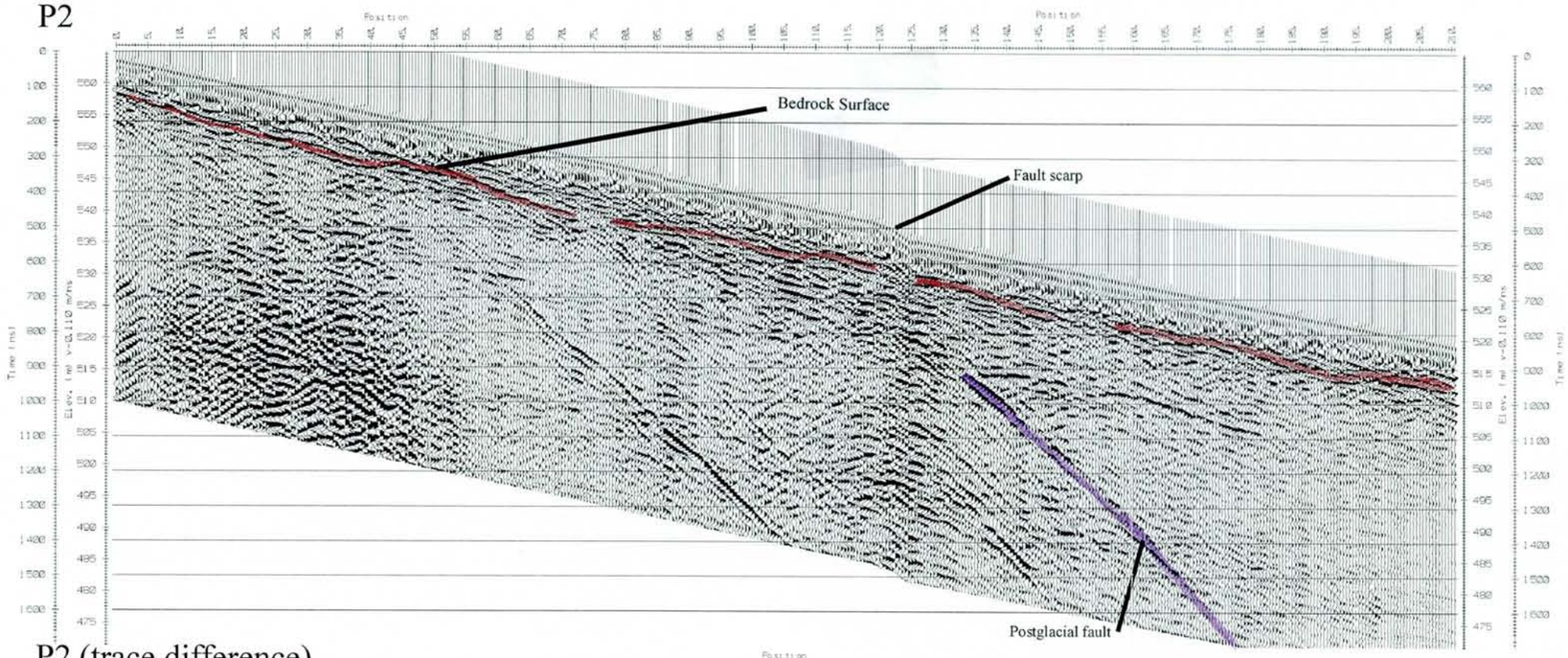

P2 (trace difference)

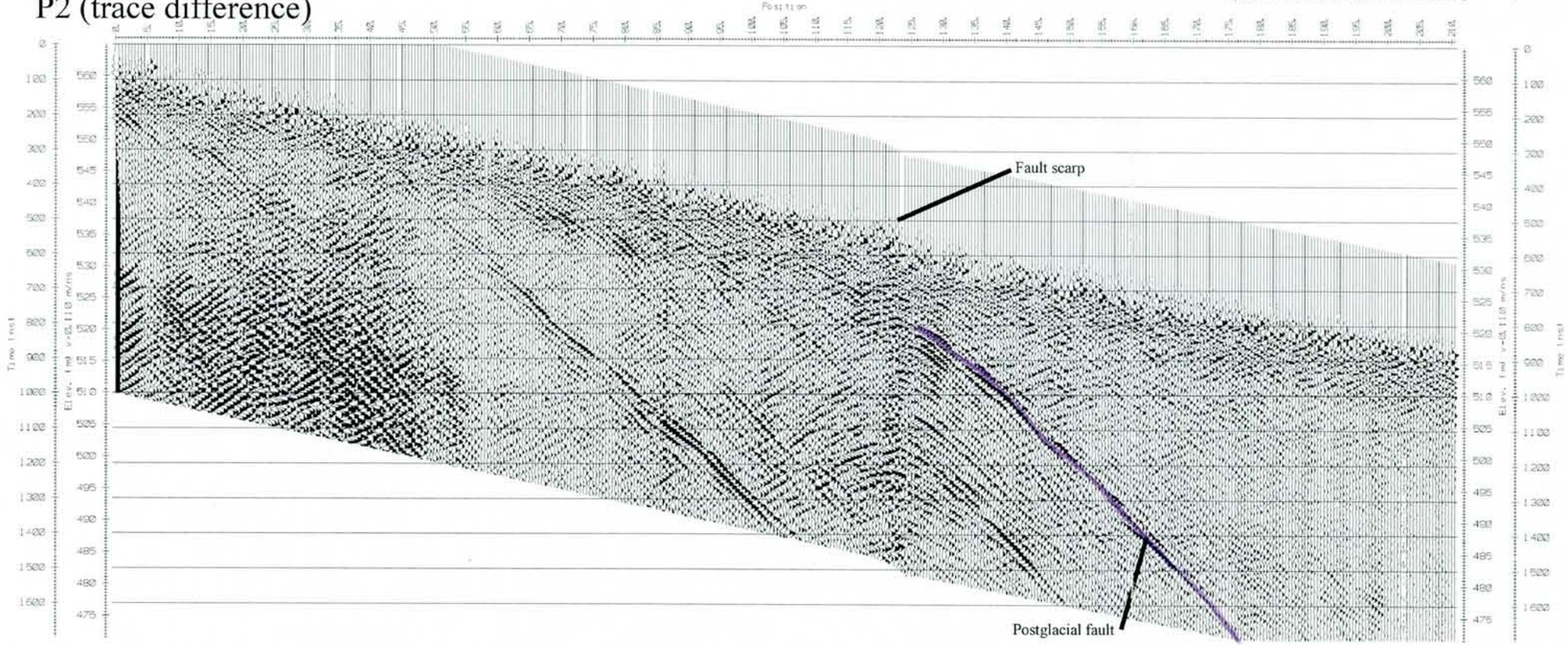

Figure 5.2.3. Terrain corrected GPR profile 2 at Kåfjord. Top: GPR record, 'normal' presentation. Bottom: GPR record with trace difference applied.

P3

Possible bedrock can be seen as gently dipping reflectors at depths of 5-10 m. The most prominent dipping reflectors can be seen in the south-western part of the profile. However, these do not seem to have a surface expression. Most likely, they represent fractures/faults that have not been active during Holocene. A fainter, dipping reflector can be seen between position 100 (517 m.a.s.l.) and 115 (502 m.a.s.l.). This reflector probably represents a fault having its surface expression at position 85-90 in terms of an elevation offset, which can be traced continuously to profiles 1 and 2. As concluded for these profiles, the fault probably has been active after the last deglaciation. The reflector can be followed further towards depth on the trace difference processed record. Although it is very faint, it can be seen to have a more gentle dip towards depth. This could be in favour of both tectonically and gravitationally induced faulting. As mentioned earlier, a prolonging of the profile towards the valley bottom to the north-east could shed some light on the possibility that the fault could be gravitational induced. Gently dipping reflectors can be seen between position 75 (519 m.a.s.l.) and 90 (515 m.a.s.l.), and between position 115 (503 m.a.s.l.) and 175 (491 m.a.s.l.). These resemble the reflector interpreted as the groundwater table in profile 2, but appear at a different elevation level. Also, they are discontinuous and have an offset between position 90 and 115. Another reflector with the same dip can be seen between position 45 (501 m.a.s.l.) and 85 (493 m.a.s.l.). The dip of these reflectors is c. 10°, which corresponds with the observed foliation from surface mapping (Zwaan, in prep.). The reflectors could represent fracturing parallel to the foliation in this area, but this is still far from conclusive.

Fidnajohka, Masi

This area has been subject to previous extensive geophysical investigations (Olesen *et al.* 1990a, 1990b, 1992a). The presence of a postglacial fault is evident in this area. The fault is named the Stuoragurra fault, and can be traced in a SW-NE direction for 80 kilometers. The fault has a reverse sense of movement. Previous GPR measurements with a 400 V transmitter (Olesen *et al.* 1992a) failed to delineate the subsurface extension of the postglacial fault. A more powerful transmitter system (1000 V) has now been utilised to try to delineate the fault.

A GPR profile has been measured along profile 807. From position 160 (level 5 m) to position 235 (level -15 m) a very distinct, gently dipping reflector can be seen. Refraction seismics and percussion drilling (Olesen *et al.* 1992a) show that this reflector represents the bedrock surface. Another (fainter) dipping reflector can be seen from position 151 (level 2 m) to position 177 (level -10 m). This reflector is enhanced on the trace difference record, and it appears shallower towards the terrain surface. Due to limited penetration, it cannot be followed far towards depth. Drillhole 5 cut the postglacial fault at a depth of c. 25 m along the drillhole, whereas the reflector on the GPR record is shallower (16-17 m). The dip of the foliation and postglacial fault is c. 30° (Olesen *et al.* 1990a, 1990b, 1992a), which is about the same as the dip of the reflector. Although the reflector doesn't depict the position of the postglacial fault, it probably represents a shallower fracture associated with the faulting. The 'ringy' reflection pattern between position 145 and 150 is probably due to very moist surface conditions.

5.2.5 Conclusions

GPR measurements have been carried out across presumed postglacial faults at Kåfjord, Troms and Fidnajohka, Finnmark, Norway. The purpose of the measurements was to map the subsurface extension of the faults, and to clarify whether the Nordmannsvik fault (Kåfjord) is a gravitational induced fault or a true tectonic, postglacial fault.

At Kåfjord, three GPR profiles have been measured across a linear terrain feature in till expressed as an elevation offset. The GPR records show that the feature is a surface expression of a structure dipping 45-50° towards the north-east. For two of the profiles (P1 and P2), a relatively constant dip of the structure towards the north-east indicates tectonic faulting. Profile 3 shows a gentler dipping of the structure towards depth which is in favour of gravitational induced faulting. To try to resolve this ambiguity, further investigations should include prolonging GPR profiles 2 and/or 3 to the valley bottom in the north-eastern direction, to investigate the possibility of a gravitational induced fault. Also, a more extensive structural geological mapping programme should be carried out in the area.

At Fidnajohka, a postglacial, reverse fault has been subject to previous extensive investigations. One GPR profile has been measured across the central part of the structure. The GPR record delineates a structure parallel to the dip of the foliation and postglacial fault, which may represent a fracture associated with faulting.

5.3 MARINE GEOLOGIC INVESTIGATIONS OF NEOTECTONIC FEATURES IN THE RANA AND TJELDSUNDET AREAS

By Oddvar Longva, Leif Rise and John Dehls, NGU

5.3.1 Introduction

Shoreline displacements or earthquake episodes which may indicate neotectonic movements, have been reported in both the Rana area, Nordland county, and Tjeldsundet area, Troms county. To study these, reflection seismic profiling was performed

5.3.2 The Rana area

A vigorous earthquake in Rana in 1819 led to rockfalls and landslides, and standing waves were reported from large distances of the fjords in the area (summarized in Olesen *et al.* 1994). Standing waves could have been generated by strong local crustal movements or by slides triggered by the earthquakes.

In order to test if sediments were faulted by neotectonism or if slides related to neotectonism could be seen, a seismic survey was done in selected fjord areas in Rana (Fig. 5.3.1)

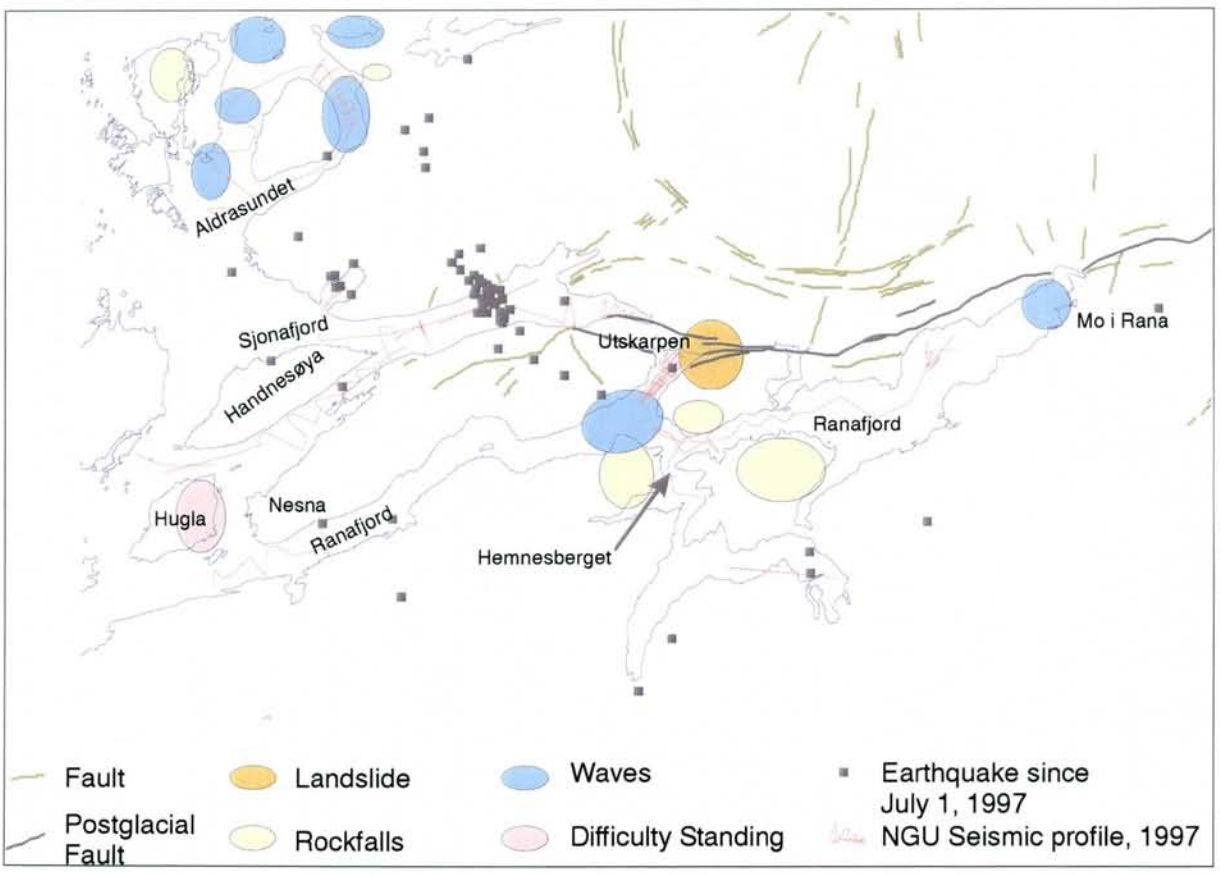

Fig. 5.3.1 Seismic tracklines from cruises 9704 and 9707 in the fjords of the Rana area. Standing waves reported after the 1819 earthquake are marked by blue ellipses (Muir Wood 1989b). Earthquakes registered by NORSAR since July 1997 are marked by black dots.

Methods

The cruises in Rana were performed by NGU's vessel "Seisma" in weeks 32, 33 and 40. The seismic sources used were primarily TOPAS, an ultra-high resolution (down to dm level) parametric source and secondly Geopulse Boomer, a high resolution seismic source (< 1 ms). Two lines were performed by a 15 cubic inch Sleevegun, a medium resolution seismic source. All seismic data was plotted on an EPC 9800 analogue printer and simultaneously taped digitally in TOPAS format, which later has been reformatted into SEGY.

Results

The seismic records have been studied. No (or perhaps one weak evidence of) neotectonic displacement of sediments related to faults has been found. A number of sediment slides have been recorded and there is evidence of slides everywhere where standing waves were reported in 1819 (Fig. 5.3.1). The ages of these slides are not known, but the stratigraphic positions indicate that some of them are fairly young.

Regional interpretation of seismic records

Utskarpen

Lines 9704001 - 9704004 (TOPAS, 001 sweep 250 ms, 002 - 004 sweep 125 ms)

These lines cover the bay of Utskarpen. A landslide was triggered onshore by the 1819 earthquake. The bay is characterised by thick glacial marine and marine sediments interrupted by slide deposits (Fig. 5.3.2). The frequency of slides is highest in the upper part of the sediments, most likely of Holocene age. The sediment succession has a marked slide escarpment with a gradient of c. 15 ° towards the steep side of the main fjord, the Ranafjord. No faults are seen.

Hemnesberget

Lines 9704005 - 9704007 (005 TOPAS, sweep 125 ms, 006 and 007 Boomer, sweep 250ms)

These lines run from the south and west of Hemnesberget and into the deepest part of Ranafjorden north of Hemnesberget.

Acoustically layered glacial marine and marine sediments including several generations of slide deposits south and west of Hemnesberget (Fig. 5.3.3) fill the fjord. The slides seem to have occurred both in the late glacial and postglacial time. These deposits are truncated to the north by a sharp slide escarpment tilting c. 15 ° towards the Ranafjord. Several slide units can be distinguished in the deeper part of the Ranafjord.

Ranafjord

Lines 9704008 - 9704010 and 9707016 (Boomer, sweep 500 ms)

These lines run in the central part of the Ranafjord from Hemnesberget towards Mo i Rana. Local basins have acoustically layered sediments. No faults were recognised. An area outside Mo, covered by lines 009 and 010, contained slide deposits in the postglacial unit.

Line 9704016 from the outer part of the Ranafjord south of Nesna, showed acoustically layered sediments without evidences of faults or any indications of slide activity.

Sjona

Lines 9704011-9707012 (TOPAS, sweep 125 ms), 9707017-9704018 (Boomer, sweep 500 ms) and 9707001-9707002 (Sleevegun, sweep 500 ms).

In the inner part of Sjona, on the southern side of the fjord, is a marked cliff with rockfalls, which has been interpreted as a fault escarpment (Olesen *et al.* 1994, Fig. 4.). No neotectonic movements could be seen in sediments below the cliff. Slides from the shallow inner part of the fjord have moved into the deeper part and well-defined slide scars could bee seen.

In the central part of Sjona, covered by lines 970417, 970418 and 9707001 and 9707002, there are no faults or distinct slide units detected. The fjord is deep and side reflections reduced the quality of the records.

Litle Sjona

Lines 9704013-9707014 (TOPAS, sweep 125 ms), 9707015 (Boomer, sweep 500 ms).

Lines 013 and 014 from the sound of Litle Sjona, between Nesna, Hugla and Handnesøya show a shift of sedimentary environment from the late glacial to the postglacial time, with current dependent deposition in the latter. No faults could be detected.

Line 9707015 runs across a Younger Dryas end moraine. Low penetration.

Aldrasundet

Lines 9707019 - 9707020 (Boomer, sweep 250 ms) and 9707021 - 9707022 (TOPAS, sweep 125 ms).

Outer fjord basins south-west of Aldra, have layered sediments, with no indications of faults. In the main sound south-east of Aldra, till covered by current deposits constitutes the sea-bottom. The sound north-east of Aldra is deeper and contains layered sediments, which have been exposed to slide activities. There is one example of disturbances of the seismic layering that may be an effect of faulting or alternatively due to water escape/clastic dike formation (Fig. 5.3.4) (Obermeier 1996). The acoustic layering seems to be broken and the surface may have been slightly warped. However, this disturbance lies within an area where the upper sediments are relatively young slide deposits (Fig. 5.3.5), and the disturbances may be related to sliding.

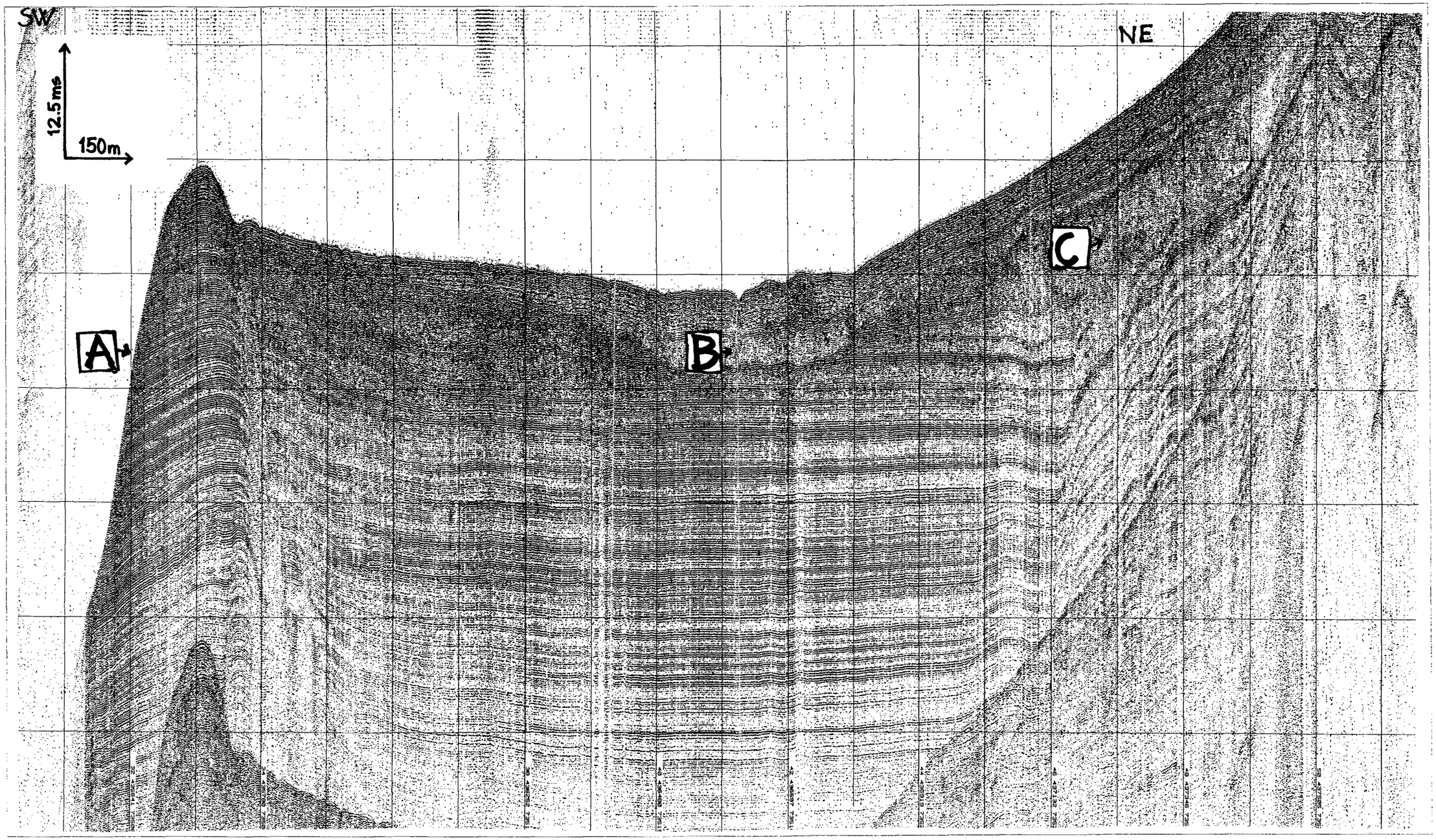

Fig. 5.3.2. Slide escarpment and slide deposits in glacial marine sediments in the bay of Utskarpen. A: marked slide escarpment towards the deep Ranafjord with a gradient of c. 15^{o}, B and C: slide deposits. Seismic line 9704001 (TOPAS registration).

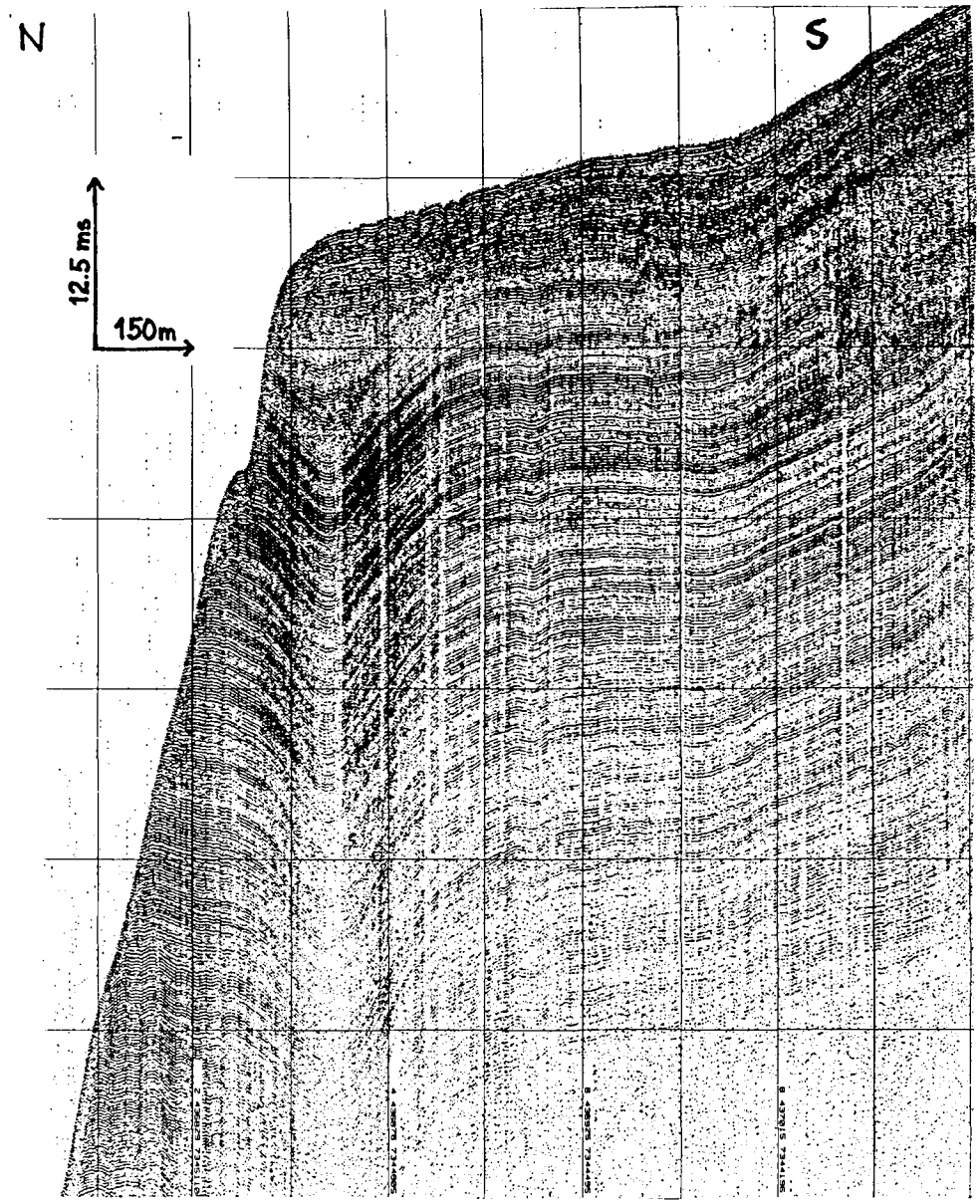

Fig. 5.3.3. Slide escarpment outside Hemnesberget. The slope towards the Ranafjord has a gradient of approximately 15 °. Seismic line 9704005 (TOPAS registration).

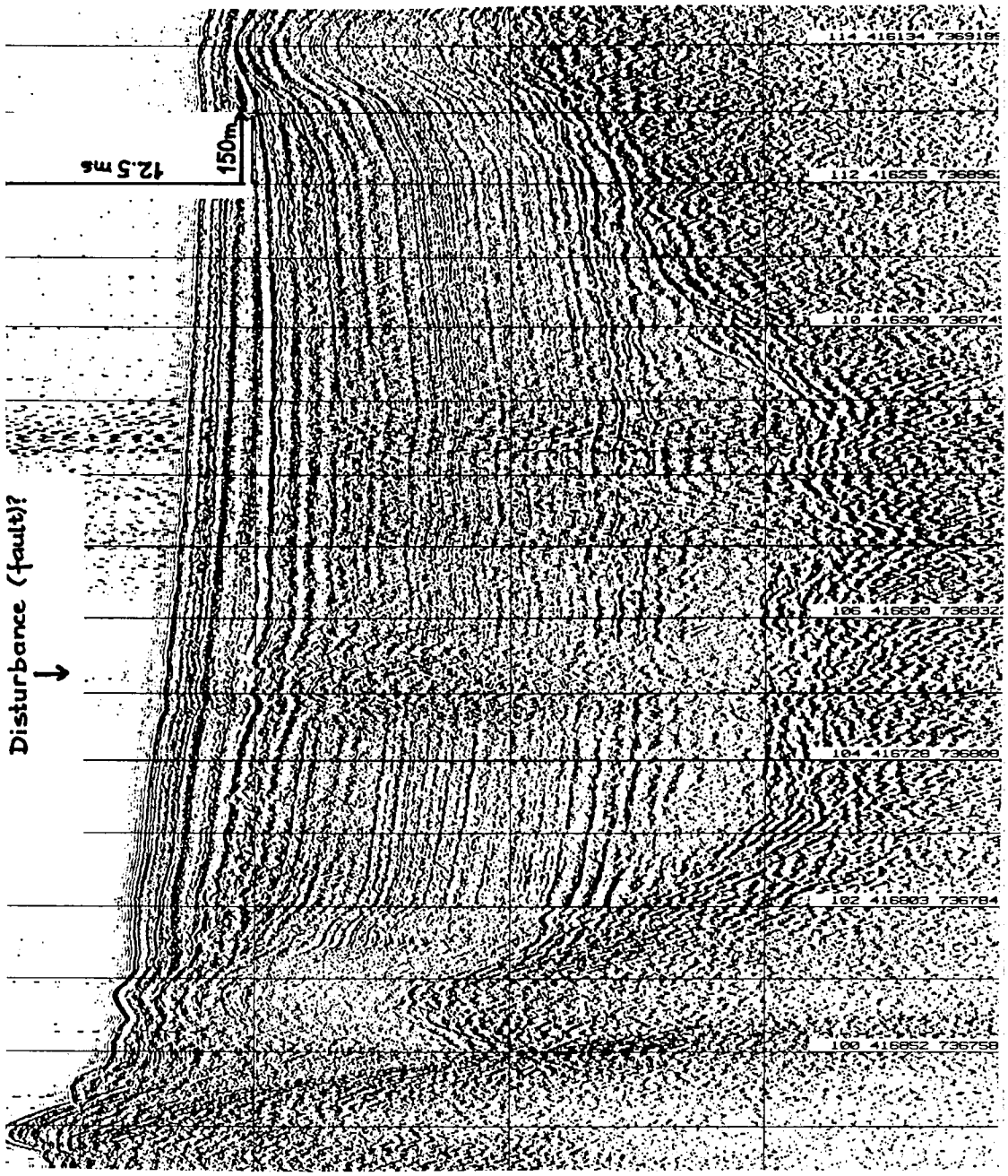

Fig. 5.3.4. Possible water escape/clastic dike formation through glaciomarine sediments in Aldrasundet. Seismic line 9704023 (TOPAS registration).

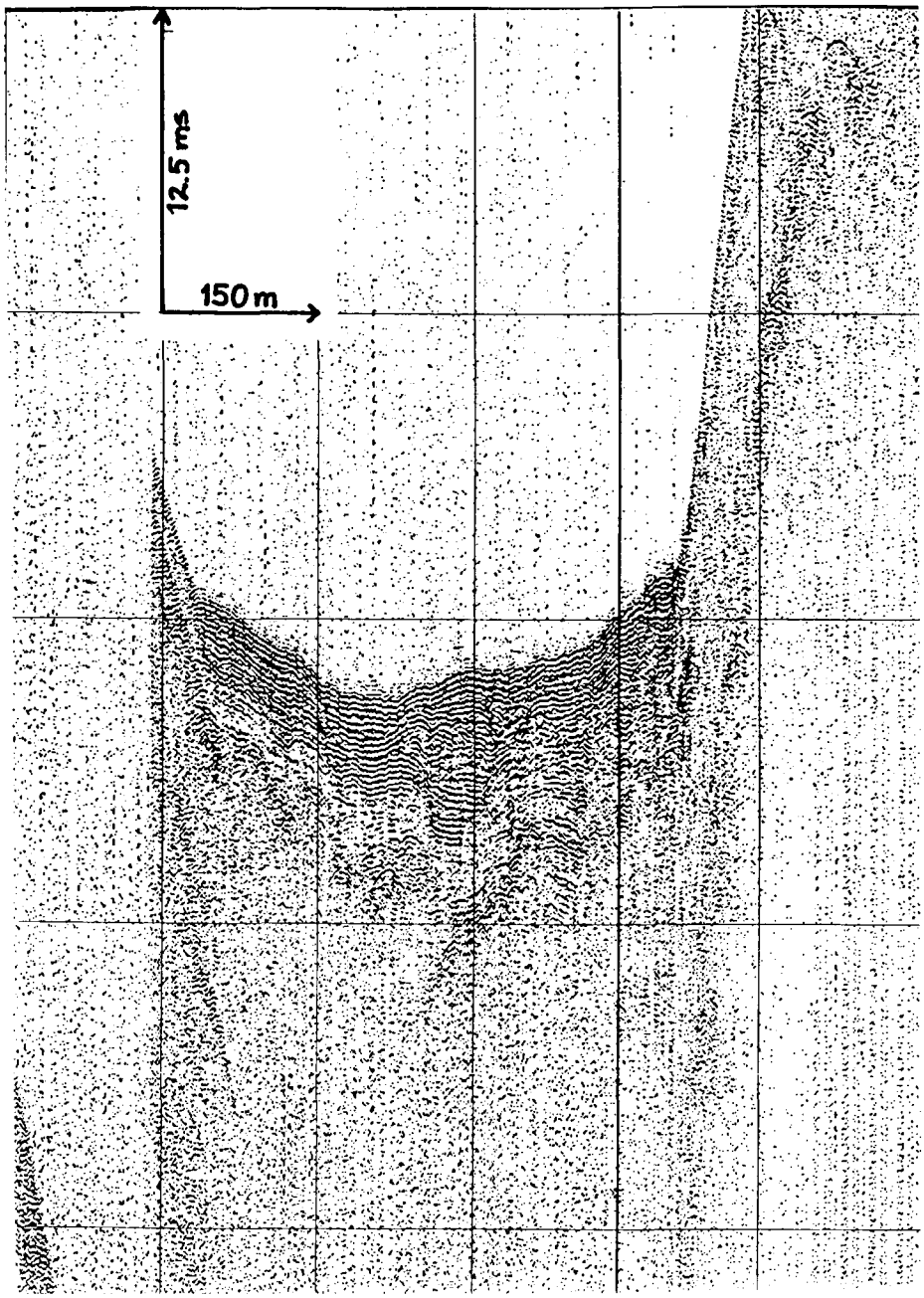

Fig. 5.3.5. Slide deposits in the northern part of Aldrasundet. Seismic line 9704023 (TOPAS registration).

5.3.3 The Tjeldsundet area

In Tjeldsundet, a narrow sound along a tectonic lineament, Grønlie (1922) reported displacements of shorelines across the sound, which he interpreted as due to neotectonic movements along the Tjeldsundet. To test if such movements could be seen by displacements of sediments, a seismic survey and a bathymetric survey were undertaken. Fig. 5.3.6 shows a shaded relief image based on the bathymetry and includes the seismic track-lines.

Methods

The seismic survey, cruises 9704 and 9706, lines 9704023 and 9706010, was done by NGU's vessel "Seisma" utilising high-resolution seismics (TOPAS). The Norwegian Hydrographic Service (SKSK), using their vessel "Sjømåleren" equipped with a Simrad multibeam echosounder (EM 500), did the echosounding.

Results

The shaded relief image (Fig. 5.3.6), based on the bathymetric measurements, shows clearly the tectonic zone of Tjeldsundet, but no neotectonic movements can be detected as escarpments in the sediments along the fault zone.

There are relatively little sediments in the narrowest part of the sound, and the sediments are definitely reworked by strong currents (Fig. 5.3.7). In the deeper and wider parts of the sound the sediment infilling is more extensive (Fig. 5.3.8), but we have so far not been able to detect young neotectonic movements from displacements and disturbance of internal sedimentary structures.

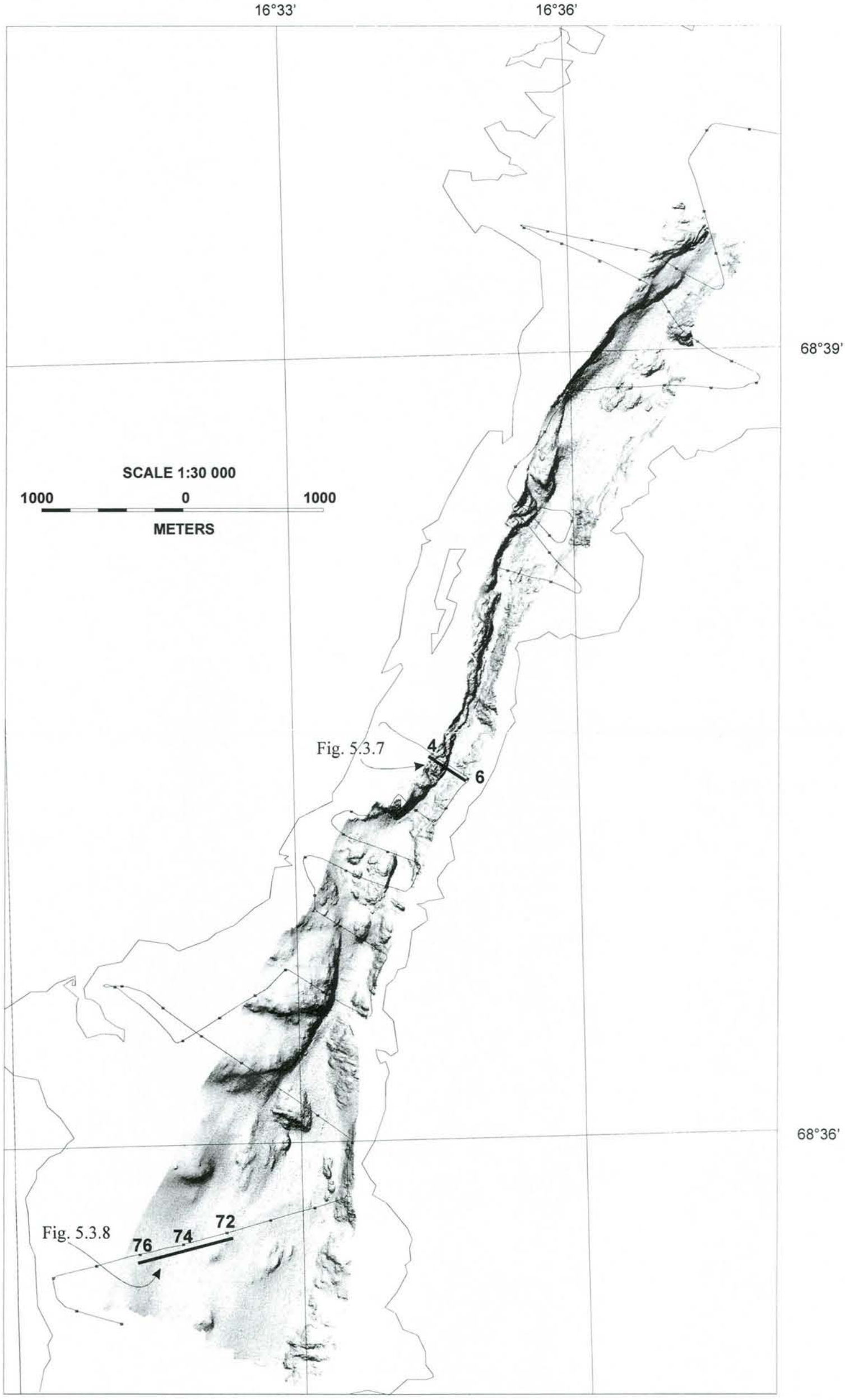

Fig. 5.3.6. Shaded relief image of the Tjeldsundet. The image is illuminated from the north-west and is based on multibeam echosounding bathymetry. The track-lines for seismic profiles 9704023 (northern line) and 9706010 (southern line) are shown (both TOPAS registration). The numbered dots refer to positions annotated on the analogue plots of the seismic lines.

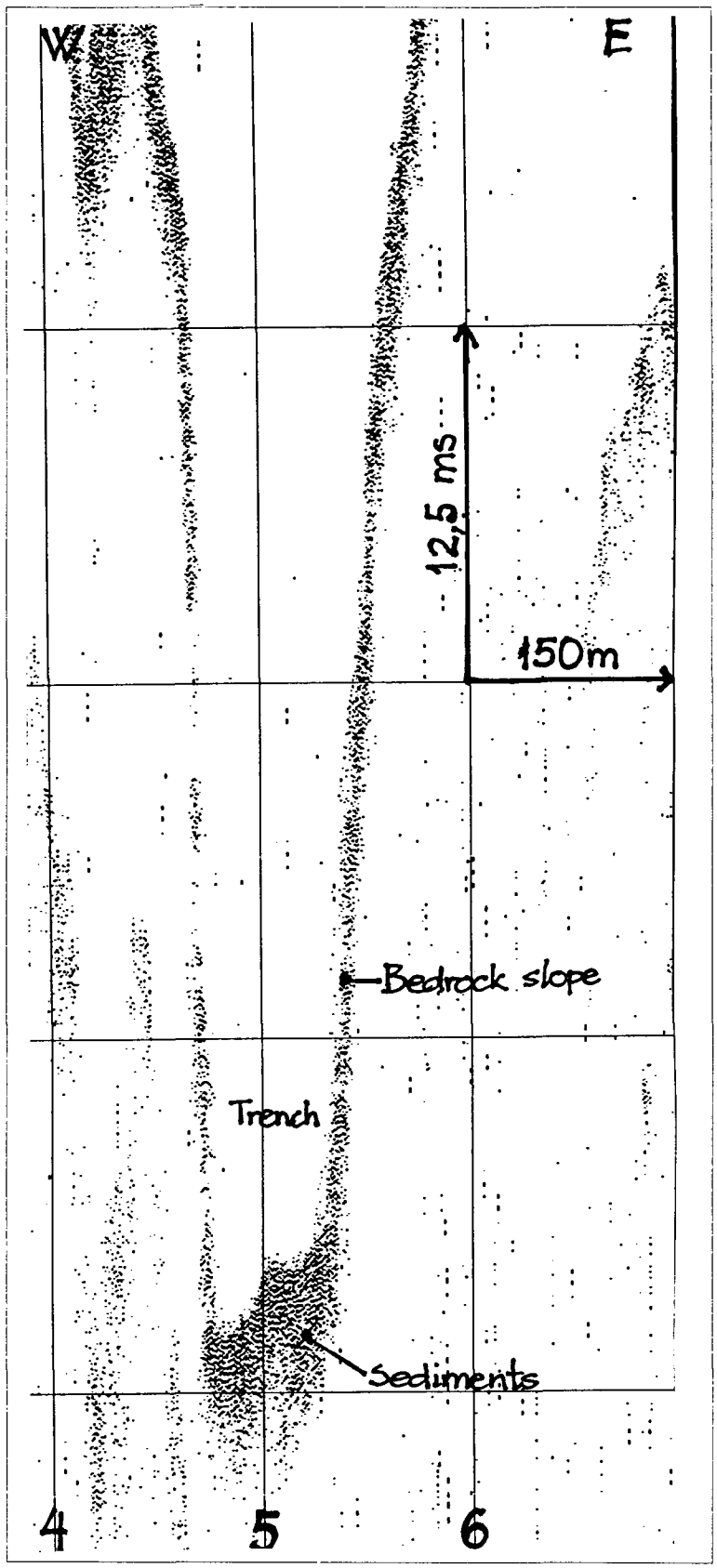

Fig. 5.3.7. The deep trench of Tjeldsundet with steep sides of bare rock and a 2-3 m thick layer of sediments in the center. The sediments show poor acoustic lamination and no faults can be seen. The position of the section is given in Fig. 5.3.6.

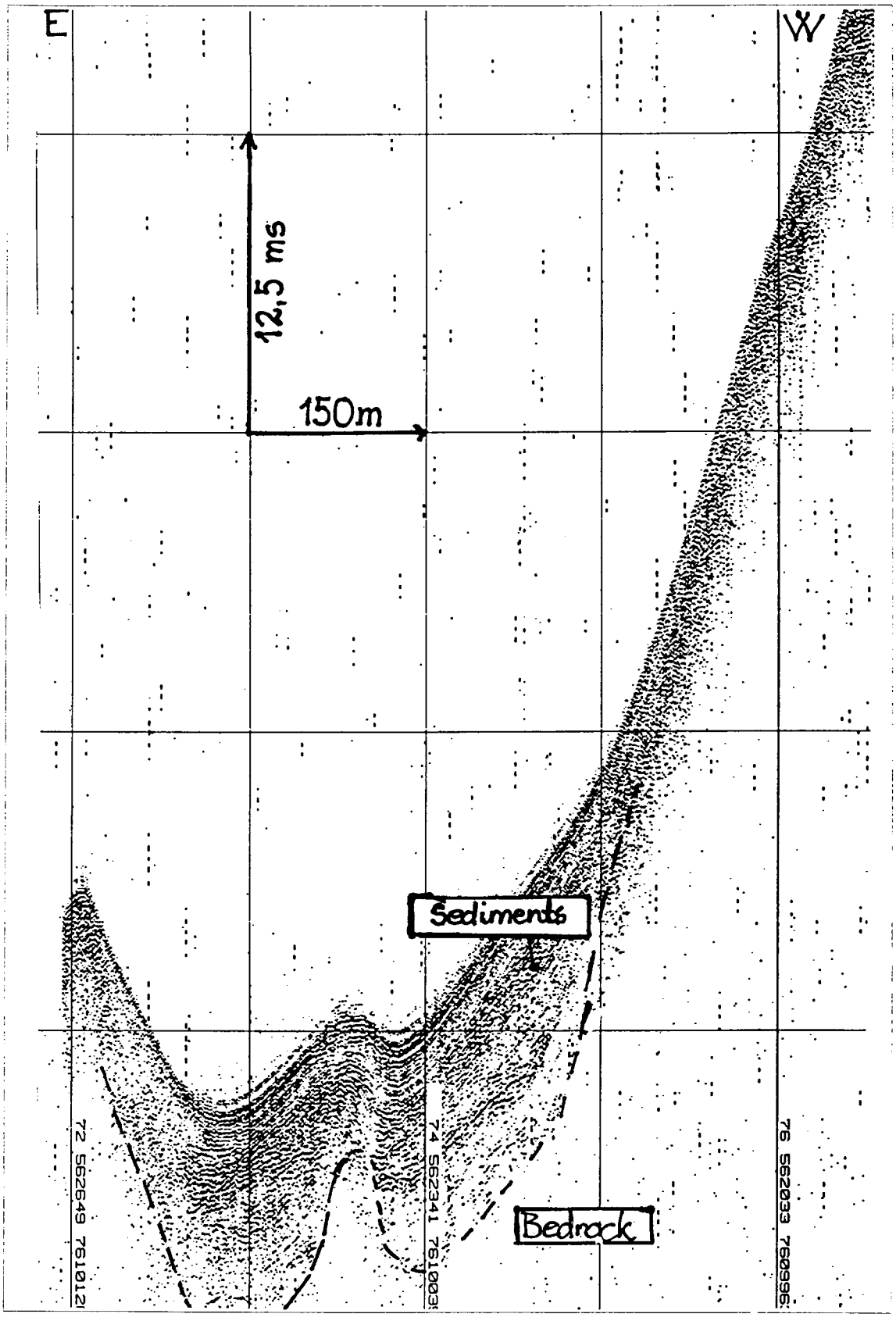

Fig. 5.3.8. Acoustically layered sediments from a wider part of the sound (for location, see Fig. 5.3.6). There are no displacements of the sediments that may indicate neotectonic crustal movements.

5.4 QUATERNARY STUDIES MAINLY IN THE SJONA - RANAFJORDEN AREA WITH SOME ADDITIONAL INFORMATION FROM OTHER AREAS IN NORTHERN NORWAY

By Lars Olsen, NGU

5.4.1 Deformation structures in the Rana area.

In the search for possible earthquake derived indicators in Quaternary loose deposits we have focused on the mapping of deformational structures in sand in the Utskarpen - Straumbotn area (Figs. 5.4.1 & 5.4.2). This area is chosen for two reasons. Firstly, the Båsmoen fault runs across this area (Olesen *et al.* 1994, 1995). Secondly, one of the locations of the major earthquake influences of the 1819 magnitude 5.8-6.2 earthquake (Muir Wood 1989b) in the Ranafjorden area is the area adjacent to the bay of Utskarpen (Heltzen 1834).

During the mapping we have tried to differentiate between two types of deformational structures in sand:

1. ***- Sand with mosaic-like or clast supported conglomeratic structures (Figs. 5.4.3-5.4.5), and***
2. ***- Sand with various kinds of deformational structures different from type 1 (Figs. 5.4.6-5.4.9).***

The cause of type 1 structures is thought to be heavy shaking of sand in water-saturated condition, resulting in partly liquefaction of fine sand and silt, fractionation or breakage of laminae and layers of fine to medium sand, and partly rotation and dislocation of sand clasts produced in this way. A number of processes may have led to structures of type 2, including earthquake, bioturbation, cryoturbation, abrupt change of groundwater flow and groundwater level, and iceberg disruptions and other glaciotectonics.

Heavy shaking of the land surface may be caused by earthquake, abrupt loading on the ground surface as a result of avalanches, rock fall debris, iceberg drop, and modern "heavy traffic," and other mechanisms (explosions, lightening/thunderstorms, etc.). We think that other causes than earthquake can be excluded in 6-7 localities of type 1 sand in the Trøndelag - Nordland region (Fig. 5.4.1), and therefore, in these cases we think that the type 1 deformational structures are diagnostic features of earthquake.

As age control of the deformational events associated with the type 1 and 2 sands in the Sjona - Ranafjorden area, we have used the generalised shoreline displacement for the Elsfjorden - Korgen area to the south (Bergstrøm 1994, Olsen *et al.* 1996). This is a very tentative approach because of the character of the generalised sea-level data (Fig. 5.4.10), and also the low precision of some of the sea-level estimates which is based on altitude relative to present sea-level and inferred water-content in the sand during deformation.

It is possible to draw a much more precise shoreline displacement curve for the Utskarpen - Straumbotn area than mentioned above, but in that case we need C14-dating of marine shells or other organic material which represent the most distinct postglacial sea-level zones. We suggest that such a curve should be worked out during the next year, together with a further mapping of type 1 and 2 sands in the present study area and other selected areas.

The main results from the 1997 field-season, and selected previous background data, are shown in Fig. 5.4.11, which is a frequency diagram of type 1 and 2 sand plotted versus time.

It is clear that the type 2 deformational structures occur in several parts of the Holocene, whereas type 1 occurs only prior to 5000 years before present (BP). Most of the type 1 cases seem to coincide in time with the period of the maximum Tapes transgression some 7000-7500 years BP. With a likely earthquake origin of the type 1 structures it is interesting to notice that the tsunami which is thought to have originated from the same postulated major earthquake which initiated the Storegga submarine avalanche, is dated to ca. 7200 years BP (Bondevik *et al.* 1997). It has been stated that earthquake magnitudes of at least 5.5-6.0 are required to get liquefaction in sand (McCalpin 1996), and it is quite possible that an earthquake of this magnitude is needed to develop deformational structures similar to those of type 1 sand.

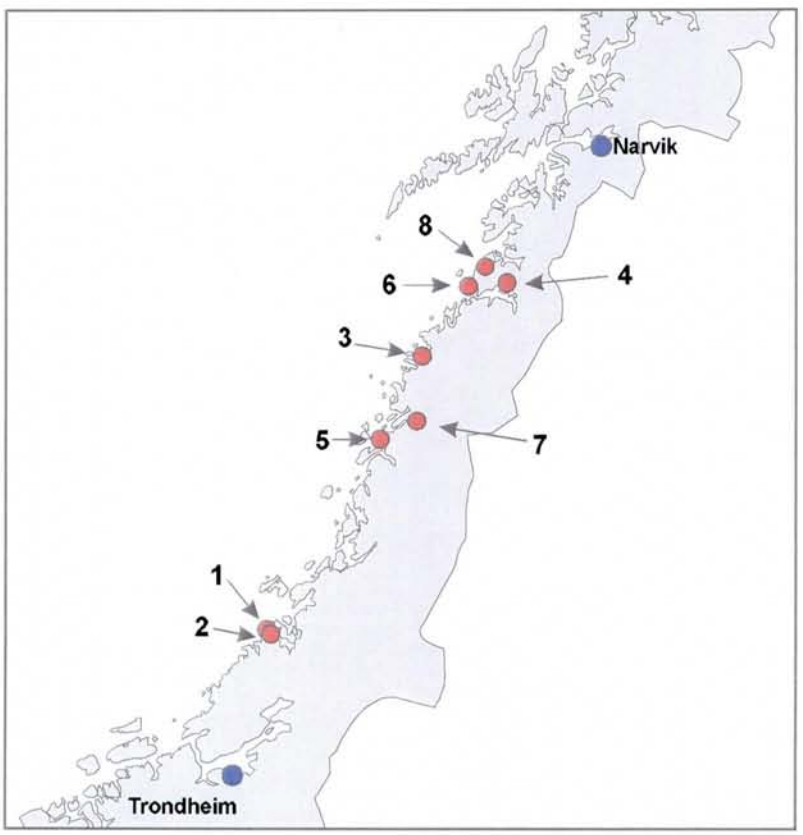

Fig. 5.4.1. Localities (1-8) with occurrences of deformed sand where the deformational event is thought to originate from earthquake activity. Dot no. 7 indicates one such locality in the Utskarpen – Straumbotn area where most of the 1997 fieldwork was done.

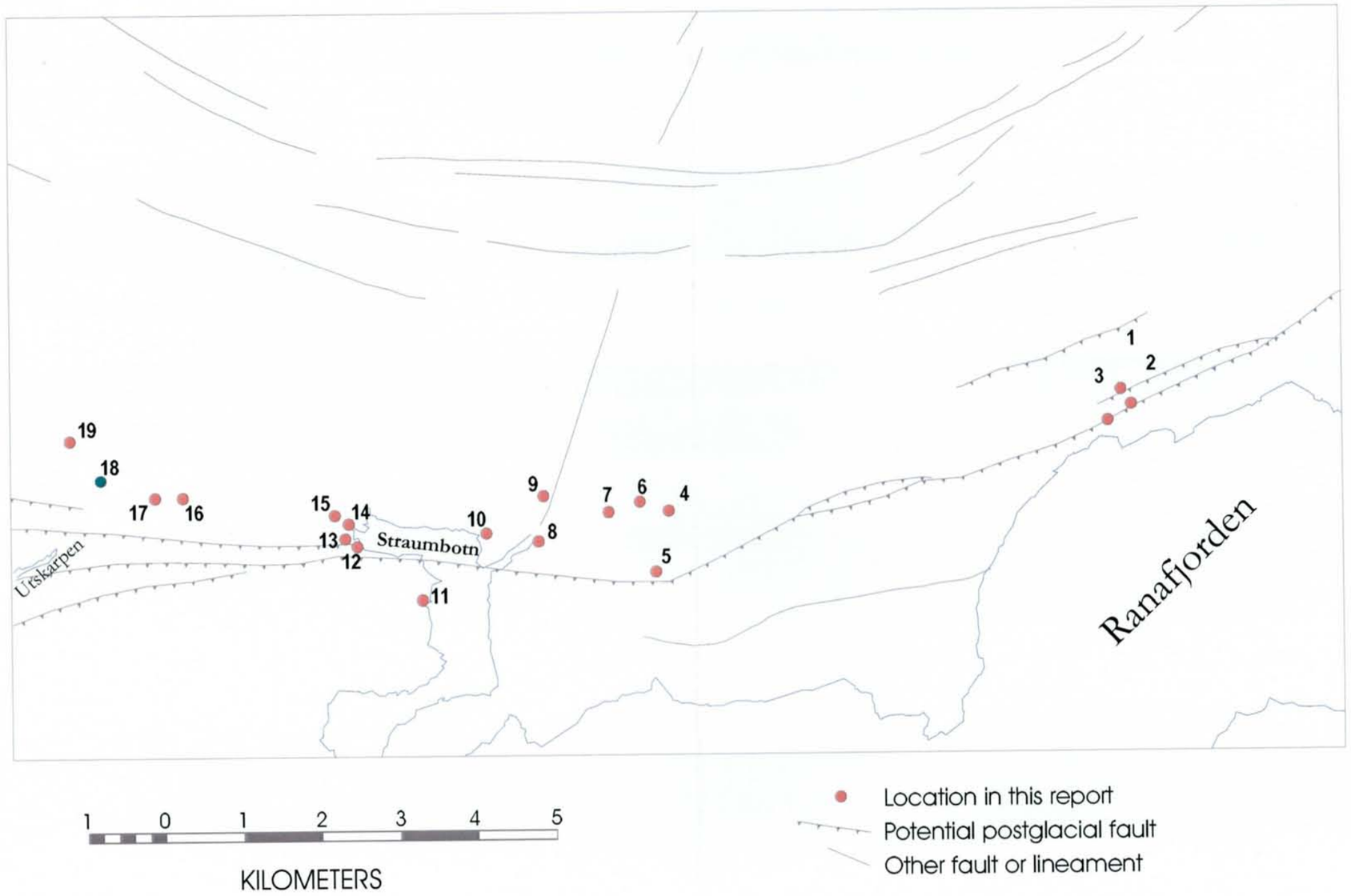

Fig. 5.4.2. Localities (1-19) with occurrences of deformed sediments in the Utskarpen-Straumbotn area where most of the 1997 fieldwork was done. The green dot (location 18) represents type 1 deformation. The red dots represent type 2 deformation..

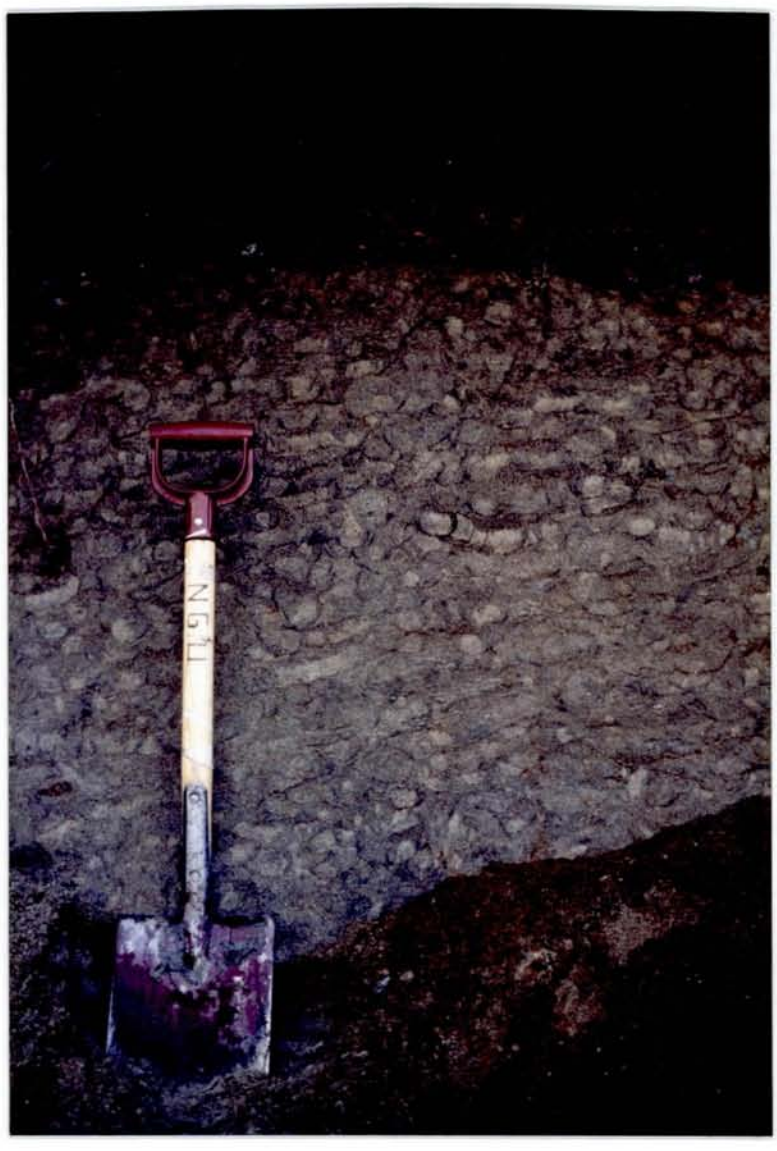

Fig. 5.4.3. Sitter, N-Flatanger, N-Trøndelag (No. 1 in Fig. 5.4.1). Sand with deformational structures of type 1. See text.

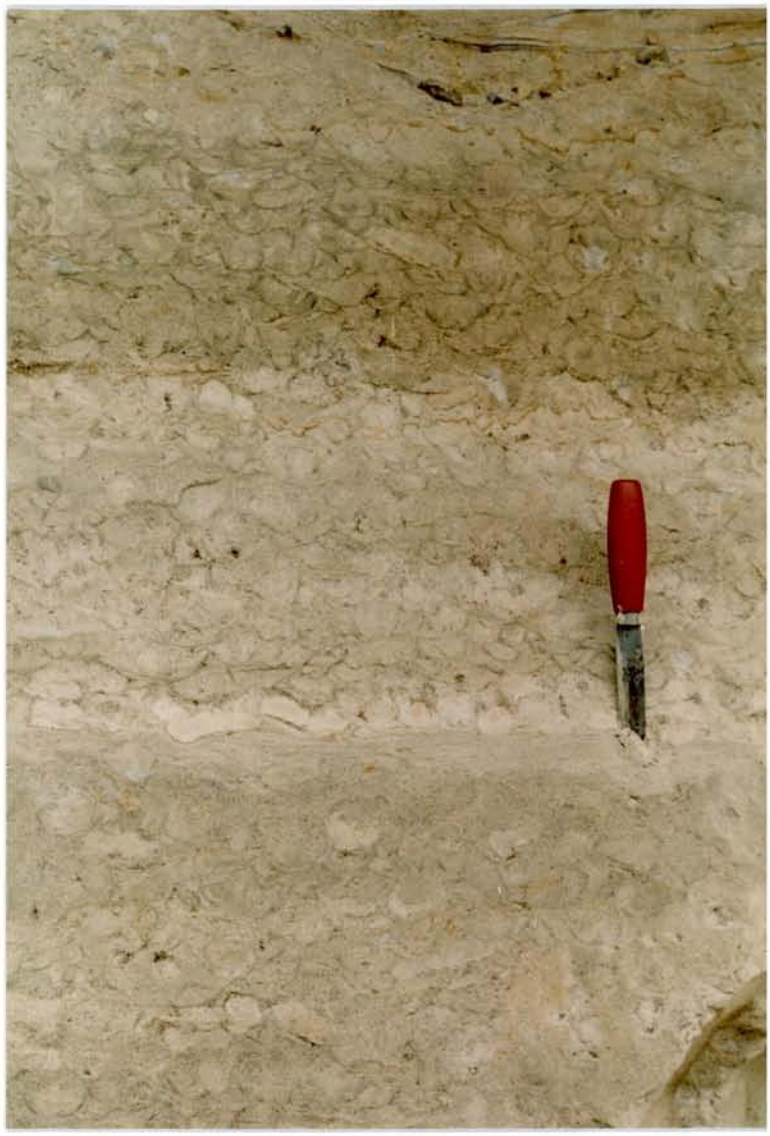

Fig. 5.4.4. Halsa, Meløy, Nordland (No. 3 in Fig. 5.4.1). Sand with deformational structures of type 1.

Fig. 5.4.5. Forsum, Utskarpen (No. 7 in Fig. 5.4.1). Sand with deformational structures inferred to be of type 1. Deformed sand facies located ca. 35 m a.s.l.

Fig. 5.4.6. Deformed sand with water-escape structures and traces of partial liquefaction in a section from the gravel pit in the ice-marginal delta at Forsbakken, Straumbotn. The delta top-surface has an altitude of ca. 120 m a.s.l., corresponding to the marine limit in this area. The deformation sand facies is located a few metres from the top (115-117 m a.s.l.). The deformed sand is mapped as type 2 sand. See text.

Fig. 5.4.7. Deformed sediments dominated by fine sand and silt alternating with gyttja-bearing sandy beds. The section is located 3-4 m a.s.l. and 5-10 metres north of the Båsmoen Fault at Straumbotn, western margin (No. 12 in Fig. 5.4.2). The deformed sediments are mapped as type 2 sands, and the deformation here is thought to have been caused mainly by bioturbation, however earthquake activity may have caused some of these disruptions.

Fig. 5.4.8. Deformed sand of fine to medium sand in two main units separated by a rusty sand in a 10-15 cm thick horizon with a sharp erosive lower boundary. The section is located 3-4 m a.s.l. and 5-10 metres north of the Båsmoen Fault zone at Straumbotn, eastern margin. The structures in the lower sand unit resemble a type 1 sand with a fine-grained structure, whereas the upper sand is clearly a type 2 sand.

Fig. 5.4.9. Deformed sand ca. 10 m a.s.l. at Straumbotn, western margin (No. 14 in Fig. 5.4.2), mapped as a type 2 sand.

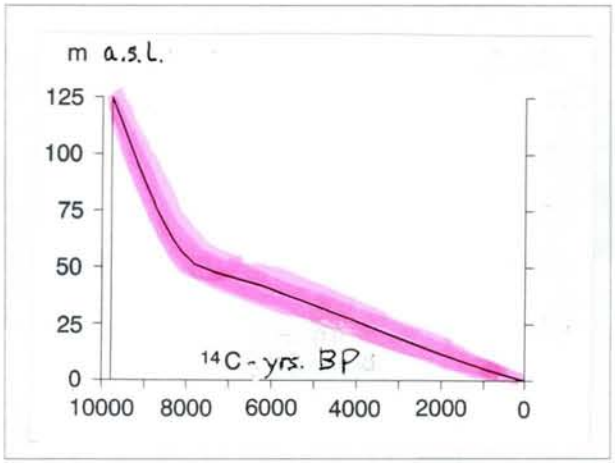

Fig. 5.4.10. Generalised shoreline displacement curve from the Elsfjord-Korgen area (after Olsen et al. 1996).

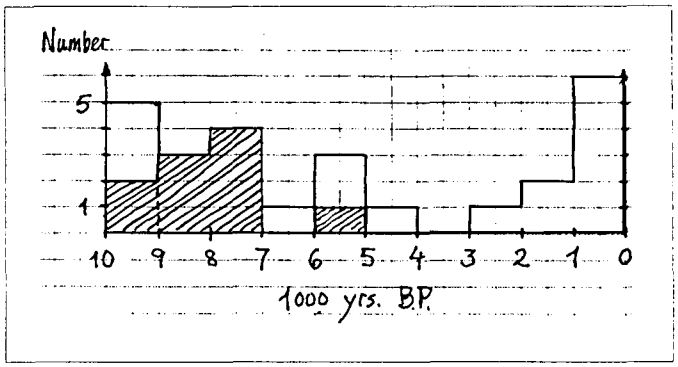

Fig. 5.4.11. Frequency diagram of type 1 (shaded) and type 2 sands plotted versus time. See text for further explanation.

5.4.2 Sand cone on a complex terrace located close to the Stuoragurra Fault, Masi - kame or sand blow origin?

A sand cone located in an elongated 2-3 m deep and 40-50 m long depression on a complex glacial-deglacial terrace along Ingajohka, Masi, has previously been suggested to be a possible sand blow cone produced by earthquake (Olesen *et al.* 1990a). This hypothesis was based on the location west of Masi in the vicinity of the Stuoragurra Fault, which was active during the last deglaciation, and on the cone morphology. The cone has an almost circular meter-deep depression on top, and, therefore, the overall morphology resembles a sand 'volcano'. To decide whether there has been some kind of central eruption from sediments underneath the cone, and subsequent collapse into the feeding pipe leaving a depression on the top, or the total structure simply is a result of melting ice, we dug a trench through the cone this field-season. The excavation revealed a structure that strongly suggests formation as a kame (Figs. 5.4.12-5.4.13).

The channel where the complex sand cone is located, is inferred to be a subglacial meltwater channel which started abruptly in the southeast and was directed towards the valley in the NNW. It is possible, though not likely because of the large dimensions (?), that this almost 50 m long channel was initiated as a depression caused indirectly by an earthquake. Thus, the initial depression may have been a result of collapse into the void from where earthquake derived liquefied material was removed. It is also possible that the sand unit 3 in the cone (Fig. 5.4.12) is produced by sand blow along a conduit starting outside the excavated section in the southeast, and continuing subparallel to the surface in the excavated zone towards the NNW. If this was the case, then this event must have happened before the inland ice-sheet melted on northwestern Finnmarksvidda some 9300 years BP. However, there are no distinct structures or depositional units which cannot derive from a normal kame, and the last depositional events recorded here are, in any case, represented by the glaciofluvial gravely stony unit 2 and the ablation melt-out/flow till unit 1.

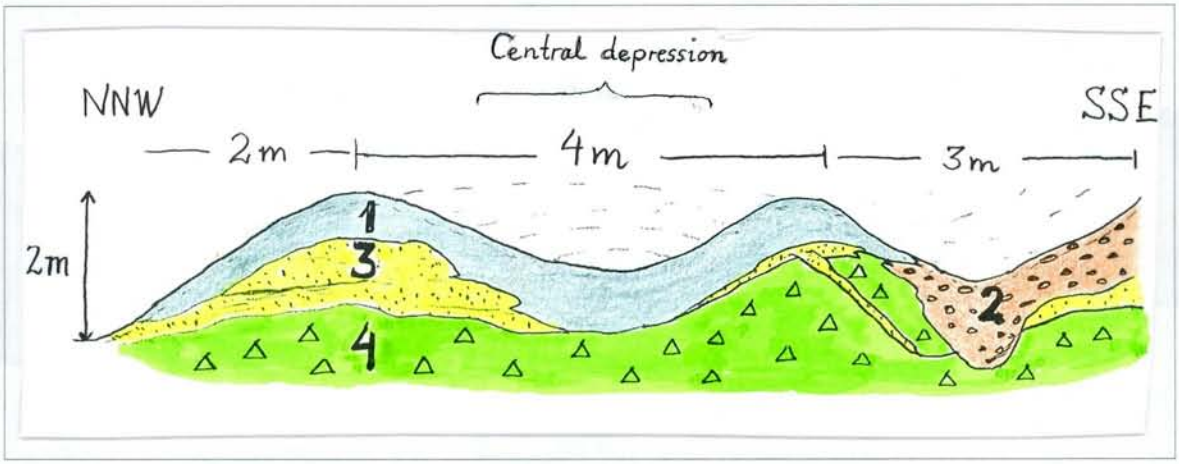

Fig. 5.4.12. Excavated section in a complex sand cone at Ingajohka, west of Masi. See text for further description. Units: 1 – Diamict sandy material, ablation melt-out till or flow till; 2 – Cobbles and pebbles, glaciofluvial material, clast supported; 3 – Sand and gravelly sand, glaciofluvial material, some flow structures, ripples etc.; 4 – Sandy till, matrix supported, dominated by fine sand, envelopes of medium sand wrapped around pebbles and cobbles and sporadically occurring in separate lenses.

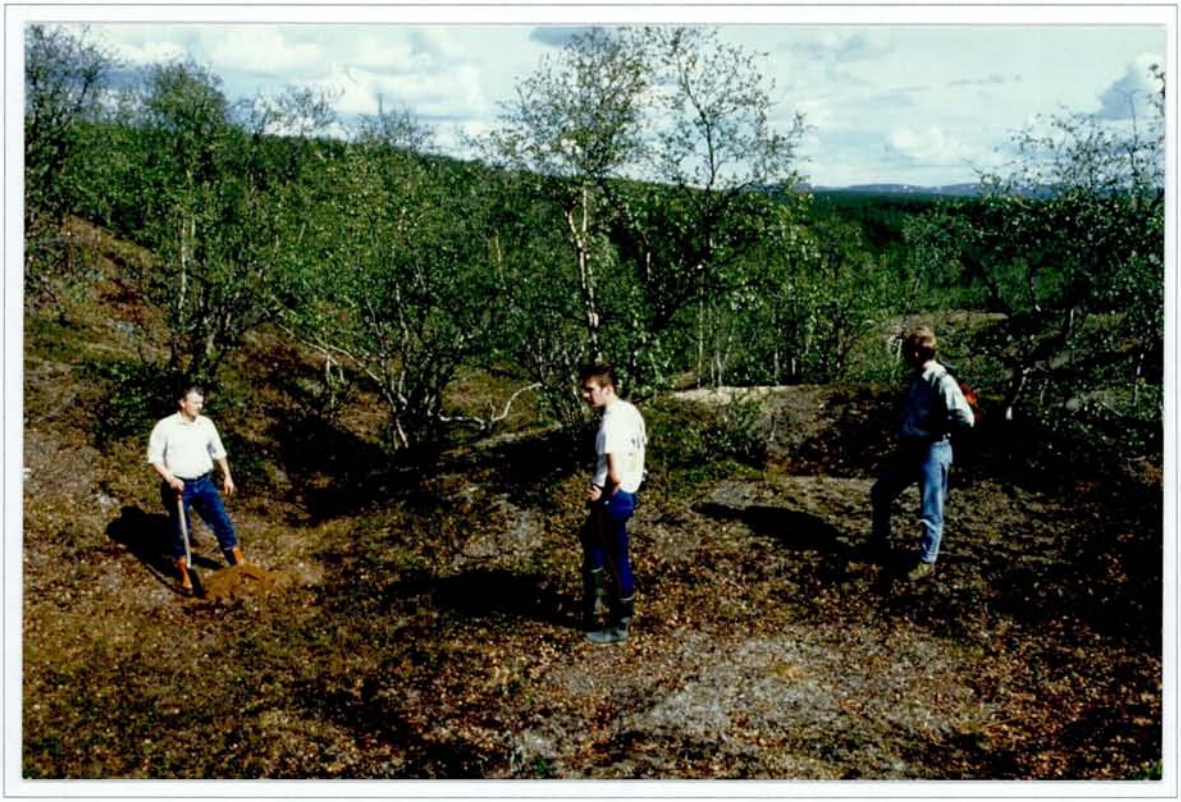

Fig. 5.4.13. The complex sand cone at Ingajohka. View towards the Ingajohka valley to the NNW. The excavated section shown in Fig. 5.4.12 was trending towards the NNW along a profile which started where the person to the right stands. Photograph by O. Olesen.

6 GEODESY (TASKS 5, 6 & 7)

6.1 REPORT ON GPS OBSERVATION CAMPAIGNS

By Lars Bockmann, Norwegian Mapping Authority

6.1.1 Nordfjord

Reconnaissance and Station Selection

Reconnaissance and site selection for the GPS observations was carried out by Lars Bockmann and John Dehls in the period 25-27 June 1997, following preparatory examination of maps and air photographs by Odleiv Olesen. A total of 15 stations (Fig. 6.1.1) were selected and monumented with specially made bolts. Each bolt was equipped with a protective cap, and was threaded so that any instrument screwed onto it would be force-centred.

The sites were selected having regard to geological requirements, while also seeking the best possible GPS observational conditions. The open rocky terrain, with little vegetation, gave considerable freedom of choice and good access to bedrock. However, it was not always possible to ensure a free line of sight over 10° elevation angle due to the high mountains in the region.

Full station description documentation was made for all points, together with photographs, in order to assist with recovering the stations at a later date.

Fieldwork

The GPS field observation campaign was carried out in the period 20-30 October 1997 by Torbjørn Nørbech and Lars Bockmann of the Norwegian Mapping Authority. A total of eight Ashtech Z12 geodetic GPS receivers together with Dorne & Margolin choke ring antennas were used.

The standard specifications for such observations within the Norwegian Mapping Authority, where different post-processing computer systems are to be used, is that GPS observations are recorded continuously at each station for a minimum of two full days. Further, where receivers have to be moved from station to station for different observational sessions, then the various sessions must always include at least two common stations where the receivers remain unmoved. As usual, GPS data was recorded at 30 second intervals, all visible satellites over 10° elevation angle being tracked.

Unfortunately, the observational period included some of the heaviest snowfalls for many years. This resulted in at times up to 10 cm of snow covering the GPS antennas, and it is not yet clear whether this will have had an effect on the end results. Nevertheless, despite the difficulty of movement and transportation caused by the inclement weather, snow cover to the antennas was carefully removed, and the times of removal carefully noted so that the observational records could be correlated.

In the end, observations at 14 of the 15 stations were completed, while the observations at the fifteenth station had to be abandoned, for a variety of reasons.

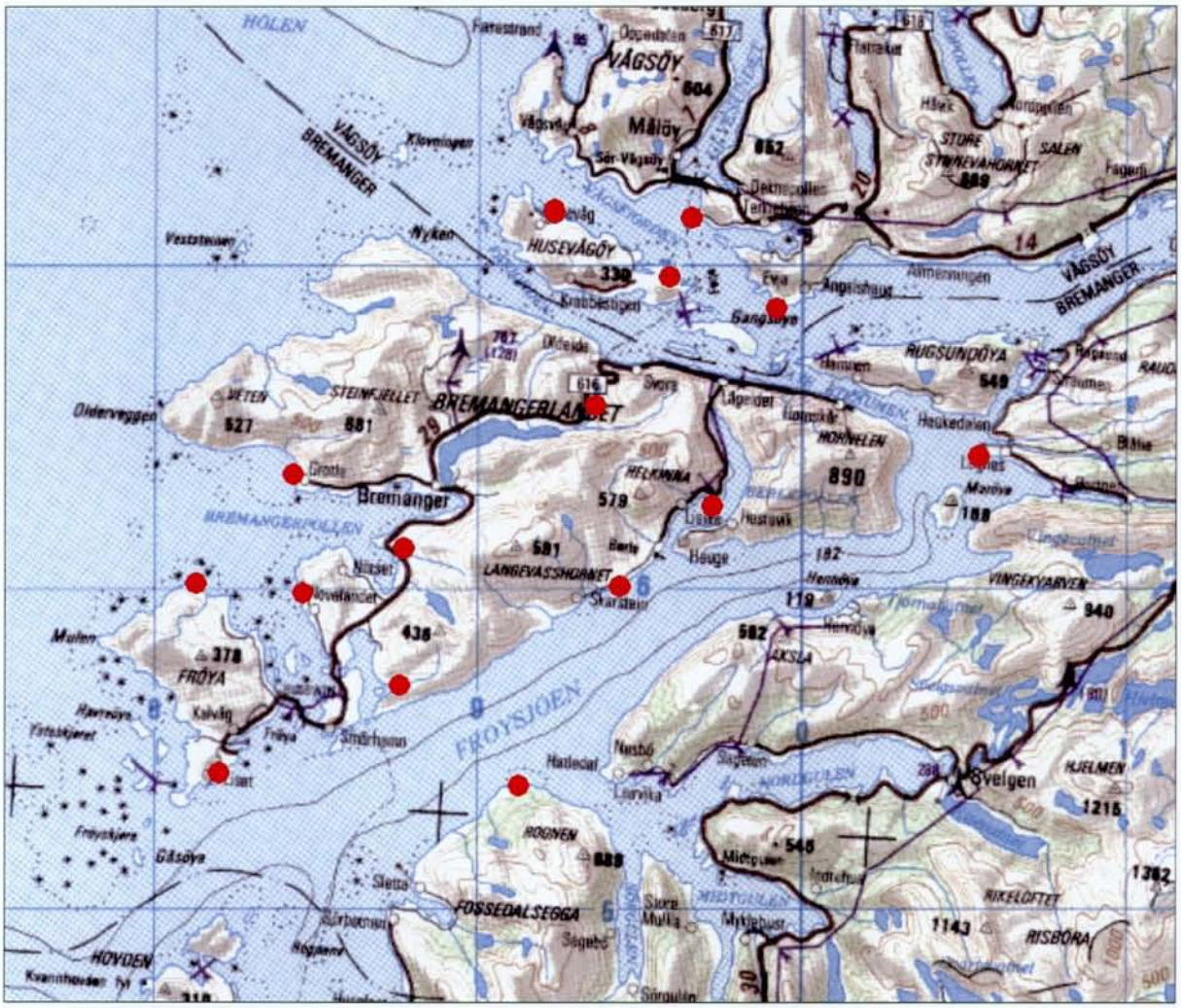

Fig. 6.1.1. GPS net station locations in Nordfjord.

Bolt Verticality

Not all of the station bolts were found to be truly vertical in their emplacement. This was important since different GPS antennas have different electrical centre heights, and it was therefore necessary to accurately establish the axes of the bolts so that all observations could subsequently be reduced to the same physical mark.

A specially made 30 cm cylinder was made for this purpose. The cylinder was internally threaded so that it could be screwed onto the bolt. The cylinder therefore functioned effectively as a bolt extension, and had the effect of magnifying the non-verticality of the bolt itself so that its axes could be established by means of spirit level and compass. The uncertainty of these measurements was considered to be no greater than 1 mm, based on the length of the above described 30 cm bolt extending cylinder.

For actual measurements, therefore, the centring uncertainty (in mm) would be the actual height of the antenna over the bolt in centimetres, divided by 30 cm, and multiplied by 1 mm. The antennas used during this observing campaign had electrical centre heights, given by the manufacturer, of 11,8 cm for single frequency measurements, and 7,7 cm for dual frequency measurements.

Antenna Calibration

All the antennas used were calibrated on completion of the field campaign. These measurements were carried out at the Norwegian Mapping Authority's offices in Hønefoss. One of the antennas was selected as a reference, to which all of the others were then compared. At least one full day's GPS observations were recorded with each antenna in turn, and the post-processed results thus gave the comparative offsets between each antenna and the reference antenna, and enabled a systematic confirmation of the antenna offset values given by the antenna manufacturer.

The same procedure will be followed for the next GPS observing campaign, taking care that the same reference antenna is used.

These additional measurements are most important if the highest accuracies are to be achieved. The additional calibration observations could, in fact, have been avoided if it had been possible to guarantee that the same antennas would be used again on the same stations as in this present campaign. Such a guarantee, however, is not considered a practical possibility, and therefore re-calibration for the next campaign will be essential.

Post-processing of the recorded observations will be completed during the winter of 1998.

6.1.2 Masi

Reconnaissance and Station Selection

Reconnaissance and station selection was completed by Odleiv Olesen, John Dehls and Lars Bockmann during the period 14-16 August 1998. In this case, the reconnaissance was more difficult than in the Nordfjord area, because bedrock is considerably less accessible. Nevertheless, with the help of geological maps suitable observing sites were successfully identified. A total of 14 stations (Fig. 6.1.2) were monumented with bolts in the same way as in the Nordfjord area and the appropriate records were made, again as described above.

Field Observations

The GPS observations in this area were recorded during the period 2 to 14 October by Torbjørn Nørbech and Lars Bockmann using the same receivers and methods as are described above for the Nordfjord campaign, including the procedures for ascertaining the verticality of the actual bolts.

Two of the loaned GPS receivers were found to be equipped with only 1MB of internal memory, while the remaining receivers had 3MB. This resulted in that the 1MB receivers had to have their recorded data downloaded twice each day, while the 3MB could continue for up to two whole days without downloading. The daily routine of changing batteries, downloading data, confirming antenna centring and indeed moving instruments had therefore to take account of this factor, and led to very long working hours during the campaign.

Post-processing of the recorded observations will be completed during 1998.

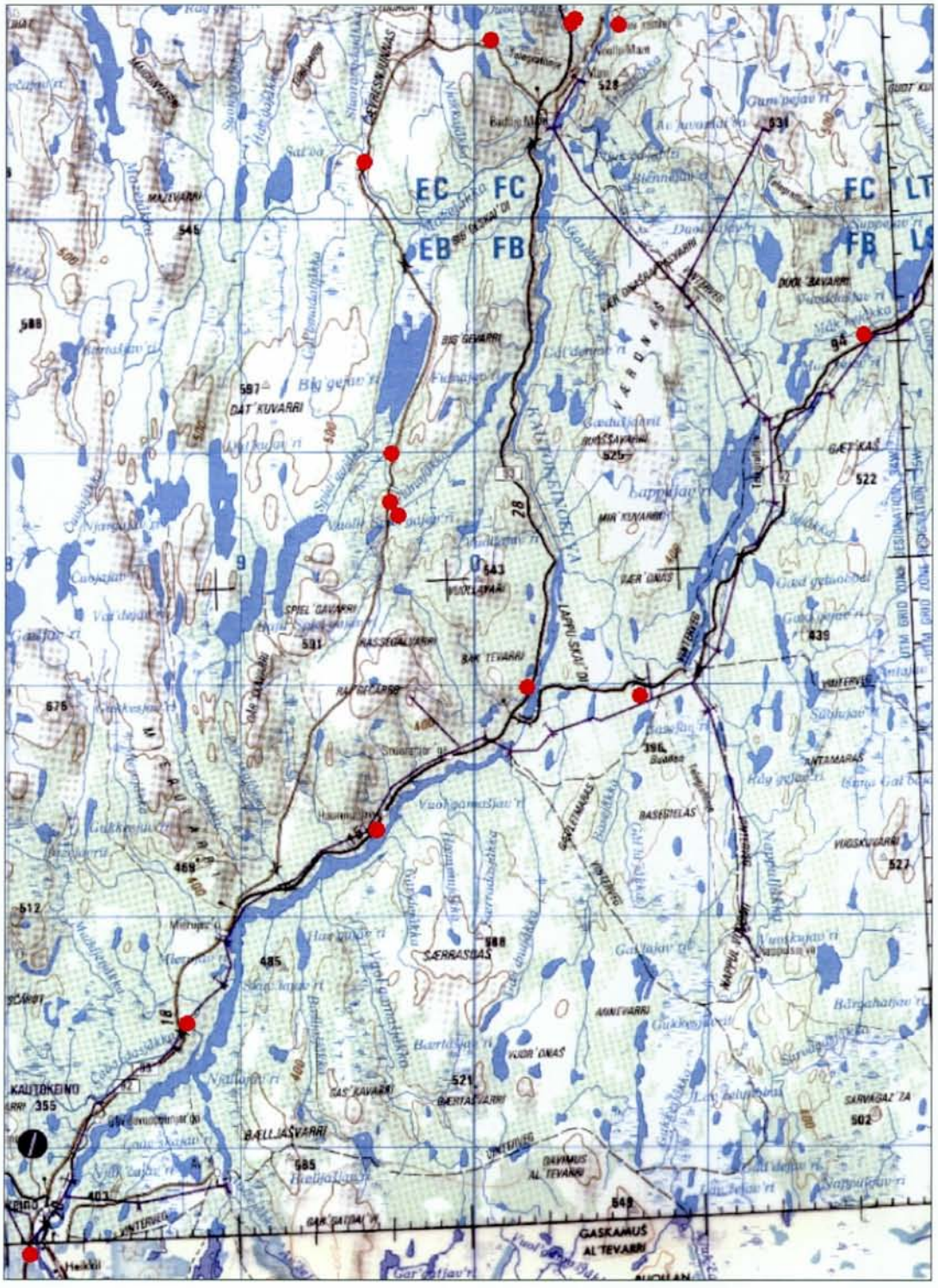

Fig. 6.1.2. GPS net station locations in the Masi area.

6.1.3 Yrkje

Monitoring the possible neotectonic movements at Yrkje by geodetic methods was originally suggested by the late Professor Karl Anundsen of the University of Bergen. Preliminary reconnaissance, station selection and monumentation was completed in 1983. Since then, several surveys have been carried out in order to determine the positions of the various monuments relative to each other.

Monitoring Horizontal Movements

At Yrkjevågen, 3 concrete pillars had been built on each side of a possible active fault, as planned by the late Professor Jon Holsen of the Norwegian Institute of Technolgy, University of Trondheim. The Professor then measured the angles within this network a total of four times in the period 1984 to 1987 using a high precision Kern DKM2A theodolite. A further re-measurement of the angles was made in 1993, although the results were not fully adjusted.

On November 22nd 1997 the network was measured anew by Leif Grimstveit and Sigvald Olli of the Norwegian Mapping Authority. This time, the side distances were measured using the very precise Kern Mekometer ME5000 electro-optical distance meter. These measurements now need to be adjusted by the method of least squares, so that they can be compared with Holsen's results.

Monitoring Vertical Movements

Also In 1983, 2 to 5 benchmarks had been set in rock at each of 7 different sites in the Yrkje district. This work had been planned and managed by Sivert Bakkelid from the Norwegian Mapping Authority. The elevation differences between the benchmarks at each site were measured several times with the Wild NI3 precision level during the years 1983-90.

All of these elevation differences were measured anew in late November 1997 by Leif Grimstveit and Sigvald Olli from the Norwegian Mapping Authority, using the Zeiss DiNi11 digital level. These measurements are more easily adjusted than those obtained using the Mekometer, and the comparison with earlier results is simpler.

6.2 NEOTECTONICS IN THE RANAFJORDEN AREA, NORTHERN NORWAY: PRELIMINARY REPORT ON THE GPS MEASUREMENTS DONE IN 1997

By Terje Skogseth, NTNU

In 1994 a GPS network with 18 points, numbered from 9401 to 9418, was established. The network was designed to measure the geological strain in the Ranafjord.

The points in the network are situated in three profiles across the fjord. There are 7 points in the 22 km long eastern profile at Mo, 5 points in the 19 km long profile at Utskarpen and 6 points in the 25 km long western profile at Nesna. The distances between the profiles are approximately 25-30 km. See figure below

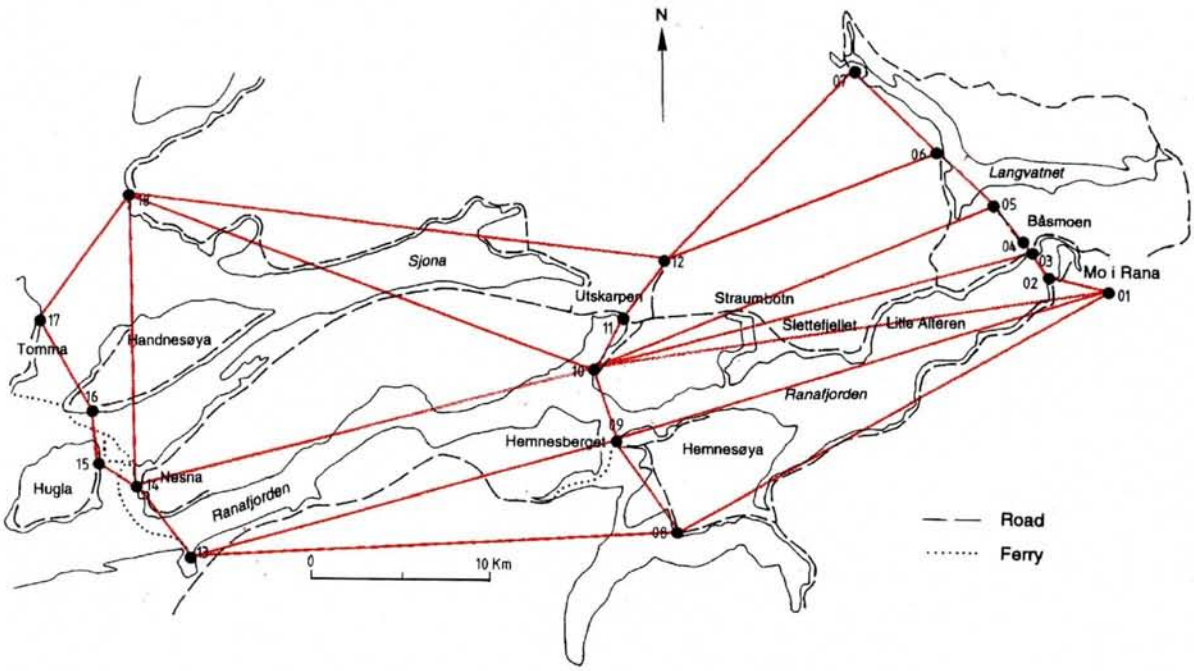

Fig. 6.2.1. GPS net 1997. Points (numbered 01-18). Vectors measured in 1997 (28 lines).

In 1997, the GPS network was measured for the second time. The fieldwork was carried out in week 37 in 1997 by staff from Department of surveying and mapping, NTNU. Four GPS-receivers were used. All 4 receivers were Leica SR9500 sensors with Leica CR344 controllers.

In 1997 a total of approximately 28 vectors were measured. A vector is calculated from simultaneous observations with two GPS receivers. As we used four receivers in this project, we were able to measure three independent vectors simultaneously.

The network is built up by triangles and quadrangles, as the lines in the figure above shows. The measuring time for the vectors within the three profiles was at least 1 hour (vectors shorter than 10 km), and the vectors between the profiles were measured for about 3-4 hours (vectors up to 30 km long.)

In 1997 we also connected our GPS network to the official national Norwegian network (SK network), established by Statens kartverk (the Norwegian Mapping Authority) by measuring between 4 points in the SK network and 4 points in our network at Mo and Utskarpen. One of

the SK points we used, is a national point of first order. By these measurements, we will be able to connect and calculate our GPS net in the EUREF89 reference frame (or datum), we will have exact absolute coordinates for the calculations of our GPS net. This is an important advantage when calculating the measured vectors, as the accuracy of a vector is also dependent of good absolute (preliminary) coordinates. The SK net was measured in 1997, and we hope to use the final results of the calculations of the SK net, in out work.

We have done some preliminary calculations of the vectors, to check the quality and if there are any problems getting a solution of the different vectors.

The final calculations of the GPS-vectors and the adjustments of the GPS network as measured in 1997, will be carried out as a student project, supervised by Terje Skogseth. The results will be ready in May 1998.

7 SEISMICITY (TASK 10)

7.1 SEISMICITY IN THE RANAFJORD AREA

By Erik Hicks, Hilmar Bungum and Conrad Lindholm, NFR-NORSAR

7.1.1 Summary

As a part of the NEONOR project, a six-station seismic network in the Ranafjord area was installed by NORSAR in June 1997, and has been operative since the beginning of July 1997. A total of 167 seismic events have been located as of Dec. 1, 1997, with 95 of these being probable earthquakes occurring within the network, with M_L (local) magnitudes ranging from 0.1 to 2.3. To support this study, a local magnitude scale was calibrated to the region.

A large number of the earthquakes recorded are concentrated in a NW-SE trending zone under the Sjona fjord, with shallow depths around 4-6 km. Five focal mechanisms solutions have been determined, including one composite solution from the Sjona group and four single event solutions for earthquakes with magnitudes (M_L) ranging from 1.7 to 2.7, the latter ones determined through full waveform modelling. The inferred directions of maximum compressive stress are significantly different from the Fennoscandian average (including regions offshore Mid Norway), indicating that regional and local sources of stress are more important in this case.

7.1.2 Introduction

An earthquake of magnitude around 6.0 occurred in the Ranafjord area on 31 August 1819, causing widespread damage, numerous rockfalls and liquefaction phenomena as well as observed disturbances to the sea over a wide area (Muir Wood 1989b). This earthquake is the largest recorded in Scandinavia in historical times. The seismic activity in this region is still higher than in most other onshore regions in Norway (Bungum *et al.* 1991).

The purpose behind the Mo i Rana seismic network is to monitor the possible seismic activity in this region, and particularly along and nearby the Båsmoen fault running E-W north of Ranafjorden. This fault shows signs of postglacial tectonic activity, and is subject to geological investigations and to GPS measurements of deformation across the fault as part of the NEONOR project.

7.1.3 Technical Installations

The seismic network consists of six vertical-component seismometers deployed within an area of approximately 50x30 km around Ranafjorden in northern Norway. Fig. 7.1.1 shows a map of the six stations. Five of the stations relay data via radio (UHF and VHF) to a central station, where they are discriminated and digitized. The sixth station is connected directly to the digitizer. The digitized data are continuously fed via modem and a permanent landline to NORSAR at Kjeller, outside Oslo, where the data are processed and analyzed.

Detailed plans for the network layout were made at a meeting at the NORSAR Maintenance Center in Hamar in the beginning of June 1997, attended by Paul Larsen, Kjell Arne Løken and Erik Hicks from NORSAR, Alf Nilsen from the University of Oslo and Carlos Aranda from the University of Bergen. The technical part of the installation was discussed, and possible sites for the sensors were found based on 1:50.000 maps.

Alf Nilsen then departed for Mo i Rana with the instruments and other equipment on June 6, 1997, and used the first days to evaluate the possible sites, including verification of radio transmission.

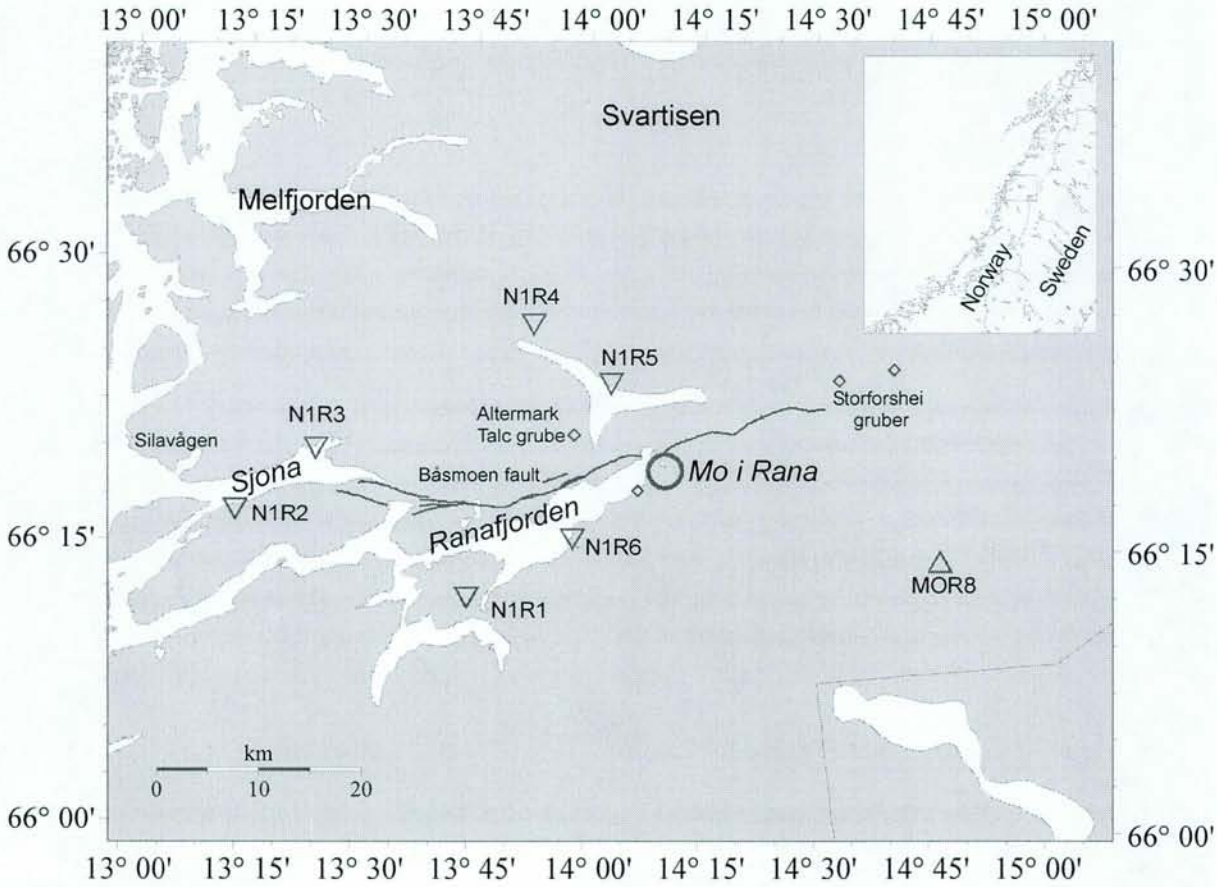

Fig. 7.1.1. The six NEONOR stations (N1R1-N1R6), and the MOR8 station operated by the University of Bergen as part of the NNSN. The Båsmoen fault is shown by a solid line. Active mines are shown by diamonds.

The following criteria needed to be fulfilled for each location:

1. 230V AC available nearby.

2. Accessibility by car.

3. Permission from landowner.

4. Approximate line of sight between transmitting and receiving stations.

5. Distance between transmitting and receiving station less than ~30 km.

6. Bedrock, preferably with 50-80 cm soil cover.

7. Distance to noise sources as great as possible.

8. Free location of the radio mast.

Six locations were found that fulfilled these criteria to a reasonable extent, including a site for the central station that also needed a sheltered location for the discriminator, digitizer and modem, and the possibility of installing a phone line.

Carlos Aranda arrived in Mo i Rana on June 9, 1997, at which time the seismometers and radio masts were installed. A schematic figure of a typical station is shown in Fig. 7.1.2. Technical information regarding the installation is given in appendix A (updated with changes made during fieldwork in October).

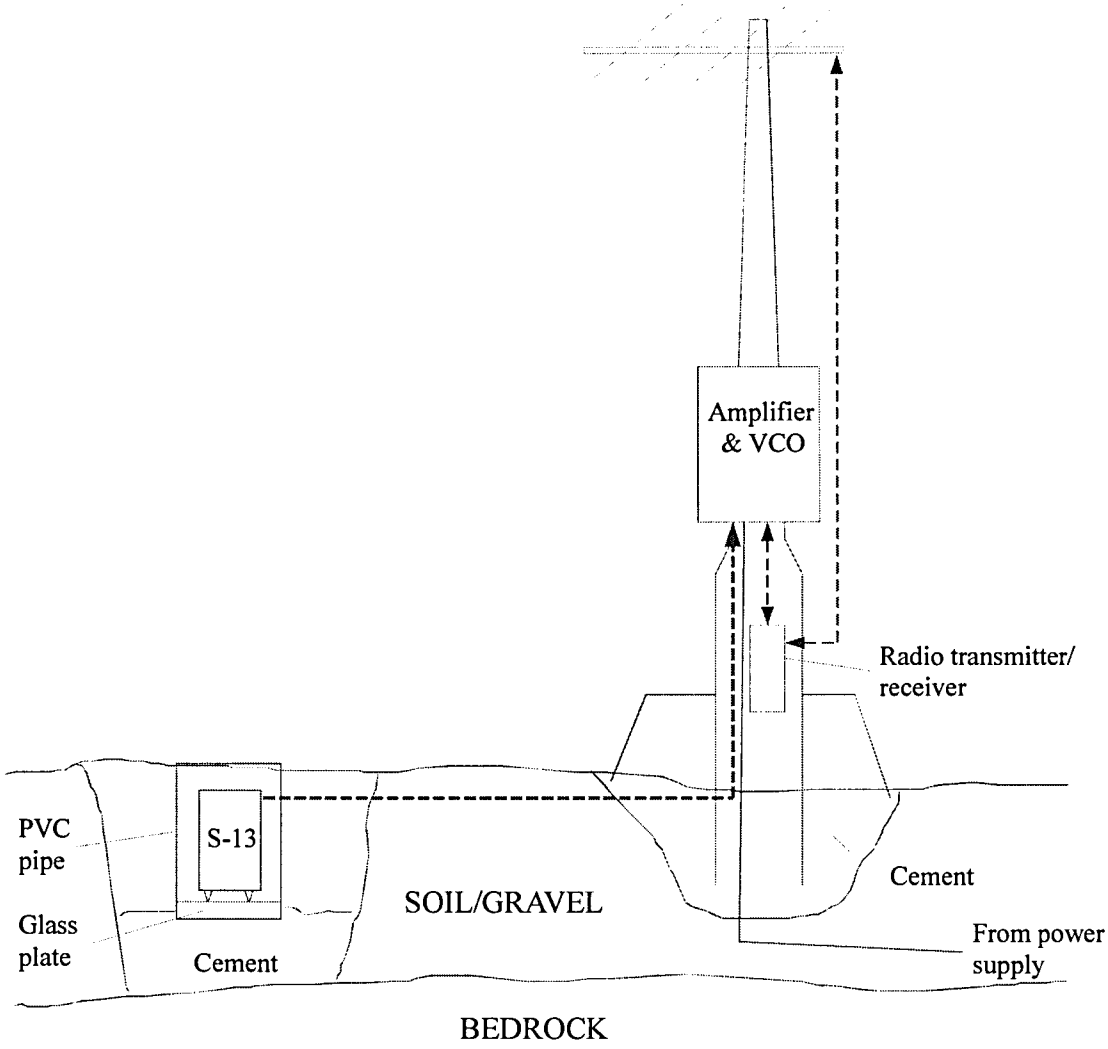

Fig. 7.1.2. Schematic representation of a single station.

Due to the lost time caused by shipping delays of the radio masts from Hamar to Mo i Rana, there were some tasks that could not be completed before departure. One problem was that no signal was received from station No. 4 (N1R4), and there was little time to evaluate and adjust gain and filter settings.

Further fieldwork was therefore performed on the network from October 28-31, 1997, by Kjell Arne Løken and Erik Hicks, with the aim to correct these problems. Station 2 (N1R2) had also developed intermittent problems during October, which also needed attention. There was an unsuccessful attempt at using VHF to transmit directly from station 3 (N1R3) to the central station (N1R6), thus making N1R2 and N1R3 independent of the repeater at station

no. 1 (N1R1) which is located atop Hemnesberget, and thereby sensitive to weather related problems.

The problem with N1R4 was traced to a bad multiplexer on the VCO board at N1R5, and the UHF radio link from N1R5 to the central station was replaced with VHF. The problem with N1R2 was traced to a problem with the transmitter at N1R3, and was fixed when the transmitter at N1R3 was changed to VHF. Unfortunately, the VHF transmitter at N1R3 was unable to reach the central station, so data from N1R2 and N1R3 are still relayed via NIR1. A large radio mast near the NlRl site appears to induce some noise in the network, this mainly affects the data from NlRl, but may occasionally also affect all of the Stations 2 to 5. This problem could not be corrected without removing Station 1, but was alleviated somewhat by changing the VCO frequency. The lowpass filters on all stations were lowered from 25 Hz to 12.5 Hz, while the gain at all stations was adjusted to 60 dB (see Appendix A for more details).

7.1.4 Data Analysis

As soon as the data became available in real time at NORSAR, a fully automated data acquisition and analysis system was developed. About one week of continuous data are kept on disk at any time, with selected intervals permanently stored.

Several seismic events are normally detected by the data acquisition system each day, with local (within the network) and nearby (within approx. 150-200 km) events selected for localization. Data for other seismic events (more distant and teleseismic earthquakes) are saved without further analysis. A sample seismogram from the six stations is shown in Fig. 7.1.3.

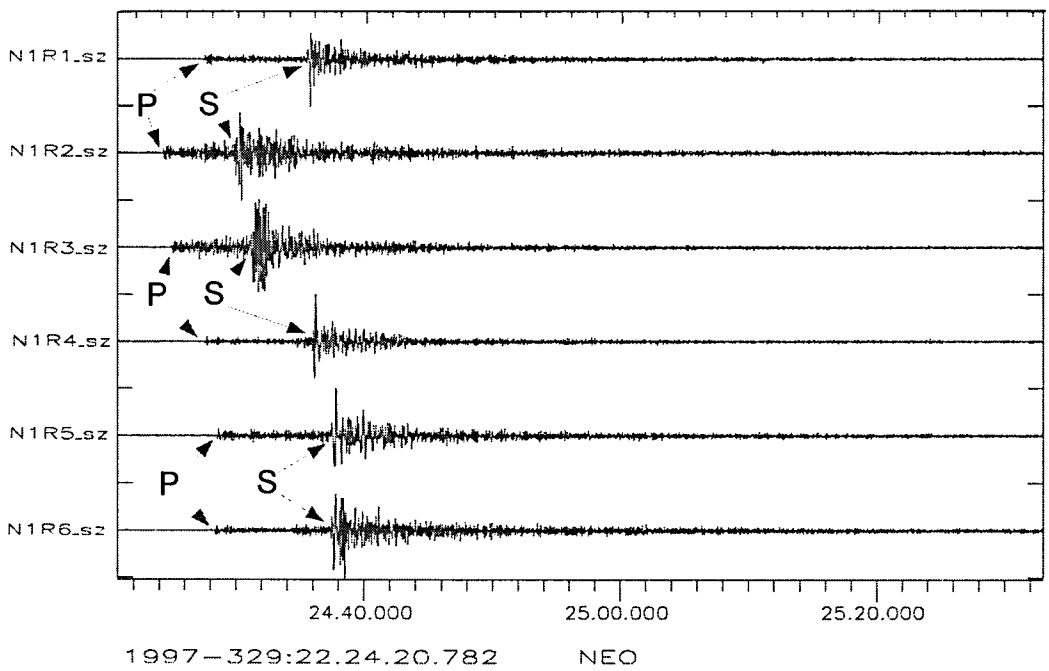

Fig. 7.1.3. Seismogram from the earthquake of 21 November 1997, 22.24.16 GMT. The P (pressure) and S (shear) wave arrivals are indicated.

A common problem lies in separating real earthquakes from man-made explosions, possibly originating from mines, construction sites, etc., a problem that increases with decreasing magnitude. There are two active mines within the network area (Altermark Talc grube and Storforshei gruber), which are visible in the recorded data to a varying degree. Once a few shots from a certain mine are registered, however, it becomes a simple matter to filter these from further analysis, as shots in the same mine will produce virtually identical seismograms (the

automatic detection system will still save the data regardless). Data from the NNSN MOR8 (Norwegian National Seismic Network; (Havskov *et al.* 1992) station 30 km east of Mo i Rana (operated by the University of Bergen) and other available stations are used to constrain the location whenever available.

The automatic phase arrival detection processing for the NEONOR network is done using NORSARs own data acquisition software. Each trace is filtered in seven frequency bands (between 0.8 and 12 Hz), and detections based on signal to noise ratio for each band are found. The threshold of detection is set individually for each band, to reduce false detections from noise. If there is a detection for three or more stations within a set time interval, two minutes of data is automatically saved to file, for later analysis and location using the SEISAN software package from the Institute of Solid Earth Physics, University of Bergen.

7.1.5 Results

Event locations

As of December 1, 1997, a total of 167 seismic events have been located by the network, 28 of these within distances of 50 and 200 km from the network (outside Fig. 7.1.4). A total of 42 probable local explosions have been located and removed from the maps, mainly from a talc mine a few kilometers northwest of Mo i Rana and from Storforshei Gruber around 40 km east of Mo i Rana.

This leaves approximately 95 probable local earthquakes from the beginning of July to the end of November 1997. Fig. 7.1.4 shows a map of the earthquakes around the Ranafjord area, while Fig. 7.1.5 also includes events at greater distances.

There are three notable groups of earthquake epicenters in Fig. 7.1.4, all of which lie in the western part of the network. The group in Sjona contains around 40 earthquakes, with the largest having a magnitude of 1.6. Depths are mainly around 4-6 km, which is very shallow for earthquakes. The epicenters have a NNW-SSE trend, which complies with lineations and topographic features in the area. Although one would expect the scatter in epicenter location for these events to be larger in this direction due to the dependency on the arrival times at stations N1R2 and N1R3, the existing lineation in the area in addition to the composite focal mechanism solution determined for this group supports the theory that this is indeed a real trend.

Another group of 10 epicenters is seen some 10 km further west along the Sjona fjord. The earthquakes detected here have magnitudes ranging from around 0.9 to 1.8, but the detection threshold is also slightly higher due to the greater distance to the stations. Focal depths here are around 8-11 km. Four events in this group are larger than M_L 1.5.

The third group is found around 10- 15 km north of Sjona, and includes the largest earthquake so far detected within the network, with a magnitude of M_L 2.3. There are seven earthquakes in this group, with three of them being of magnitude 1.0 and larger. The focal depths are also around 8-12 km for this group.

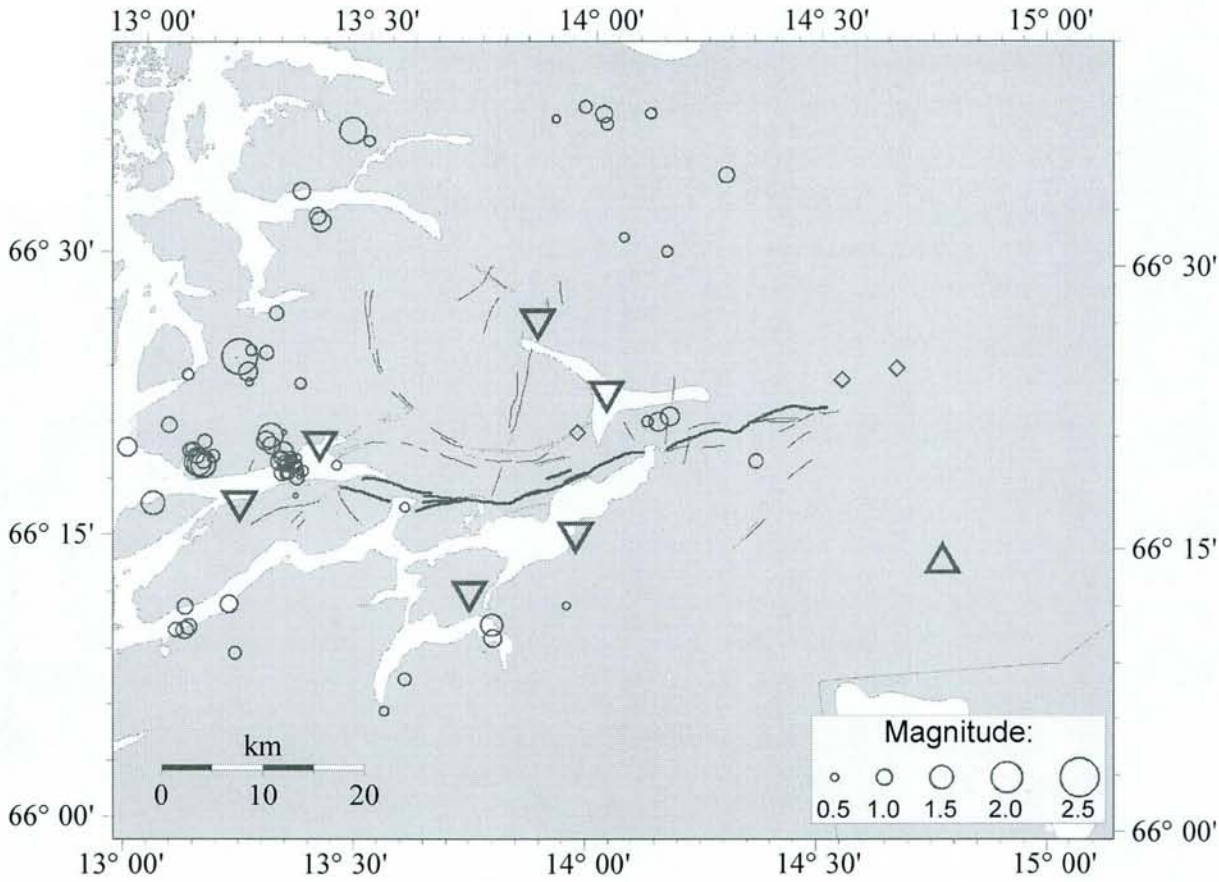

Fig. 7.1.4. Local seismicity of the Ranafjord area. Magnitude range from M_L 0. 1 to 2.3. The stations are represented by triangles. Active mines in the area are shown by diamonds. Faults and cracks courtesy of NGU. Thick lines represent the mapped potential postglacial Båsmoen fault.

The remaining local epicenters are fairly well scattered, with some of the largest ones being located along the Nesna peninsula. The earthquakes located to the south of the Båsmoen fault are of the greatest neotectonic interest, as the fault has a shallow (30°) dip towards the south.

Focal mechanisms

A total of five focal mechanism solutions have been determined, for the events listed in Table 1 (one composite solution and four individual ones).

The focal mechanisms are plotted in Fig. 7.1.6, along with the 1997 background seismicity as obtained from the NEONOR network.

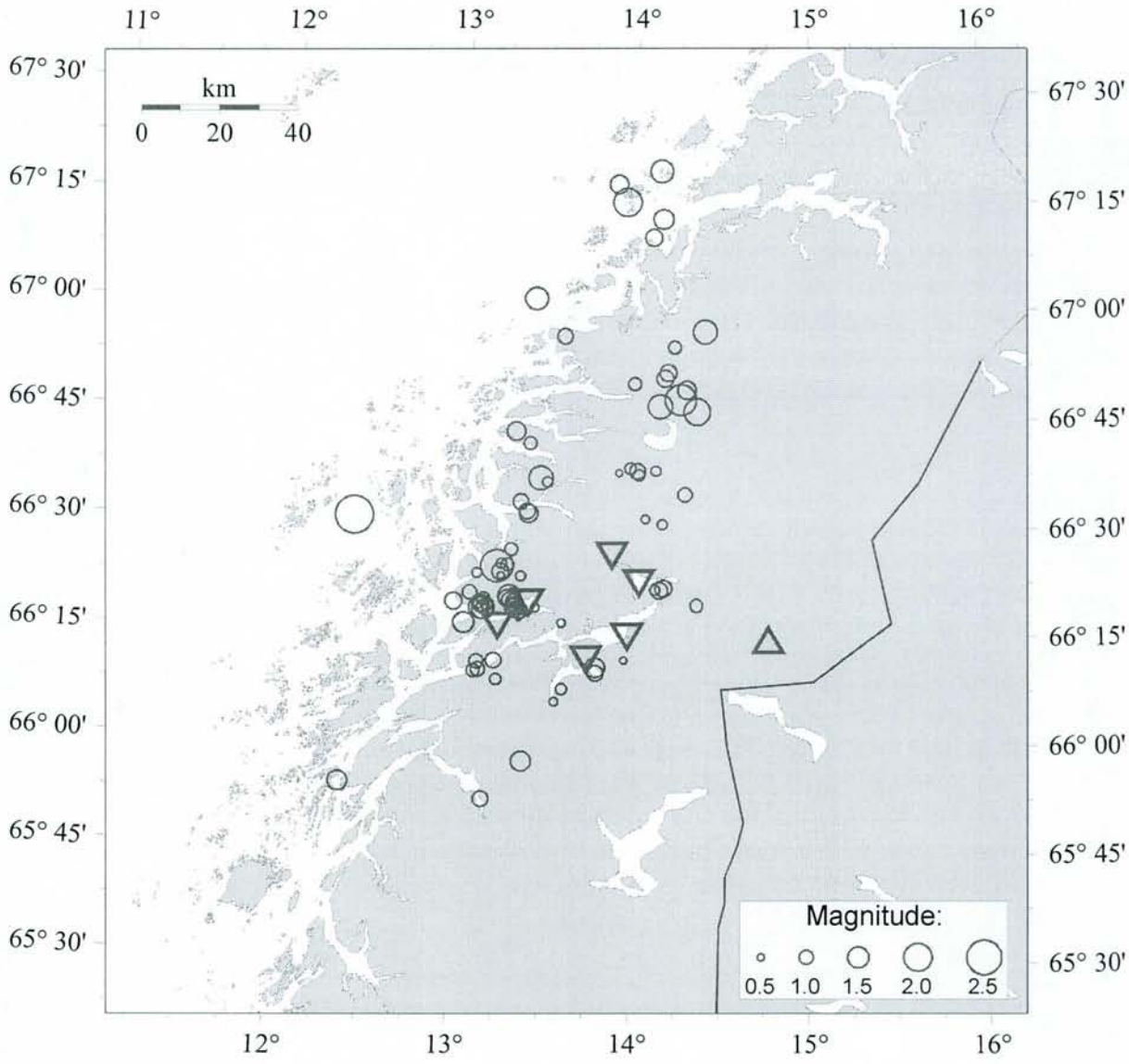

Fig. 7.1.5. Earthquakes located by the NEONOR seismic network, magnitudes 0.1 to 2.7.

Date	Lat.	Lon.	Depth	Mag.	P-trn	P-plng	T-trn	T-plng
Comp.1	66.31	13.32	5 km	N/A	167	48	270	11
971121	66.41	13.22	7 km	2.3	208	29	302	7
971125	66.52	12.40	11 km	2.7	77	29	343	7
971128	66.32	13.14	11 km	1.7	74	58	299	23
971128	66.32	13.15	11 km	1.8	74	58	299	23

Table 1. Focal mechanisms determined by using data from the NEONOR seismic network. The composite solution is determined by first motion polarities only, the other four are determined by first motion polarities combined with full waveform modelling.

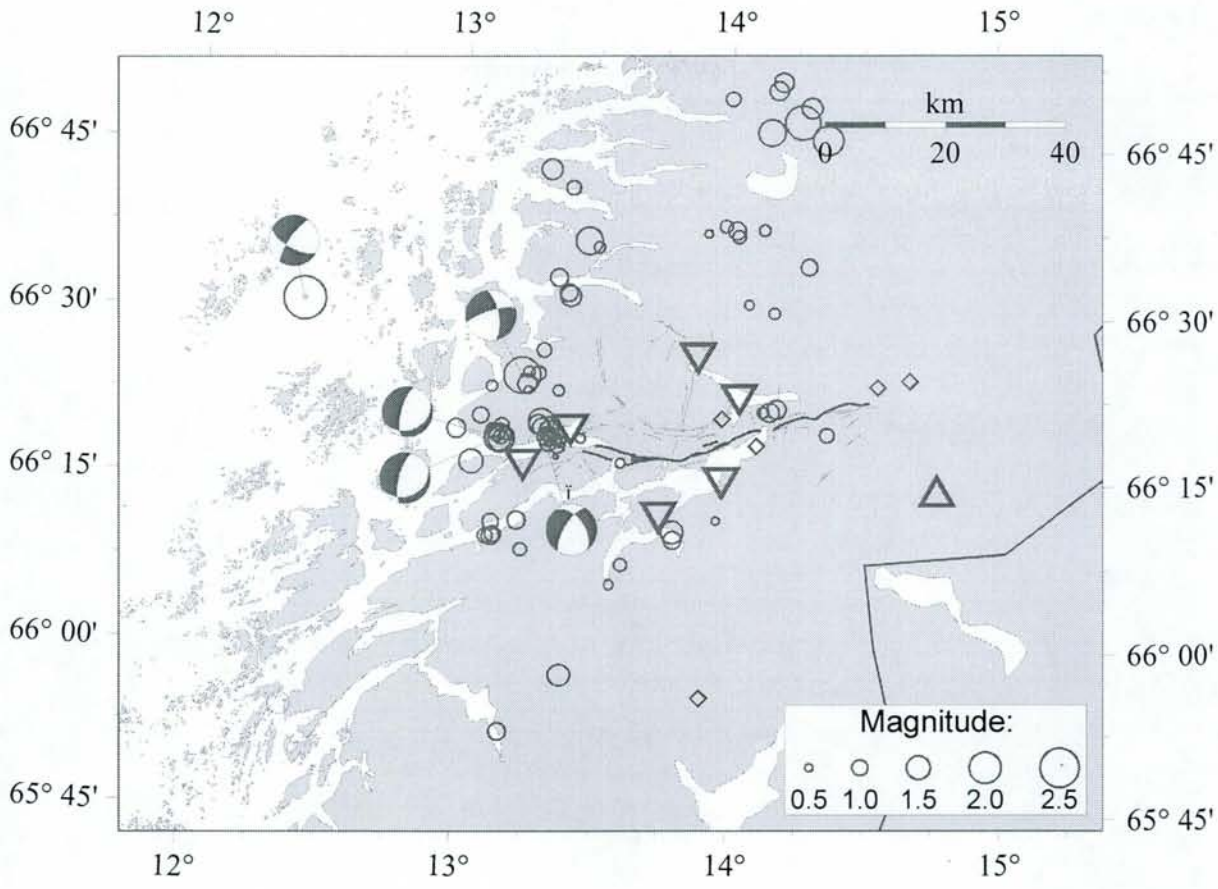

Fig. 7.1.6. Focal mechanism solutions as determined using data from the NEONOR stations. The background seismic activity (July-November 1997) is plotted with symbols proportional to magnitude.

The composite focal mechanism in Table 1 and Fig. 7.1.6 is determined from the larger number of earthquakes that appear to be concentrated around a NW-SE trending line under Sjona (Fig. 7.1.4). The focal mechanism has one nodal plane conforming to this direction, which strengthens the assumption that this trend is real. There is also a system of lineations and cracks in this area with approximately the same trend. The first motions are very consistent within this group, implicating a static stress and slip regime. The inferred direction of maximum compression appears to be roughly N-S, in contrast to the regional stress field for this area, which has an ENE-WSW trend (Fig. 7.1.7).

One of the largest earthquakes detected within the network is also located in this Sjona group, with a local magnitude of 1.6. The polarities from this event do not, however, fully comply with those from the smaller ones, for reasons not yet fully understood.

The other focal mechanisms were determined by waveform modelling (using Herrmann's code) of the events, using the first motion polarities to constrain possible solutions. All four focal mechanism solutions within the network show a rotation with regard to the regional stress field, while the focal mechanism for the large event further west has a maximum horizontal compressive stress direction that is closer to the regional trend.

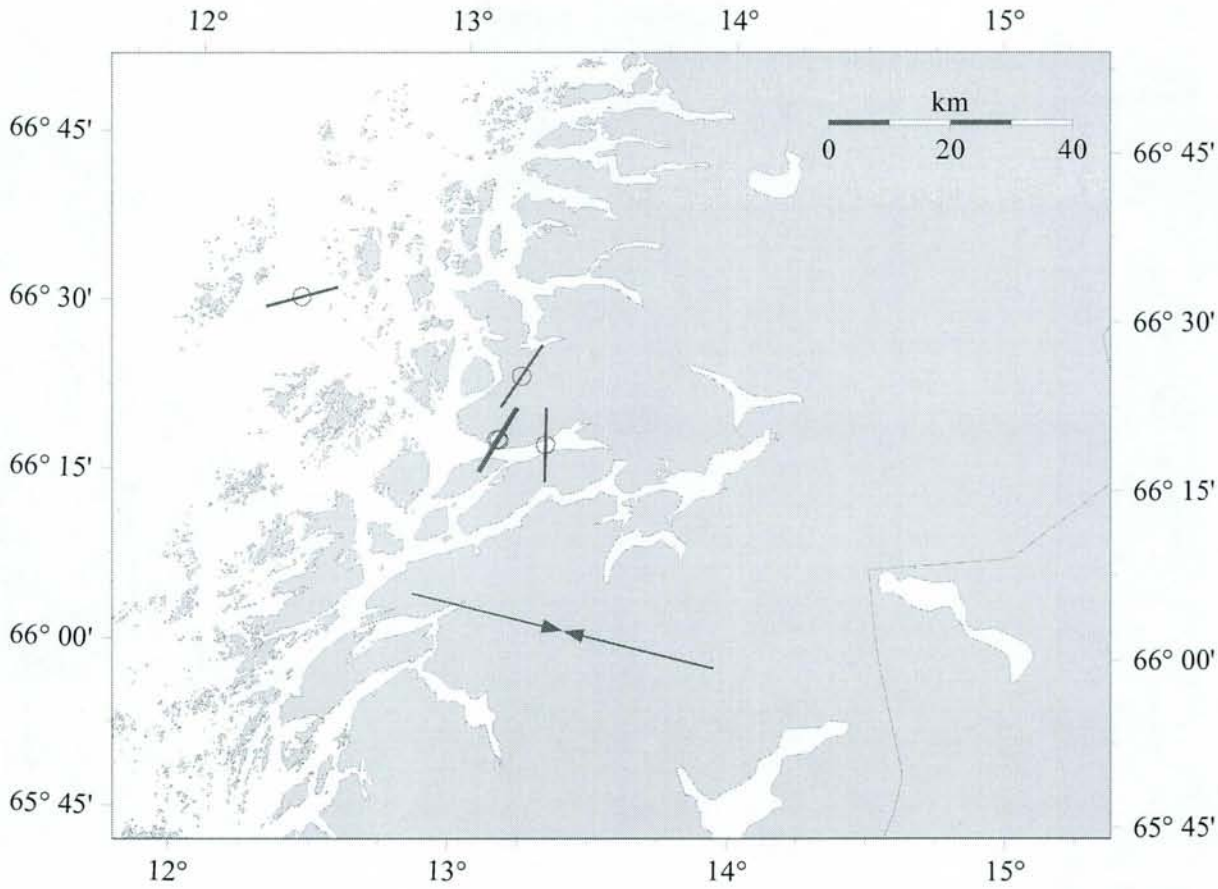

Fig. 7.1.7. Directions of maximum horizontal compressive stress derived from the focal mechanism solutions. The large arrows represent the approximate direction of the regional stress field, derived from offshore earthquake focal mechanism solutions and borehole break-outs, in addition to overcoring stress measurements onshore (Hicks 1996).

Magnitude and depth distributions

The magnitude distribution plot shown in Fig. 7.1.8 indicates that the detection threshold is around magnitudes (M_L) of 0.9. The magnitudes have been calibrated in relation to the NNSN stations nearby (MOR8, Namsos and Lofoten) using a regression relationship. The magnitudes will be recalculated once system response information is available for the network. Most of the activity within the network has local magnitudes between 0.5 and 1.5, and all of the earthquakes have shallow foci with depths mainly ranging from 4-6 km.

Fig. 7.1.9 shows a plot of the depth distribution within the network. The activity observed slightly further north, around Melfjorden, appears to be somewhat less shallow, with depths around 8 km. There are also some events originating below the large Svartisen glacier 40 km north of the network, these events have a wide range of depth estimates.

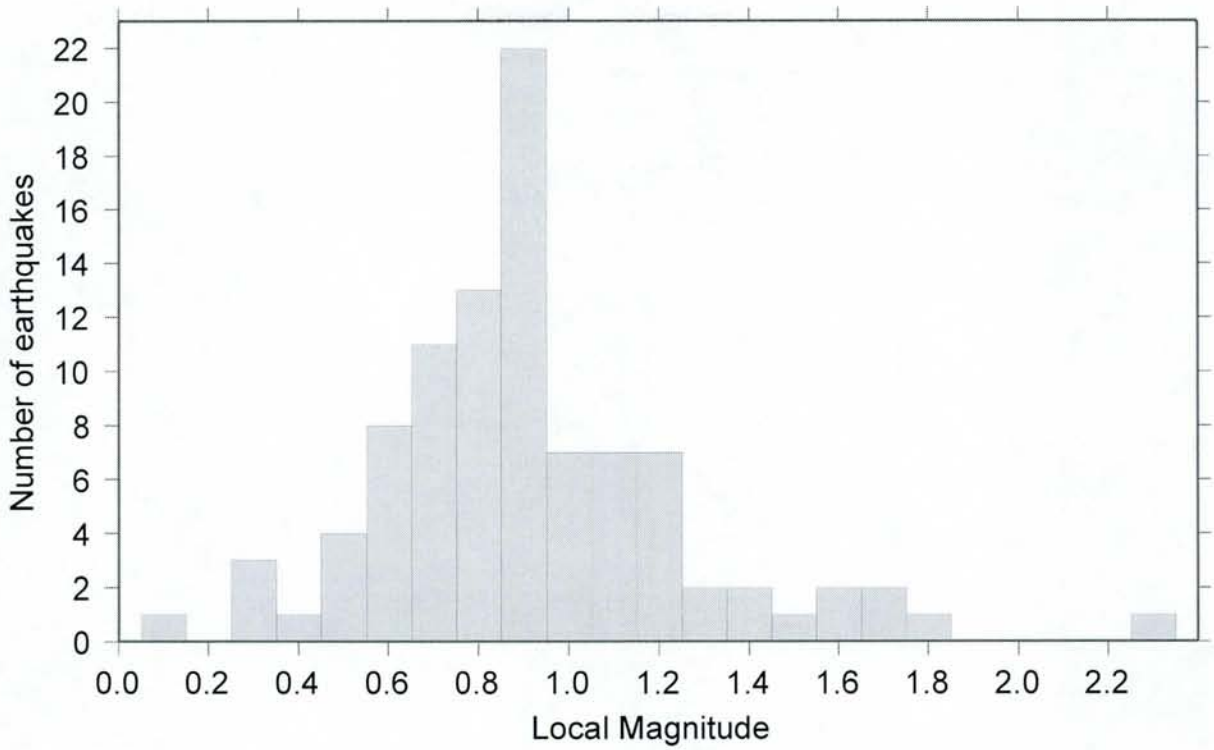

Fig. 7.1.8. Magnitude distributrion for the earthquakes in the Ranafjord area determined by the NEONOR network (probable explosions removed). Note that the threshold of detection drops below M_L 0.9.

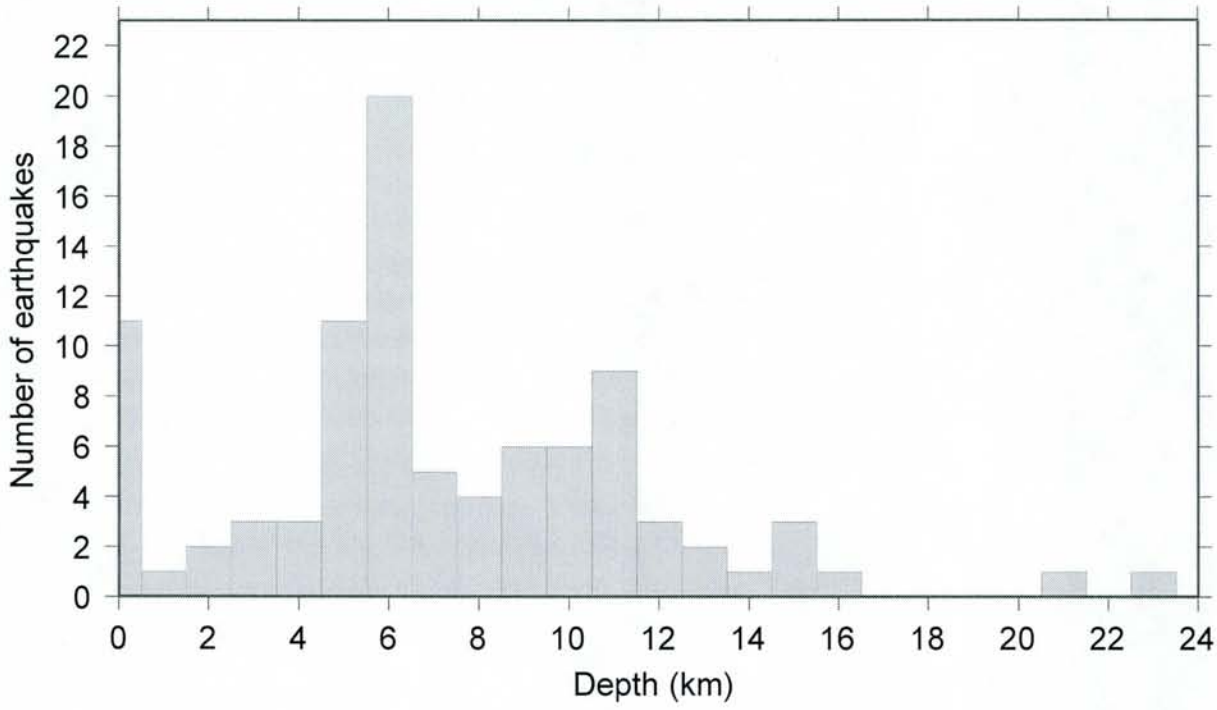

Fig. 7.1.9. Depth distribution of the earthquakes within the network (probable explosions removed).

Moreover, a cluster of earthquakes originating below the Silavågen fjord further west along the Sjona fjord have depths around 10 km. These earthquakes are slightly larger (magnitudes 1.0 to 1.8), but the threshold of detection is slightly lower for these events as they are located just outside the network.

It should be noted that the depths observed (4-6 km) are quite shallow compared to what is generally the case in Norway (5-30 km), but typical for what has been found from other coastal areas in northern Norway where earthquake swarms have been studied, such as in Meloy (Bungum *et al.* 1979) and in Steigen (Atakan *et al.* 1994).

Results are also available on the World Wide Web, in the form of maps, event lists and more detailed monthly bulletins. The URL is "http://www.norsar.no/NEONOR/".

7.1.6 Conclusions

The Rana region has been known for a long time to be one of the seismically most active in Norway, as demonstrated in many studies (e.g. Byrkjeland 1996). Over the last few years, the region has been studied in details by NGU (e.g. Olesen *et al.* 1994), and identified as one of the areas outside of the Finnmark/Lapland region with the best chances for postglacial faulting to be identified and documented. In Masi, the Stuoragurri postglacial fault has already been found to be clearly (albeit weakly) seismically active (Bungum & Lindholm 1997).

The seismic array installed in the Ranafjord area in the summer of 1997 turned out to be very successful in that it started to record significant local activity already from the very first day, as documented in the present report.

The main findings so far can be summarized as follows:

The study confirms the region as being seismically active, as the network has identified of the order of a hundred earthquakes from the region, with magnitudes from 0.1 to 2.3. With a detection threshold of around 0.9, it seems that the improvement with respect to the national network is more than one order of magnitude, as confirmed also by the fact that the national (NNSN) network has reported only six of the NEONOR earthquakes. There are no indications that the activity these last months has been significantly different from long term averages, even if no larger event has been experienced.

Some of the seismic activity documented here is clearly related to the Båsmoen fault, but with important qualifications, in particular one related to the Sjona group of events, where an oblique normal composite focal mechanism supports a NW-SE delineation, possibly indicating some kind of transform mechanism with respect to the main Båsmoen fault.

The focal mechanisms obtained indicate a NNE-SSW maximum compression, as distinctly different from the average Fennoscandian WNW-ESE direction, which is commonly accepted to be related to the first order source of stress from the ridge push force (Bungum *et al.* 1991). In mid Norway, however, this direction has been found mostly for offshore events (Byrkjeland 1996), and we interpret the present finding for the coastal region to be related more to regional and local second and third order sources of stress (density inhomogeneities, flexural stresses, topographic loads, geological features, etc.) than to first order (plate motion related) effects, as indicated both by the Meløy (Bungum *et al.* 1979) and the Steigen earthquake sequencies (Atakan *et al.* 1994).

The shallow focal depths reported on here are both interesting and important, and is one of several topics which will receive special attention as more data and results become available from the NEONOR seismic network in the Rana region.

Appendix 7.1: Revised Technical Information, Mo I Rana

This document contains technical information concerning the NEONOR seismic network in Mo i Rana. Some of the information was revised during fieldwork on the network October 28-31, 1997.

Station no. 1 (NIRI) - Vettahaugen

Latitude:	66° 12' 28.2" N
Longitude:	13° 44' 24.6" E
Height above MSL:	690 m
Contact:	Per Jørgen Drage, Tel.: 75193251 Mob.: 94890365
Seismometer SN:	1697
Gain:	60 dB
Highpass filter:	0.2 Hz
Lowpass filter:	12.5 Hz
VCO freq.:	2380 Hz
Receiver freq.:	173.900 MHz from station no. 3 (N1R3) - Nordsjona
Transmitter freq.:	441.600 MHz to central point (N1R6) - Dalselv

Station no. 2 (NIR2) - Lillevik (Nesna)

Latitude:	66° 16' 53.4" N
Longitude:	13° 14' 00.3" E
Height above MSL:	61 m
Contact:	Kristian Lillevik, Tel.: 75057544
Seismometer SN:	1167
Gain:	60 dB
Highpass filter:	0.2 Hz
Lowpass filter:	12.5 Hz
VCO freq.:	1360 Hz
Receiver freq.:	N/A
Transmitter freq.:	441.725 MHz to station no. 3 (N1R3) - Nordsjona

Station no. 3 (NIR3) - Nordsjona

Latitude:	66° 20' 14.0" N
Longitude:	13° 24' 22.6" E
Height above MSL:	68 m

Contact:	Harry A. Nilsen, Tel.: 75163263
Seismometer SN:	1162
Gain:	60 dB
Highpass filter:	0.2 Hz
Lowpass filter:	12.5 Hz
VCO freq.:	1700 Hz
Receiver freq.:	441.725 MHz from station no. 2 (N1R2) - Lillevik (Nesna)
Transmitter freq.:	173.900 MHz to station no. 1 (N1R1) - Vettahaugen

Station no. 4 (N1R4) - Lillevand (Langvatn)

Latitude:	66° 26' 57.6" N
Longitude:	13° 52' 42.0" E
Height above MSL:	55 m
Contact:	Daniel Granlund, Tel.: 75163013
Seismometer SN:	1198
Gain:	60 dB
Highpass filter:	0.2 Hz
Lowpass filter:	12.5 Hz
VCO freq.:	2040 Hz
Receiver freq.:	N/A
Transmitter freq.:	441.625 MHz to station no. 5 (N1R5) - Hammernes (Langvatn)

Station no. 5 (N1RS) - Hammernes (Langvatn)

Latitude:	66° 23' 12.8" N
Longitude:	14° 01' 58.2" E
Height above MSL:	62 m
Contact:	Hans Leiramo, Tel.: 75169568
Seismometer SN:	1161
Gain:	60 dB
Highpass f:dter:	0.2 Hz
Lowpass filter:	12.5 Hz
VCO freq.:	2720 Hz
Receiver freq.:	441.625 MHz from station no. 4 (N1R4) - Lillevand (Langvatn)
Transmitter freq.:	174.000 MHz to central point (N1R6) - Dalselv

Central point/station no. 6 (N1R6) - Dalselv

Latitude:	66° 15' 39.6" N
Longitude:	13° 58' 11.0" E
Height above MSL:	85 m
Contact:	Olaf M. Hansen, Tel.: 75164540
Seismometer SN:	1208
Gain:	60 dB
Highpass filter:	0.2 Hz
Lowpass filter:	12.5 Hz
VCO freq.:	N/A
Receiver no. 1 freq.:	441.600 MHz from station no. 1 (N1R1) - Vettahaugen
Receiver no. 2 freq.:	174.000 MHz from station no. 5 (N1R5) - Hammernes (Langvatn)
Transmitter freq.:	N/A

All stations:

Seismometer type:	Teledyne Geotech S - 13
Amplifier:	Teledyne Geotech model 42.50
VCO:	Teledyne Geotech model 46.22

Central point:

Discriminators:	Teledyne Geotech model 46.12
Digitizer:	Nanometrics RD6

8 MODELLING (TASK 11)

8.1 Modelling of Tectonic Movements

by Willy Fjeldskaar, Rogaland Research

Fennoscandia has experienced major uplift in post-glacial time. The rate of uplift along the coasts has been so high in the past that its effects have been observed within one generation. From the 18th century onwards the rate of displacement has been intensively discussed. It is now widely accepted to be basically an isostatic response of the deglaciation history of the area.

Data on the uplift can be grouped in two: i) present rate of uplift (Fig. 8.1.1) and ii) shoreline tilts versus time (Fig. 8.1.2). These observations are mainly results of the movements of the solid earth. They are scarcely affected by movements of the sea level. The movements of the solid earth are here assumed to have glacial isostatic origin connected to the melting of the last ice sheets (Fig. 8.1.3). It is, however, not unreasonable to assume that there is a neotectonic component in the uplift rate and the paleao shoreline gradients. The general pattern of the uplift is here believed to be a result of glacial isostasy, but there may be local disturbances to this general pattern caused by tectonic processes.

The earth's response to the deglaciation in Fennoscandia is modelled using a layered viscous model with elastic lithosphere. The modelled tilting of palaeo shorelines at particular locations peripheral to the former ice load and the pattern of present rate of uplift consistent with the observations strongly suggest a low-viscosity asthenosphere. It is strongly suggested that the asthenosphere has a thickness less than 150 km and viscosity less than 7.0×10^{19} Pa s (Fjeldskaar 1994).

The most likely glacier thickness model gives a flexural rigidity of 10^{23} Nm ($t_e \approx 20$ km) at the Norwegian coast, increasing to above 10^{24} Nm ($t_e \approx 50$ km) in central parts of Fennoscandia (Fjeldskaar 1997).

The model that best fits with the observations (Fig. 8.1.4), will, probably, give a good measure of the glacial isostatic process. There will, however, be local areas that have a significant difference between the observations and the calculated uplift. This is assumed to be areas that experience tectonic movements today. This part of the project will focus on such discrepancies, and in such a way model neotectonism.

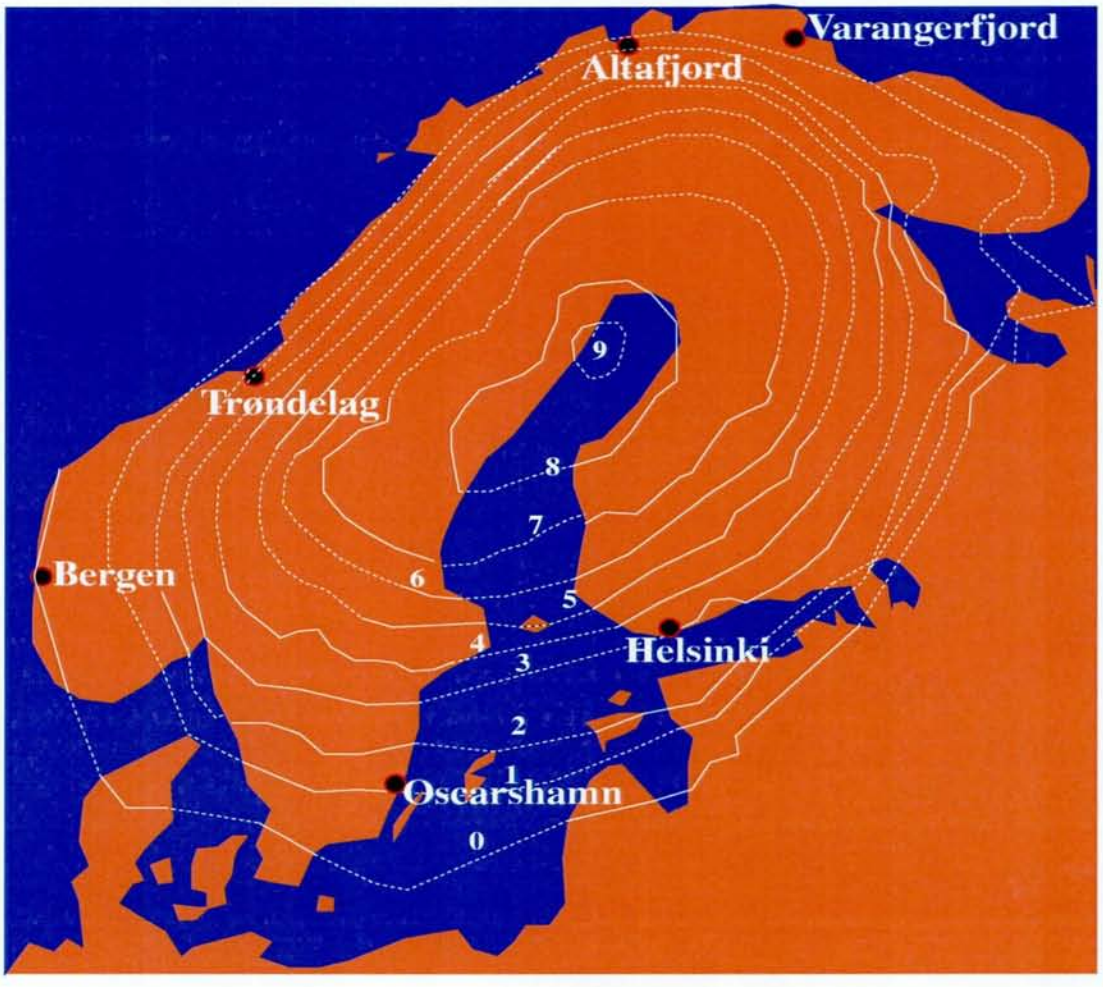

Fig. 8.1.1. Observed present rate of uplift in mm/year.

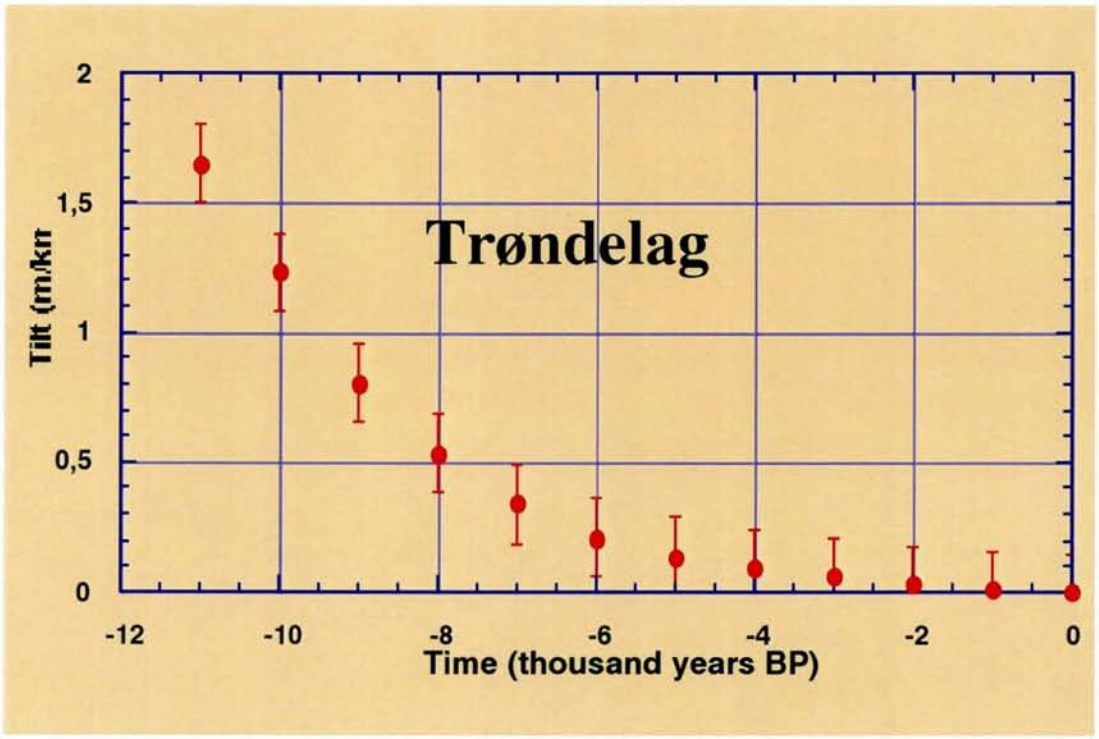

Fig. 8.1.2. Observed palaeo shoreline tilt in Trøndelag, mid Norway.

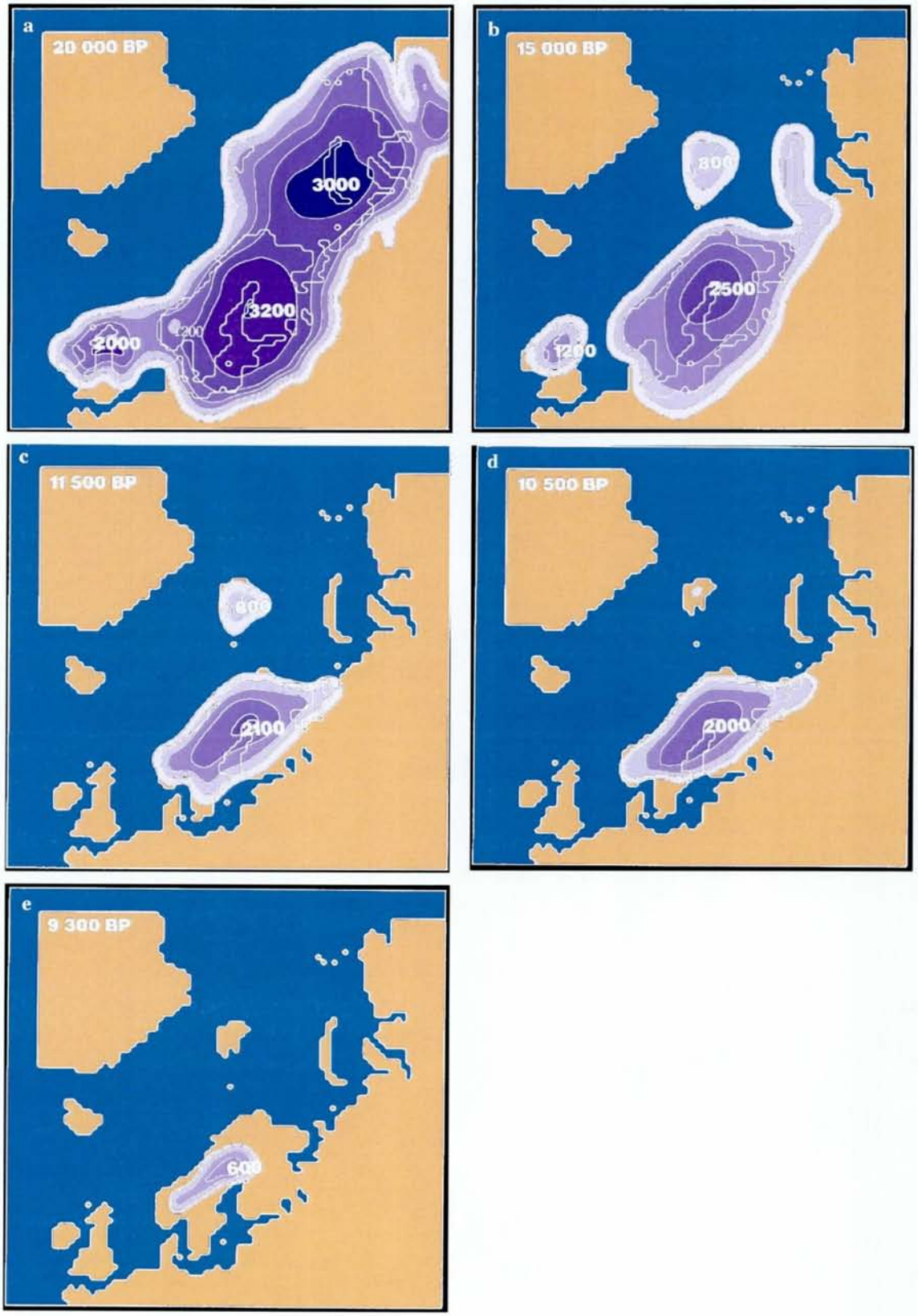

Fig. 8.1.3. Deglaciation of Fennoscandia

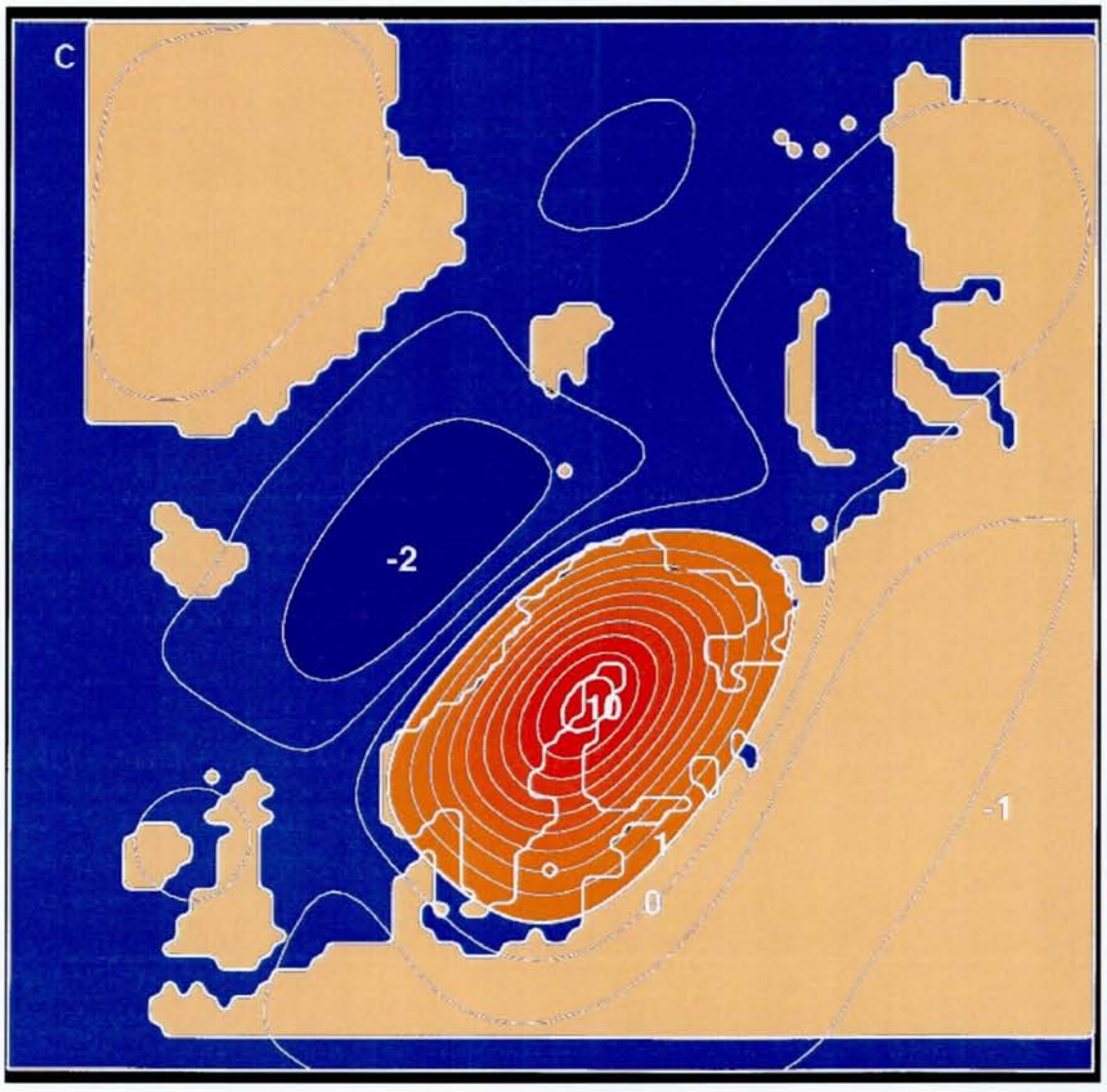

Fig. 8.1.4. Theoretical vs. observed present rate of uplift.

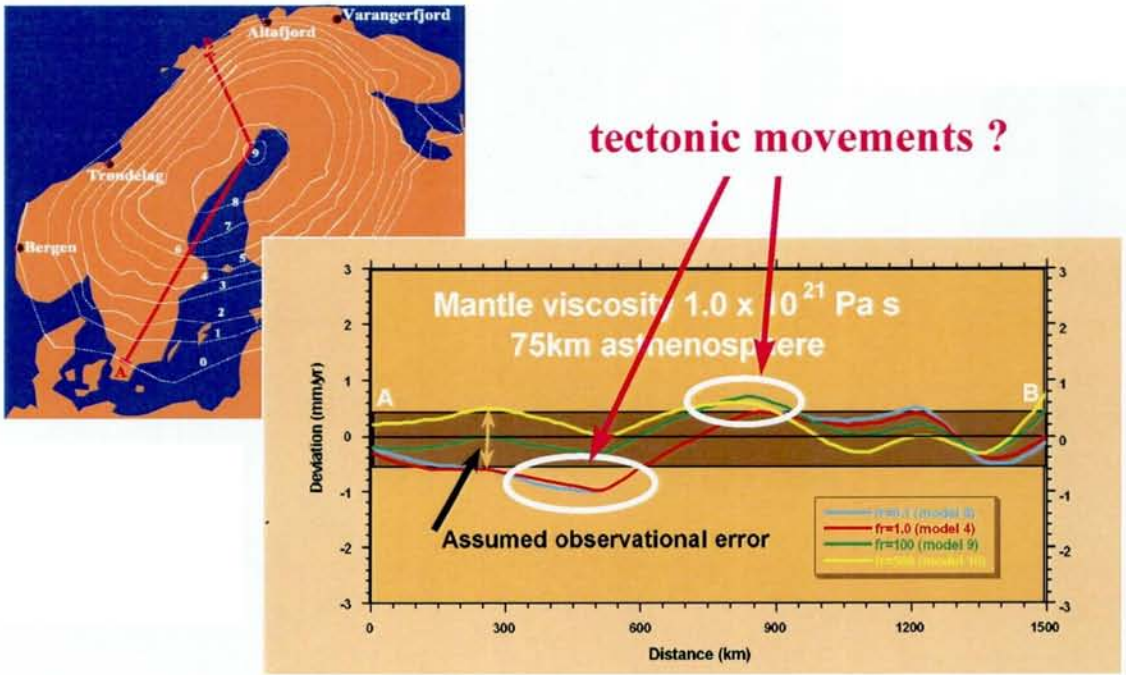

Fig. 8.1.5. Deviation between observed and theoretical uplifts, shown on a profile across Fennoscandia. Areas with deviation greater than the observational error most probably experience tectonic movements.

Acknowledgements

The NEONOR Project has received financial support from the three petroleum companies Amoco Norway, Norsk Hydro and Phillips Petroleum and the Norwegian state hydro-power company Statkraft. Mark Shahly, Chris Dart, Philip J. Goldsmith and Ivar Hågensen are representatives of the four industrial partners in the steering committee. Dagfinn Rise (Statkraft), Per Christian Alsgaard (Amoco Norway) and Pål Haremo, Bjørn T. Larsen and Tor Harald Hanssen (Norsk Hydro) have participated in the initial phase of the project. The Norwegian Research Council has financed a three-year Doctorate fellowship (Dr.Scient) at NORSAR/UiO and a two-year Post Doctorate fellowship at NGU. IKU Petroleum Research, Rogaland Research and the Norwegian University of Science and Technology (Dept. of Surveying and Mapping) are carrying out substantial parts of the research project on a contract basis. John Adams from the Geological Survey of Canada visited NGU and NORSAR in February 1996 and contributed valuable information during the planning stage of the project. To all these persons, institutions and companies we express our sincere thanks.

9 COMBINED REFERENCES

Andersen, B. G., Wangen, O. P. & Østmo, S., 1987: Quaternary geology of Jæren and adjacent areas, southwestern Norway. *Geological Survey of Norway Bulletin 411*, 55 p

Anundsen, K., 1988a: Jordskorpebevegelser. *In Geologi for fjellvandrere*. Stavanger Turistforening, Årbok 1988, 86-87.

Anundsen, K., 1988b: Landskapet forandrer seg fremdeles. *In Geologi for fjellvandrere*. Stavanger Turistforening, Årbok 1988, 88-89.

Anundsen, K., 1989: Late Weichselian relative sea levels in southwest Norway: observed strandline tilts and neotectonic activity. *Geologiska Föreningens i Stockholm Förhandlingar* 111, 288-292.

Anundsen, K. & Gabrielsen, R. H., 1990: Neotectonics, Sunhordaland region. Guide to Excursion. *Structural Geology Group, UiB/NRSC Report 5*, 29 p

Anundsen, K., Grimstveit, L., Harsson, B. G. & Holsen, J., submitted: Anundsen, K., Grimstveit, L., Harsson, B.G. & Holsen, J. in prep.: Measurements of neotectonic movements in southern Norway: Implications for former ice thickness estimates. *Norsk Geologisk Tidsskrift*.

Atakan, K., Lindholm, C. D. & Havskov, J., 1994: Earthquake swarm in Steigen northern Norway: an unusual example of intraplate seismicity. *Terra Nova* 6, 180-194.

Bakkelid, S., 1990: Innmåling av rur- og tangrandmerker i Nordland. *Statens kartverk report 3/1990*, 90 p

Bargel, T. H., Boyd, R. & Dahl, R., 1995: The geology of the Narvik District, A journey in time and space, *Geological Survey of Norway, Trondheim, 351 p.*

Beck, A. C., 1968: Gravity faulting as a mechanism of topographic adjustment. *New Zealand Journal of Geophysics* 11, 191-199.

Bergstrøm, B., 1994: Elsfjord: Kvartærgeologisk kart 1927 III - M 1: 50 000. Geological Survey of Norway.

Bøe, R., 1990: Regionalseismisk undersøkelse i ytre del av Boknafjorden. *NGU Rapport 90.093*, 7 p

Bøe, R., Sørensen, S. & Hovland, M., 1992: The Karmsundet Basin, SW Norway: stratigraphy, structure and neotectonic activity. *Norsk Geologisk Tidsskrift* 72, 281-283.

Bondevik, S., Svendsen, J. I., Johnsen, G., Mangerud, J. & Kaland, P. E., 1997: The Storegga tsunami along the Norwegian coast, age and runup. *Boreas* 26, 29-53

Brekke, H. & Riis, F., 1987: Tectonics and basin evolution of the Norwegian shelf between 62° and 72°N. *Norsk Geologisk Tidsskrift* 67, 295-322.

Brøgger, W. C., 1884: Spaltenverwerfungen in der Gegend Langesund-Skien. *Nyt Magazin for Naturvidenskaberne* 28, 253-419.

Bungum, H., Alaskar, A., Kvamme, L. B. & Hansen, R. A., 1991: Seismicity and seismotectonics of Norway and surrounding continental shelf areas. *Journal of Geophysical Research* 96, 2249-2265.

Bungum, H., Hokland, B. K., Husebye, E. S. & Ringdal, F., 1979: An exceptional intraplate earthquake sequence in Meløy. *Nature* 280, 32-35.

Bungum, H. & Lindholm, C., 1997: Seismo- and neotectonics in Finnmark, Kola Peninsula and the southern Barents Sea. Part 2: Seismological analysis and seismotectonics. *Tectonophysics* 270, 15-28.

Byrkjeland, U., 1996: *Seismotectonics of the Norwegian Continental Margin, 620-7 1ON.* Cand. Scient thesis, University of Oslo Norway, 146.

Fanavoll, S. & Dahle, A., 1990: Earthquake hazard and loads in the Barents Sea. *ESARC Report* 13, SF60.4022.00/01/90 (restricted).

Fejerskov, M., Lindholm, C., Larsen, B. T. & Nøttvedt, A., in press: Stress map, North Atlantic Area, Scale 1:3 million. *Integrated Basin Studies, Dynamics of the Norwegian Continental Margin (IBS-DNM).*

Fenton, C., 1991: *Neotectonics and palaeoseismicity in North West Scotland.* Ph.D. thesis, University of Glasgow Glasgow, 403.

Fenton, C., 1994: Postglacial faulting in eastern Canada. *Geological Survey of Canada, Open file report 2774*, 98 p

Feyling-Hanssen, R. W., 1966: Geologiske observasjoner i Sandnes-området. *Geological Survey of Norway* 242, 26-43.

Fiedler, A., 1992: *Kenozoisk sedimentasjon i Lofotenbassenget langs vestlige Barentshavmarginen.* Cand. Scient. thesis, University of Oslo Norway, 114.

Fjeldskaar, W., 1994: Viscosity and thickness of the asthenosphere detected from the Fennoscandian uplift. *Earth and Planetary Science Letters* 126, 399-410.

Fjeldskaar, W., 1997: The flexural rigidity of Fennoscandia inferred from the post-glacial uplift. *Tectonics* 16(4), 596-608.

Fugelli, E. & Riis, F., 1992: Neotectonism in the Jæren area, southwest Norway. *Norsk Geologisk Tidsskrift* 72, 267-270.

Gade, H. G., 1986: Brief overview of the physical oceanography. *In* Hurdle, B. G. (ed.), *The Nordic Seas*. Springer Verlag, New York, 183-189.

Granberg, E., 1992: *A basin modelling study of the Vøring Basin.* Diploma thesis, University of Trondheim Norway.

Grønlie, O. T., 1922: Strandliner, moræner og skjælforekomster i den sydlige del av Troms fylke. *Norges geologiske undersøkelse Nr. 94*

Grønlie, O. T., 1923: Har Høgtuva steget i vor tid? *Naturen* 7, 139-141.

Grønlie, O. T., 1939: Some remarks on the land area in Nordland between the glacier Svartisen, and the frontier. *Norsk Geogr. Tidsskr* 7, 399-406.

Havskov, J., Kvamme, L. B., Hansen, R. A., Bungum, H. & Lindholm, C. D., 1992: The northern Norway seismic network: Design, operation and results. *Bulletin of the Seismological Society of America* 82(481-496).

Heltzen, I. A., 1834: Ranens Beskrivelse, *Rana Museums og Historielag*, Mo i Rana, 290 p

Hicks, E. C., 1996: *Crustal stresses in Norway and surrounding areas as derived from earthquake focal mechanisms and in-situ stress measurements*. Cand. Scient thesis, University of Oslo Norway, 163.

Holmsen, G., 1916: Om strandlinjers fald omkring gabbroomraader (Summary in English). *Norsk Geologisk Tidsskrift* 4, 7-20.

Holtedahl, H., 1959: Den norske strandflate med særlig henblikk på dens utvikling i kystområdene på Møre. *Norsk Geogr. Tidsskr.* 16, 285-305.

INQUA, 1982: International Association for Quaternary Research (INQUA) Commission Reports 1978-1982. *In Striolae 1982:1 (INQUA Newsletter 4)*, 36-38.

Jahn, A., 1964: Slopes morphological features resulting from gravitation. *Z. Geomorph. Suppl* 5, 59-72.

Janocko, J., Landvik, J. Y., Larsen, E. & Sejrup, H. P., 1997: Stratigraphy and sedimentology of Middle to Upper Pleistocene sediments in the new Grødeland borehole at Jæren, SW Norway. *Norsk Geologisk Tidsskrift* 77, 87-100.

Janocko, J., Landvik, J. Y., Larsen, E., Sejrup, H. P. & Steinsund, P. I., 1998: Middle and Late Quaternary depositional history reconstructed from two boreholes at Lågjæren and Høgjæren SW Norway. *Norsk Geologisk Tidsskrift*, in press.

Jibson, R. W., 1996: Using landslides for paleoseismic analysis. *In* McCalpin, J. P. (ed.), *Paleoseismology*. Academic Press, San Diego, 397-438.

Johnsen, E., 1981: Kvartære trekk fra Beiarns geologiske historie. *In Årbok for Beiarn, Beiarn historielag*. Egil Trohaugs Forlag a.s, Bodø, 93-106.

Karpuz, M. R., Gabrielsen, R. H., Engell-Sørensen & Anundsen, K., 1991: Seismotectonic significance of the 29 January 1989 Etne earthquake, SW Norway. *Terra Nova* 3, 540-549.

King, E. L., Sejrup, H. P., Haflidason, H., Elverhøi, A. & Aarseth, I., 1996: Quaternary seismic stratigraphy of the North Sea Fan: Gacially fed gravity flow aprons, hemipelagic sediments and large submarine slides. *Marine Geology* 130, 293-315.

Kujansuu, R., 1964: Nuorista sirroksista Lapissa. Summary: Recent faults in Lapland. *Geologi* 16, 30-36.

Lagerbäck, R., 1979: Neotectonic structures in northern Sweden. *Geol. Fören. Stockh. Förh* 100 (1978), 271-278.

Lagerbäck, R., 1990: Late Quaternary faulting and paleoseismicity in northern Fennoscandia, with particular reference to the Lansjärv area, northern Sweden. *Geol. Fören. Stockh. Förh.* 112, 333-354.

Lagerbäck, R., 1992: Dating of Late Quaternary faulting in northern Sweden. *Journal of the Geological Society of London* 149, 285-291.

Larsen, E., 1992: Quaternary stratigraphy at Jæren, SW Norway: Paleoenvironments, climatic change and faulting. *Geological Survey of Norway, Internal Report 92.002*, 21 p

Lindholm, C., Bungum, H., Hicks, E., Fejerskov, M., Larsen, B. T. & Nøttvedt, A., in press: Seismicity and earthquake focal mechanisms, North Atlantic Area, Scale 1:3 million. *Integrated Basin Studies, Dynamics of the Norwegian Continental Margin (IBS-DNM)*.

Longva, O. & Thorsnes, T., 1997: Skagerrak in the past and at the present - an integrated study of geology, chemistry, hydrography and microfossil ecology. *Geological Survey of Norway, Special Publication 8*, 98 p

Løset, F., 1981: Neotectonic movements in Norway. Literature review of neotectonic movements in Norway, and results from field investigations on Hardangervidda. *Norwegian Geotechnical Institute (NGI), Internal Report 40009-7*, 13 p

Lundquist, J. & Lagerbäck, R., 1976: The Pärvie Fault: A late-glacial fault in the Precambrian of Swedish Lapland. *Geol. Fören. Stockh. Förh.* 98, 45-51.

Mangerud, J., Sønstegaard, E., Sejrup, H.-P. & Haldorsen, S., 1981: A continuous Eemian-Early Weichselian sequence containing pollen and marine fossils at Fjøsanger, western Norway. *Boreas* 10, 137-208.

Mauring, E., Olesen, O., Rønning, J. S. & Tønnesen, J. F., 1997: Ground-penetrating radar profiles across postglacial faults at Kåfjord, Troms and Fidnajohka, Finnmark. *Geological Survey of Norway, Report 97.174*, 16 p

Mauring, E. & Rønning, J. S., 1990: Refleksjosseismiske målinger ved Oppstad på Jæren, Hå, Rogaland. *Geological Survey of Norway, Report 90.148*, 16 p

McCalpin, J. P., 1996: Paleoseismology, *Academic Press*, 598 p

McCalpin, J. P. & Irvine, J. R., 1995: Sackungen at the Aspen Highlands Ski Area, Pitkin County, Colorado. *Environ. & Engin. Geosci.* 1, 277-290.

Mokhtari, M., 1991: *Geological model for the Lofoten continental margin.* Dr. Scient. thesis, University of Bergen Norway, 184.

Mokhtari, M. & Pegrum, R. M., 1992: Structure and evolution of the Lofoten continental margin, offshore Norway. *Norsk Geologisk Tidsskrift* 72, 339-355.

Muir Wood, R., 1989a: Extraordinary deglaciation reverse faulting in northern Fennoscandia. *In* Gregersen, S. & Basham, P. W. (ed.), *Earthquakes at North-Atlantic passive margins: neotectonics and postglacial rebound.* Kluwer Academic Publishers, Dordrecht, The Netherlands, 141-173.

Muir Wood, R., 1989b: The Scandinavian Earthquakes of 22 December 1759 and 31 August 1819. *Disasters* 12, 223-236.

Muir Wood, R., 1993: A review of the seismotectonics of Sweden. *Swedish Nuclear Fuel and Waste Management Co. Technical Report 93-13*, 225 p

Muir Wood, R., 1995: Reconstructing the tectonic history of Fennoscandia from its margins: The past 100 million years. *Swedish Nuclear Fuel and Waste Management Co. Technical Report 95-36*, 107 p

Muir Wood, R. & Forsberg, C. F., 1988: Regional crustal movements on the Norwegian continental shelf, ELOCS (Earthquake Loading on the Norwegian Continental Shelf) Report 1-3, *Norwegian Geotechnical Institute, Oslo, NTNF/NORSAR, Kjeller and Principia mechanica Ltd.*, London, 148 p

Muir Wood, R. & King, G. C. P., 1993: Hydrological signatures of earthquake strain. *Journal of Geophysical Research* 98, 22035-22068.

Myrvang, A., 1993: Rock stress and rock stress problems in Norway. *In* Hudson, J. A. (ed.), *Comprehensive rock engineering. Vol. 3, Rock testing and site characterization.* Pergamon Press, 461-471.

Obermeier, S. F., 1996: Using Liquefaction - Induced Features for Paleoseismic Analyses. *In* McCalpen (ed.), *Paleoseismology.* Academic Press, 331-396.

Olesen, O., 1988: The Stuoragurra Fault; evidence of neotectonics in the Precambrian of Finnmark, northern Norway. *Norsk Geologisk Tidsskrift* 68(2), 107-118.

Olesen, O., Gjelle, S., Henkel, H., Karlsen, T. A., Olsen, L. & Skogseth, T., 1994: Neotectonic studies in the Ranaford area, northern Norway. *Geological Survey of Norway, Report 94.073*

Olesen, O., Gjelle, S., Henkel, H., Karlsen, T. A., Olsen, L. & Skogseth, T., 1995: Neotectonics in the Ranafjorden area, Northern Norway. *Bulletin - Norges Geologiske Undersøkelse* 427, 5-8.

Olesen, O., Henkel, H., Lile, O. B., Mauring, E. & Ronning, J. S., 1992a: Geophysical investigations of the Stuoragurra postglacial fault, Finnmark, northern Norway. *Journal of Applied Geophysics* 29(2), 95-118.

Olesen, O., Henkel, H., Lile, O. B., Mauring, E. & Rønning, J. S., 1990a: Detailed geophysical investigations of the Stuoragurra postglacial fault, Finnmark, northern Norway. *Geological Survey of Norway Report 90.160*, 24 p

Olesen, O., Henkel, H., Lile, O. B., Mauring, E., Rønning, J. S. & Torsvik, T. H., 1992b: Neotectonics in the Precambrian of Finnmark, northern Norway. *Norsk Geologisk Tidsskrift* 72, 301-306.

Olesen, O., Roberts, D., Henkel, H., Bernt, L. O. & Torsvik, T. H., 1990b: Aeromagnetic and gravimetric interpretation of regional structural features in the Caledonides of West Finnmark and North Troms, Northern Norway. *Geological Survey of Norway, Bulletin* 419, 1-24.

Olesen, O., Roberts, D. & Olsen, L., 1992c: Neotectonic studies in Finnmark 1992. *Geological Survey of Norway Report 92.325*, 15 p

Olsen, L., 1989: Bæivašgied'di, 2033 III kvartærgeologisk kart - M 1:50 000. Geological Survey of Norway.

Olsen, L., Sveian, H. & Blikra, L. H., 1996: Korgen: 1927 II. Kvartærgeologisk kart - M 1:50 000. Geological Survey of Norway.

Reusch, H., 1888: Bømmeløen og Karmøen med omgivelser, *Geological Survey of Norway*, 423 p

Reusch, H., 1901: Nogle bidrag til forstaaelsen af hvorledes Norges dale og fjelde er blevne til. *Geological Survey of Norway Bulletin* 32, 125-217.

Riis, F., 1996: Quantification of Cenozoic vertical movements of Scandinavia by correlation of morphological surfaces with offshore data. *Global and Planetary Change* 12, 331-357.

Roberts, D., 1991: A contemporary small-scale thrust-fault near Lebesbye, Finnmark. *Norsk Geologisk Tidsskrift* 71, 117-120.

Roberts, D., Olesen, O. & Karpuz, M. R., 1997: Seismo- and neotectonics in Finnmark, Kola Peninsula and the southern Barents Sea; Part 1, Geological and neotectonic framework. *Tectonophysics* 270(1-2), 1-13.

Rokoengen, K. & Rønningsland, T. M., 1983: Shallow bedrock geology and Quaternary thickness in the Norwegian sector of the North Sea between 60°30¢N and 62°N. *Norsk Geologisk Tidsskrift* 68, 83-102.

Rokoengen, K. & Sættem, J., 1983: Shallow bedrock geology and Quaternary thickness off northern Helgeland, Vestfjorden and Lofoten. *IKU report P-155/2/83*, 44 p

Savage, W. Z. & Varnes, D. J., 1987: Mechanics of gravitational spreading of steep-sided ridges ('sackung'). *International Association of Engineering Geologists Bulletin* 35, 31-36.

Sejrup, H.-P., 1987: Molluscan and foraminiferal biostratigraphy of an Eemian-Early Weichselian section on Karmøy, southwestern Norway. *Boreas* 16, 27-42.

Sejrup, H. P., Aarseth, I., Haflidason, H., Løvlie, R., Braathen, A., Tjøstheim, G., Forsberg, C. F. & Ellingsen, K. I., 1995: Quaternary of the Norwegian Channel: glaciation history and paleoceanography. *Norsk Geologisk Tidsskrift* 75, 65-87.

Sejrup, H. P., Landvik, J. Y., Larsen, E., Janocko, J., Eiriksson, J. & King, E. L., 1997: The Jæren area, a border zone of the Norwegian Channel Ice Stream. *Quaternary Science Reviews*, in press.

Selnes, P. B., 1983: Possible neotectonic fault movements in Norway. *In* Ritsema, A. R. & Gürpinar, A. (ed.), *Seismicity and seismic risk in the offshore North Sea.* D. Reidel Publishing Company, 47-48.

Sibson, R. H., 1981: Fluid flow accompanying faulting: field evidence and models. *In* Simpson, D. W. & Richards, P. G. (ed.), *Earthquake prediction: An international review.* Maurice Ewing Ser. 4. Americal Geophysical Union, Washington, D. C., 593-603.

Sollid, J. L. & Tolgensbakk, J., 1988: Kvartærgeologisk og geomorfologisk kartlegging på Svalbard og fastlands-Norge utført ved Geografisk institutt, Univ. i Oslo. Abstract 18. *Nordiske Geologiske vintermøte, København*, 380-381.

Talbot, C. J. & Slunga, R., 1989: Patterns of active shear in Fennoscandia. *In* Gregersen, S. & Basham, P. W. (ed.), *Earthquakes at North-Atlantic passive margins: neotectonics and postglacial rebound. NATO ASI Series.*

Tanner, V., 1907: Studier öfer kvartärsystemet i Fennoskandias nordliga delar. I: Till frågan om Ost-Finmarkens glaciation och nivåförändringar. Résymé en francais. *Bull. Comm. Géol. Finl. 18*, 165 p

Tolgensbakk, J. & Sollid, J. L., 1988: Kåfjord, kvartærgeologi og geomorfologi 1:50 000, 1634 II. Geografisk institutt, Universitetet i Oslo.

Varnes, D. J., Radbruch-Hall, D. H. & Savage, W. Z., 1989: Topographic and structural conditions in areas of gravitational spreading of ridges in the Western United States. *USGS professional paper 1496*

Vogt, T., 1923: En postglacial jordskjælvs-forkastning. *Naturen* 7, 65-71.

Werenskiold, W., 1931: Ett sprekkesystem i Gudbrandsdalen. *Norsk Geologisk Tidsskrift* 12, 575-576.

Wontka, J. F., 1974: *Zur Geologie und Tektonik des Gebietes zwischen nördlichem Reisadal und Oksfjorddal, Nordreisa Kommune, Troms, Nord-Norwegen.* Diploma thesis, University of Mainz Germany, 58.

Zischinsky, U., 1969: Über Sackungen. *Rock Mechanics* 1, 30-52.